Journal of Nanomaterials

Synthesis and Application of Nanoparticles from Microorganisms and Plants

Lead Guest Editor: Naeem Khan
Guest Editors: Shahid Ali and Asif Mehmood

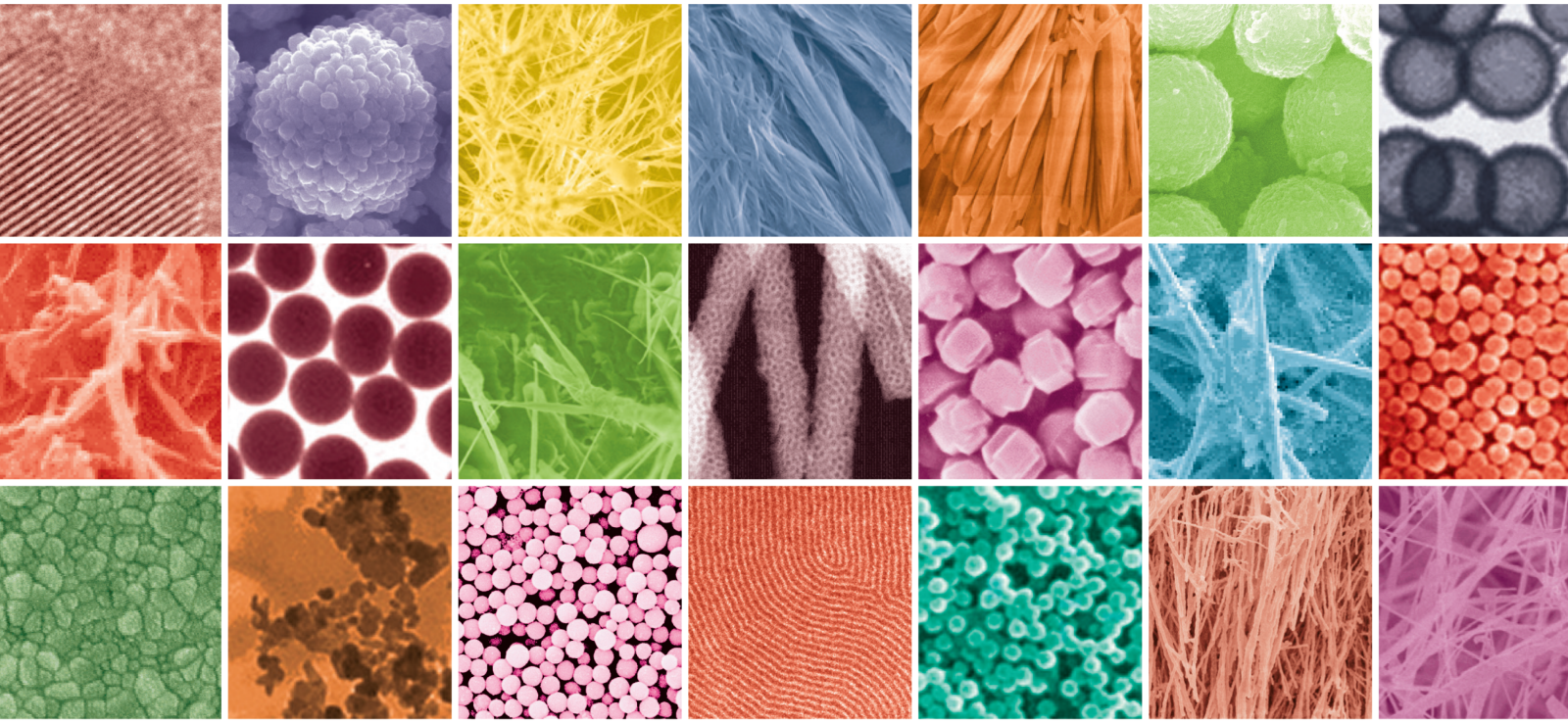

Synthesis and Application of Nanoparticles from Microorganisms and Plants

Journal of Nanomaterials

Synthesis and Application of Nanoparticles from Microorganisms and Plants

Lead Guest Editor: Naeem Khan
Guest Editors: Shahid Ali and Asif Mehmood

Contents

Hindawi
Journal of Nanomaterials
Volume 2021, Article ID 5518389, 9 pages
https://doi.org/10.1155/2021/5518389

Research Article

Comparative Study of the Silver Nanoparticle Synthesis Ability and Antibacterial Activity of the *Piper Betle* L. and *Piper Sarmentosum* Roxb. Extracts

Ngoc Hoi Nguyen,[1,2] Tran Thi Yen Nhi,[2,3] Ngo Thi Van Nhi,[1,4] Tran Thi Thu Cuc,[1,4] Pham Minh Tuan,[4] and Dai Hai Nguyen[1,2]

[1]*Institute of Applied Materials Science, Vietnam Academy of Science and Technology, Ho Chi Minh City 700000, Vietnam*
[2]*Graduate University of Science and Technology, Vietnam Academy of Science and Technology, Hanoi City 100000, Vietnam*
[3]*NTT Hi-Tech Institute, Nguyen Tat Thanh University, Ho Chi Minh City 700000, Vietnam*
[4]*Faculty of Biotechnology, Ho Chi Minh City University of Food Industry, 140 Le Trong Tan, Tay Thanh Ward, Tan Phu District, Ho Chi Minh City 700000, Vietnam*

Correspondence should be addressed to Dai Hai Nguyen; nguyendaihai0511@gmail.com

Received 18 January 2021; Revised 9 April 2021; Accepted 16 April 2021; Published 27 May 2021

Academic Editor: Shahid Ali

Piper betle (*P. betle*) and *Piper sarmentosum* (*P. sarmentosum*) are the two members of the *Piper* genus, have been reported to be rich in phytochemicals and essential oils, which showed strong reducing power, antibacterial, and antifungal activities. *P. betle* recently has been studied and applied in several commercial products in the antimicrobial respect, meanwhile its relatives, *P. sarmentosum* has been lesser-known in this field. In this study, the two *Piper* species—*P. betle* and *P. sarmentosum* were studied to compare their ability in silver nanoparticle synthesis and efficacy in antibacterial activity. *P. betle* and *P. sarmentosum* were extracted by distilled water at different temperatures and times. Subsequently, their total reducing capacity was determined by DPPH scavenging and Folin-Ciocalteu assays to choose the appropriate extraction conditions. The silver nanoparticle solutions prepared by the extracts of *P. betle* (Pb.ext) and *P. sarmentosum* (Ps.ext) were characterized by Dynamic light scattering (DLS), Zeta potential, UV-vis, and Fourier-transform infrared (FTIR) measurements. Finally, the antibacterial activity of the synthesized silver nanoparticle solutions was tested against *Escherichia coli* using the agar diffusion well–variant method. The Pb.ext showed stronger reducing power with higher total polyphenol content (~125 mg GAE/mL extract) and better DPPH activity (IC50~1.45%). Both the green synthesized silver nanoparticle solutions (Pb.AgNP and Ps.AgNP) performed significantly stronger antibacterial activity on *Escherichia coli* compared to their initial extracts. Antibacterial tests revealed that Ps.AgNP showed remarkably better growth inhibition activity as compared to Pb.AgNP. This study would contribute useful and important information to the development of antibacterial products based on green synthesized silver nanoparticles fabricated by the extracts of *P. betle* and *P. sarmentosum*.

1. Introduction

Piper betle (*P. betle*) and *Piper sarmentosum* (*P. sarmentosum*) are the two members of the *Piper* genus, which have long been consumed popularly in Southeast Asia as herbal medicines and vegetables. The *Piper* species have been reported to be rich in phytochemicals and essential oils, which showed strong antioxidant, antibacterial and antifungal activities [1]. Besides being used as a wrapper for the chewing of areca nut, *P. betle* leaves are also used as an ingredient in stimulant, antiseptic, tonic, and other ayurvedic formulations thanks to its bioactivity components such as hydroxychavicol, allylpyrocatechol, and eugenol [2, 3]. The other *Piper* species, *P. sarmentosum*, has been reported to

possess many potential bioactivities due to its bioactive compounds such as Vitamin E, carotenoids, xanthophylls, tannins, flavanoid, and phenolics [4–6]. The aerial parts of P. sarmentosum are consumed as a vegetable, and the whole plant are applied as a folk cure for headaches, asthma, joint aches, and toothache and to reduce fever in influenza patients [7]. In recent, these Piper species have extensively been investigated in a wide range of studies to provide scientific evidence for folklore claims or to find new therapeutic applications and thereafter to utilize in commercial products.

Silver nanoparticles (AgNPs) have attracted great attention worldwide over the last few decades due to their outstanding antimicrobial activities [8–11]. Owning to their nanoscale size and high specific surface area, AgNPs have the ability to penetrate bacterial cell walls and change the structure of cell membranes, leading to cell growth inhibition or even cell death [12]. Moreover, compared to other synthesis methods of AgNPs, biosynthesis using various sources such as microorganisms and plant extracts has been regarded as the green method and has been becoming the inevitable trend [13–17]. The reducing agents in these green sources would transfer their electrons to reduce silver (I) ions into AgNPs without using toxic solvents and generating harmful byproducts. Additionally, these biological molecules would cover the formed AgNPs and act as capping agents to prevent the agglomeration, reduce the toxicity, and improve the antimicrobial activity of the AgNPs [18]. Therefore, *P. betle* and *P. sarmentosum* with abundant of reducing agents are expected to be effective green sources to synthesize AgNPs.

Recently, a number of research were reported about AgNPs biosynthesis using extracts of *Piper* species. In 2014, AgNPs were synthesized by *P. betle* extract and tested their antibacterial activities on *Bacillus cereus*, *Escherchia coli*, *Klebsiella pneumonia*, and *Staphylococcus aureus*. The synthesized AgNPs performed more effectiveantibacterial activities to the pathogens [19]. In 2019, AgNPs synthesized by the aqueous extract of *P. betle* were evaluated for their effect on the postharvest physiology of cut flower [20]. In 2020, the process parameters for the synthesis of AgNPs from *P. betle* leaf aqueous extract were optimized, and the resulted AgNPs were assessed for antiphytofungal activity [21]. Even though *P. betle* has been well studied and applied in several commercial products with antibacterial and antifungal effects, *P. sarmentosum* has been still little-known in this field. Moreover, there have been several researches compared the vegetative anatomy, phenolic contents, and bioactivities between P. betle and P. sarmentosum [22, 23], but their capacities in AgNP synthesis have been not compared yet.

This study was aimed to compare the silver nanoparticle synthesis ability and antibacterial activity between *P. betle* and *P. sarmentosum* extracts. *P. betle* and *P. sarmentosum* were extracted by DIW. The appropriate extract conditions for their highest total reducing capacity were determined by DPPH scavenging and Folin-Ciocalteu assays. The solutions of silver nanoparticles prepared by the extracts of *P. betle* and *P. sarmentosum* were characterized by Dynamic light scattering (DLS), Zeta potential, UV-vis, and Fourier-transform infrared (FTIR) measurements. Finally, the antibacterial activity of the synthesized silver nanoparticle solutions was tested on *Escherichia coli* (*E. coli*) using the agar diffusion well–variant method. This study would contribute useful and important information to the development of antibacterial products based on green synthesized silver nanoparticles fabricated by the extracts of the two popular *Piper* species in Southeast Asia, *P.betel* and *P. sarmentosum*.

2. Materials and Methods

2.1. Materials. Silver nitrate ($AgNO_3$) was obtained from Guanhao High-Tech Co., Ltd. (China). Deionized water (DIW) was obtained from Milli-Q HX 7150 systems (Merck Millipore, France). pH-indicator paper was purchased from Merck (Germany). 2,2-diphenyl-1-picrylhydrazyl (DPPH), ascorbic acid, and gallic acid were purchased from Sigma (Netherland). Luria Broth (LB) broth powder and agar powder were purchased from Lab M (UK).

P. betle and *P. sarmentosum* leaves were collected in a fresh state in Ho Chi Minh City area. After being removed the diseased, damaged, or contaminated ones, the leaves were mildly dried and ground into 2-5 mm pieces using an herbal grinder. The samples were kept in plastic zip bags and stored in fridge for further experiments.

2.2. Preparation of P. betle Extract and P. sarmentosum Extract. The dried grinding sample of each species was extracted with DIW at the ratio 1 : 15 (w/v) in an Erlenmeyer flask with magnetic stirring and heating. The extract times were 1, 2, 3, 4, and 5 h, and the extract temperatures were 30, 40, 50, 60, and 70°C. Aqueous extracts of *P. betle* (Pb.ext) and *P. sarmentosum* (Ps.ext) were obtained by centrifuging the extracted mixtures at 10,000 rpm in 10 min and consequently collecting the supernatants. These extracts were kept in the fridge for further experiments within 7 days.

2.3. Determination Total Reducing Capacity of the Extracts. It was reported that extracts with higher total reducing capacity are more potential in the green synthesis of AgNPs. The total reducing capacity of plants can be estimated by electron or hydrogen-atom transfer-based assays. DPPH and Folin-Ciocalteu assays are the two-electron transfer-based assays, in which the reducing agents present in the sample transfer electrons to oxidants such as DPPH radical or to the metal ion present in the Folin-Ciocalteu reagent. DPPH and Folin-Ciocalteu assays were used to estimate the total reducing capacity of the extracts [24–26].

DPPH assay: 100 μL of the extract (Pb.ext or Ps.ext) at concentrations of 10, 20, 30, 40, and 50% (of the initial extracts) was placed into each well of 96-well plate. Methanolic solution of DPPH (0.15 mM) was added 100 μL into every well. After being shaken vigorously, the plate was allowed for reactions in dark condition at room temperature in 30min. The control was prepared as above without the extract, and DIW was used for the baseline correction. The optical density (OD) of the samples was measured at 517 nm using a microplate reader. Ascorbic acid was used as a positive control [27]. The results were expressed as inhibition percentage of the

DPPH radical in comparison to the control (taken as 100%), using the following equation:

$$\%\text{inhibition} = \left(1 - \frac{\text{OD}_{\text{Sample}}}{\text{OD}_{\text{Control}}}\right) \times 100\%. \quad (1)$$

The concentration of Pb.ext and Ps.ext that scavenged 50% of the DPPH radicals (IC50) was calculated from the DPPH absorbance plot at 517 nm versus the extract concentration.

Folin-Ciocalteu (F-C) assay: 1.0 mL of the extract (Pb.ext or Ps.ext) at concentrations of 10, 20, 30, 40, and 50% was mixed with 2.5 mL of 10% Folin-Ciocalteu reagent. After 5 min, 2.5 mL of saturated sodium bicarbonate solution was added to the reacted solution. The mixture was kept in dark condition for 30 min at room temperature, and the absorbance was reordered at 765 nm. Gallic acid was used as the standard in the concentration range of 0-50 mg/L. The results were determined from the standard curve and were expressed as gallic acid equivalent (mg GAE/mL of extract) [28].

2.4. Preparation of Silver Nanoparticles. Silver nanoparticles were green synthesized using the chosen Pb.ext and Ps.ext. The determined volumes of Pb.ext or Ps.ext were prepared in different Erlenmeyer flasks. Specific amount of silver nitrate solution (1 mM) was dropped slowly into the corresponding flasks using opened syringes to form the silver nanoparticles. The silver nanoparticles synthesized by Pb.ext and Ps.ext were named as Pb.AgNPs and Ps.AgNPs, respectively. The investigated ratios of silver nitrate solution and the leaf extract were 1 : 2, 1 : 4, 1 : 6; 1 : 8, and 1 : 10 (v/v). The reactions were performed under dark condition with magnetic stirring at room temperature in 8 h. After that, the silver nanoparticles were washed and collected by repetitively centrifuging the reacted mixtures with DIW at 10000 rpm in 10 min for each time.

2.5. Characterization of the Synthesized Silver Nanoparticles. The size, size distribution (polydispersity index, PDI), and zeta potential of the synthesized silver nanoparticles were characterized using a Zetasizer Nano SZ (SZ-100, Horiba, Kyoto, Japan) based on the dynamic light scattering (DLS). The measurement was conducted at the detection angle of 90° and the temperature of 25°C [29].

To illustrate the formation of the synthesized AgNPs, silver nanoparticle solutions with different reaction ratios and the corresponding extract were, respectively, loaded into the quartz curvets to collect their UV-vis spectrum. The measurement was performed by the Shimadzu UV-1800 machine (Shimadzu, Columbia, MD, USA) with a resolution at 1 nm and a wavelength range of 300–800 nm. DIW was used to adjust the baseline [30].

Fourier-transform infrared spectroscopy (FT-IR) was carried out by Bruker Equinox 55 FTIR spectrometer (Bruker, Ettlingen, Germany), and the KBr pellet method was used to explore the functional groups surrounding the synthesized AgNPs. Briefly, KBr was blended with each of the extracts at the ratio of 100 : 1 (w/w). The mixtures were then pelleted and recorded FT-IR spectroscopy at the wavenumber range of 500-4000 cm^{-1} [9].

The hydrodynamic size and surface charge of the synthesized silver nanoparticles were measured by dynamic light scattering (DLS) using a Zetasizer Nano SZ (SZ-100, Horiba). The measurement was determined through a Helium-neon (He-Ne) laser beam with the detection angle, and the temperatures were 90° and 25°C, respectively. Samples were dispersed in DIW prior to measurement [31].

2.6. Antibacterial Assay. Antibacterial activity was assessed against *Escherichia coli*—ATCC 25922 using the agar diffusion well–variant method. *E. coli* cultures were grown to mid-exponential phase at 37°C before being harvested and resuspended in PBS with the ratio of 100 mg wet weight cells per 1 mL PBS. Then, 1 mL of cell suspension was mixed with 10 mL of LB broth agar (containing 1.5% agar) and overlaid on the surface of solid LB agar (containing 1.5% agar) petri dishes. Four holes (8 mm in diameter, 20-30 mm apart from one to another) were then punched on the agar and 20 μL of the nanosilver suspension at the dilution of 1, 5, and 10% was dropped into the holes. DIW and each extract, which were added the same volume into every punched well, were used as blank and control, respectively. Next, the dishes were kept at about 10°C in 4–8 h for the suspension to diffuse into the agar medium. Finally, the dishes were incubated at 37°C in 24 h [32, 33]. The zones of growth inhibition were detected following the equation below:

$$\text{Growth inhibition zone(mm)} = \text{D} - \text{d}, \quad (2)$$

where D is the radius of sterile ring (mm) and d is the radius of the punched wells (mm).

2.7. Statistical Analysis. All the experiments were replicated 3 times, and the obtained results were represented as mean ± standard deviation. All experimental data were analysed by Student's t-test. $P < 0.05$ implied that two compared results were statistically significant. $P > 0.05$ indicated nonstatistical (NS) difference [30].

3. Results and Discussion

3.1. Appropriate Extraction Temperature. The collected Pb.ext and Ps.ext were determined their total polyphenol content and DPPH scavenging activity to choose the appropriate extract temperature. The extracts owning higher total polyphenol content and stronger DPPH activity would be regarded as having better total reducing capacity [24].

In general, the total polyphenol contents of Pb.ext were higher than that of Ps.ext in the same extract condition (Figure 1). The polyphenol contents in the extracts increased when the extract temperature increased. The phenolic amount of Ps.ext reached the highest values (~125 mg GAE/mL extract) when *P. betle* was extracted at 50 and 60°C. Meanwhile, that of Ps.ext was highest at the extract temperature of 60 and 70°C (~90 mg GAE/mL of extract). At other higher temperatures, the total polyphenol contents slightly decreased due to the degradation of phytochemicals

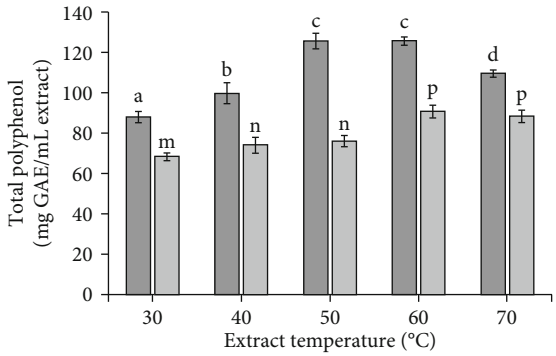

Figure 1: Total polyphenol content (mg GAE/mL) of Pb.ext (solid) and Ps.ext (pattern) extracted in 3 h at different temperatures. Bars show means ± SD. Bars with the same letters are not statistically different based on the least significant difference at $P < 0.05$.

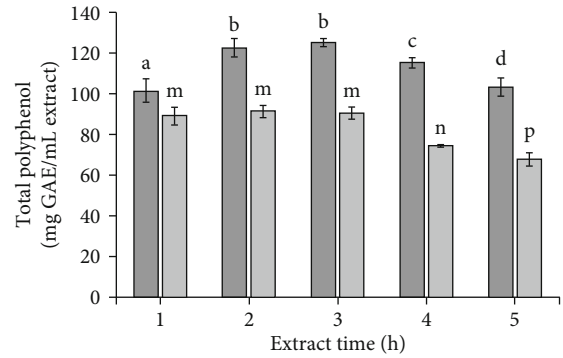

Figure 2: Total polyphenol content (mg GAE/mL) of Pb.ext (solid) and Ps.ext (pattern) extracted at 50°C and 60°C, respectively, in different time. Bars show means ± SD. Bars with the same letters are not statistically different based on the least significant difference at $P < 0.05$.

Table 1: IC50 values for DPPH scavenging activity of Pb.ext and Ps.ext extracted in 3 h at different temperatures.

	IC50 for DPPH scavenging activity (%)*				
Extract temp.	30°C	40°C	50°C	60°C	70°C
Pb.ext	2.30	2.08	1.45	1.46	1.83
Ps.ext	2.85	2.53	2.49	2.00	2.10

*IC50 value was calculated as the percentage concentration of the initial extract.

Table 2: IC50 values for DPPH scavenging activity of Pb.ext and Ps.ext extracted at 50°C and 60°C, respectively, at different times.

	IC50 for DPPH scavenging activity (%)*				
Extract time	1 h	2 h	3 h	4 h	5 h
Pb.ext	2.01	1.47	1.45	1.83	1.83
Ps.ext	2.49	2.48	2.49	2.70	2.82

*IC50 value was calculated as the percentage concentration of the initial extract.

exposed in water at high temperature. The phenolic compounds in aqueous extract of P. betle leaves were identified including a phenylpropanoid, five cinnamoyl and six flavonoid derivatives by F. Ferreres et al. [34]. In another study, Ab Rahman and her coworkers determined the phenolic compounds in Journal of Nanomaterials 3 aqueous extract of P. sarmentosum leaves were quercetin, naringin, tannic acid, and gallic acid [35]. These phenolic compounds were reported to own the redox properties which allowed them to act as reducing agents, hydrogen donors, singlet oxygen quenchers, or metal chelators. Therefore, Pb.ext and Ps.ext with high polyphenol contents were expected to perform good antioxidation and reduction.

The antioxidant capacity of Pb.ext and Ps.ext was tested by DPPH free-radical scavenging assay and the results were presented in Table 1. The Pb.ext at 50°C and Ps.ext at 60°C performed the strongest DPPH scavenging activity with IC50 values of 1.45% and 2.00% (percentage concentration of the initial extract), respectively. The results suggested that P. betle has stronger antioxidant activity than P. sarmentosum. This was consistent with the published literature about the phytochemistry and pharmacology of the two *Piper* species [36, 37]. The IC50 value of ascorbic acid as the positive control was 5.21 μg/mL, which was relevant with the previous study [38, 39]. These results suggested that *P. betle* should be extracted at 50°C and *P. sarmentosum* should be extracted at 60°C to get a better total reducing capacity.

3.2. Appropriate Extraction Time. To determine the appropriate extract time, *P. betle* and *P. sarmentosum* were extracted at the chosen temperatures for each sample at different times from 1 to 5 h. Subsequently, the total polyphenol content and DPPH scavenging activity of the obtained extracts were determined.

The phenolic contents of the Pb.ext and Ps.ext, which were showed in Figure 2. It was confirmed that *P. betle* contained a higher amount of phenolic compounds than *P. sarmentosum*. The polyphenol contents in the Pb.ext gradually increased and reached the highest value (~125 mg GAE/mL extract) when the extraction time increased from 1 to 3 h and, and then slightly decreased in the longer extraction time. For the Ps.ext, the total polyphenol reached the highest values and remained stable when the samples were extracted from 1 to 3 h (~90 mg GAE/mL extract). However, there was no statistically difference between 2 and 3 h extract samples of Pb.ext and among 1, 2, and 3 h extract samples of Ps.ext.

Additionally, the results of DPPH free-radical scavenging activity (Table 2) were consistent with the total polyphenol contents in the extracts. The Pb.ext in 2 and 3 h showed their best DPPH scavenging activity with IC50 of about 1.4%; meanwhile, Ps.ext in 1, 2, and 3 h got their lowest IC50 of about 2.4% (concentration of the initial extract). Consequently, the appropriate extract time was chosen as 2 h for *P. betle* and 1 h for *P. sarmentosum*. The correlation between polyphenol contents and DPPH scavenging activities of Pb.ext and Ps.ext suggested that the phenolic compounds of both extracts were responsible for their antioxidant activities [23]. These results also revealed that P. betle has stronger antioxidant activity as well as reducing power than P. sarmentosum. This was in line with the published literature about the two Piper species' phytochemistry and pharmacology [36, 37].

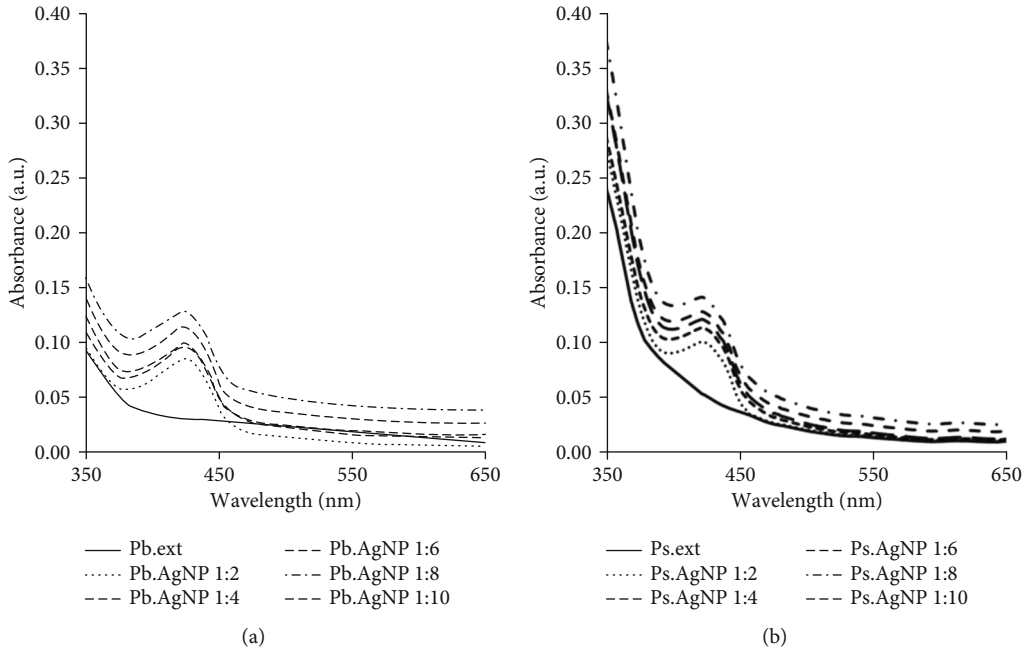

Figure 3: The UV-vis spectra of (a) Pb.ext and Pb.AgNP at different reacting ratio, and (b) Ps.ext and Ps.AgNP (b) at different reacting ratio.

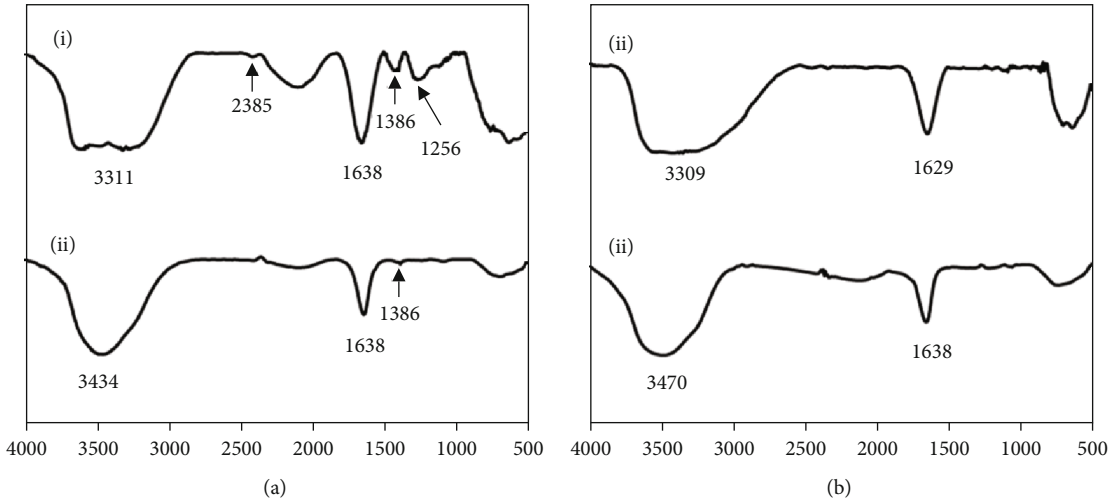

Figure 4: The FTIR spectra of (a) Pb.ext (i) and Pb.AgNP (ii) and (b) Ps.ext (i) and Ps.AgNP (ii).

Table 3: Hydrodynamic size and Zeta potential of Pb.AgNP and Ps.AgNP.

Silver nanoparticles	Pb.AgNP	Ps.AgNP
Z-average (nm)	16.28 ± 3.84	14.51 ± 2.90
Zeta potential (mV)	−23.06 ± 1.52	−19.83 ± 2.57

3.3. Characterization of the Synthesized Silver Nanoparticles. *P. betle* and *P. sarmentosum* were extracted by DIW in the chosen conditions of 50°C in 2 h, and 60°C in 1 h, respectively. Then, the obtain of each extract was used for green synthesis of silver nanoparticles with the silver nitrate solution and the leaf extract ratios of 1 : 2, 1 : 4, 1 : 6; 1 : 8, and 1 : 10 (*v*/*v*). After 8 h reacting in dark condition with magnetic stirring at room temperature, the result silver

Table 4: Growth inhibition diameter of Pb.AgNP and Ps.AgNP against *E. coli* obtained by the agar diffusion well–variant method.

Tested disk	Tested object	Growth inhibition diameter (mm)	
		Pb.AgNP	Ps.AgNP
Blank	DIW	—	—
Control	Extract	—	6.16 ± 0.27
Sample	AgNP 1%	2.85 ± 0.91	7.55 ± 0.12
	AgNP 5%	5.19 ± 0.45	12.82 ± 0.18
	AgNP 10%	8.93 ± 0.28	15.64 ± 0.14

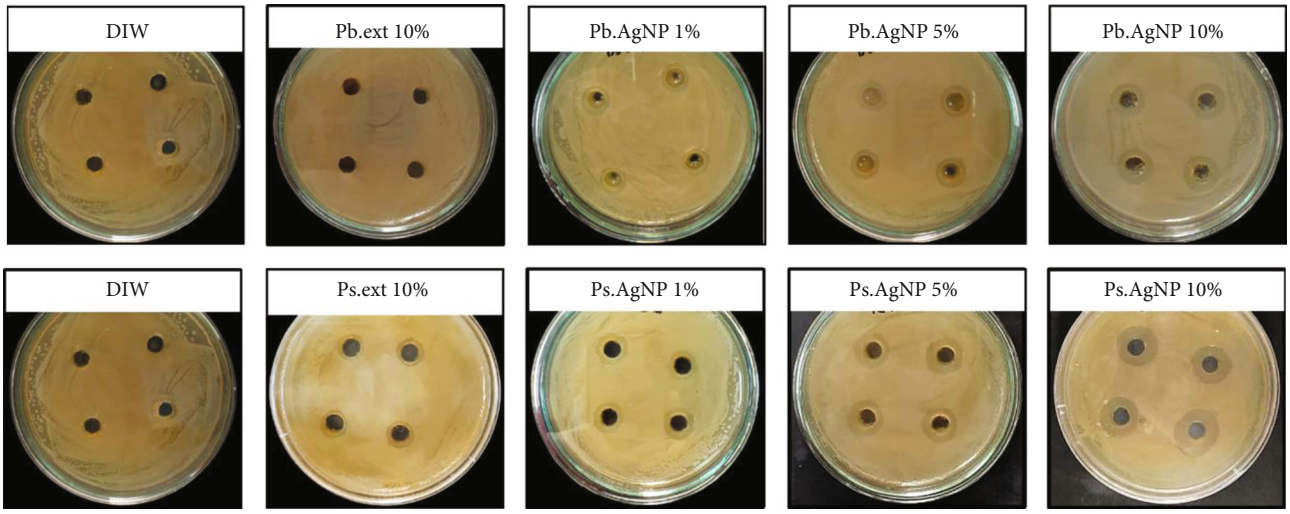

Figure 5: Antibacterial activity on *E. coli* of Pb.AgNP and Ps.AgNP at different concentrations.

nanoparticle solutions (named as Pb.AgNP 1 : x and Ps.AgNP 1 : x; where x were 2, 4, 6, 8, and 10) were separately loaded into the quartz curvets to collect their UV-vis spectrum at the wavelength range of 350-650 nm (Figure 3).

Figure 3(a) presented the UV-vis spectrum of Pb.ext and Pb.AgNP at different reacting ratios; meanwhile, Figure 3(b) presented those of Ps.ext and Ps.AgNP. The UV-vis spectra of both extracts of Pb.ext and Ps.ext showed no peak in the wavelength range of 350–650 nm. However, the UV-vis spectra of reacted mixtures of both Pb.AgNP and Ps.AgNP showed the peaks in the wavelength of 400–450 nm. This demonstrated that silver nanoparticles with a surface plasmon resonance occurred in the reacted mixtures and silver nanoparticles were synthesized [40–42]. The pointed shape of these peaks helped predict that the particle size distribution of AgNPs synthesized by Pb.ext as well as Ps.ext was relatively narrow. There was a similarity in the correlation of the reacting ratio and the absorbance between Pb.AgNP and Ps.AgNP. When the reacting ratio of silver nitrate and the extract increased, the absorbance increased and peaked at the ratio of 1 : 8, then decreased slightly at 1 : 10. These results suggested that the green synthesis process of silver nanoparticles by Pb.ext and Ps.ext got the best efficacy at the reacting ratio of 1 : 8. Therefore, both Pb.AgNP and Ps.AgNP with a ratio of 1 : 8 were used for further experiments.

The phytochemicals not only play the role of reducing silver (I) ions into AgNPs but also chelate with AgNPs which helps stabilize the biosynthesized AgNPs. Therefore, FTIR spectroscopy was performed to identify the possible biomolecules responsible for the reduction of silver (I) ions and the functional groups surrounding the synthesized silver nanoparticle. Figure 4 presented the FTIR spectra of Pb.ext versus Pb.AgNP 1 : 8 (Figure 4(a)) and the FTIR spectra of Ps.ext versus Ps.AgNP 1 : 8 (Figure 4(b)). In general, both spectra showed strong and broad peaks at the wavenumber region of 3470-3309 cm^{-1} which was attributed to O-H stretching (arising from alcohols and phenolic compounds) [43, 44]. However, the OH peaks were more broadening in the FTIR spectra of the two extracts than those of the corresponding silver nanoparticle solutions. This was due to the stronger hydrogen bonding of the phytochemical in the extracts as well as demonstrated that silver nanoparticles were capped by phytoconstituents [45, 46]. The peak at 2385 cm^{-1} was due to the O=C=O stretching vibrations indicated as CO_2. Moreover, peaks appeared at the wavenumber region of 1629-1638 cm^{-1}, which attributed to the C=C groups from alkenes [44, 47, 48], and reduced their intensity after silver reduction (Figure 4(a) and Figure 4(b)). This phenomenon revealed that the bioactive compounds in the two extracts including antioxidants, phenols, and flavonoids with abundant aromatic C=C groups took part in the reduction of silver (I) ions into AgNPs [37]. In Figure 4(a), peaks appeared at the wavenumber region of 1380-1385 cm^{-1} attributed to C-H bending vibrations of C-H (alkanes); meanwhile, the absorption band at 1256 cm^{-1} indicated the presence of C–N stretching vibrations in Pb.ext. In Figure 4(b), some peaks in Pb.ext's IR spectra were absent in Pb.ext's IR spectra. This is probably due to the abundance of bioactive compounds in *P. betle* leaf versus *P. sarmentosum* leaves, which also explains why extracted leaves of *P. betle* are more commonly used in commercial products than *P. sarmentosum* [36, 37].

The synthesized silver nanoparticles in Pb.AgNP and Ps.AgNP solutions were washed and collected by repetitively centrifuging the reacted mixtures with DIW at 10000 rpm in 10 min for each time. Subsequently, these AgNPs were dispersed in DIW for DLS and Zeta potential measurements (Table 3). The DLS measurement showed that the hydrodynamic size of Pb.AgNP and Ps.AgNP was 16.28 ± 3.84 and 14.51 ± 2.90 nm, respectively. The silver nanoparticles synthesized by Pb.ext were larger than those synthesized by Ps.ext. This was due to the higher total reducing capacity of *P. betle* compared to *P. sarmentosum* which was proved in the previous experiments. On the other hand, the negative zeta potential values of both Pb.AgNP and Ps.AgNP in the range of -30 to 0 mV suggested that the obtained silver nanoparticles were stable and did not agglomerate. These results were agreed with other green synthesized AgNPs fabricated by phytochemicals [49].

3.4. Antibacterial Activity of the Synthesized Silver Nanoparticles. In the antibacterial activity test, the blank disks were treated by DIW, and the control disks were treated by Pb.ext and Ps.ext (added DIW into the initial extracts with the ratio 1 : 8 (*v*/*v*) and then diluted 10 times). The sample disks were treated by the green synthesized nanosilver solutions, Pb.AgNP 1 : 8 and Ps.AgNP 1 : 8, at the concentrations of 1, 5, and 10%. The tested objects were tested for antibacterial ability against *E. coli* by the agar diffusion well–variant method and the results were showed in Table 4 and Figure 5.

Firstly, there was no growth inhibition area on the DIW disks, confirming that no antibacterial activity was made by DIW and the experiment was conducted under aseptic condition. Secondly, the antibacterial activity of Pb.AgNP and Ps.AgNP was concentration-dependent manner. Thirdly, at the same treated concentration of 10%, the growth inhibition areas caused by the extracts was obviously smaller than those caused by the respective nanosilver solutions. These results suggested that the green synthesized silver nanoparticles by the extracts enhanced the antibacterial activity of the initial extracts. Interestingly, no growth inhibition activity of 10% Pb.ext was observed, which demonstrated that the aqueous extract of *P. betle* at the tested concentration performed no inhibition activity on *E. coli*. This finding was consistent with the previous publication [50]. From the results of antibacterial test, it could be concluded that the antibacterial activity of Pb.AgNP on *E. coli* was totally caused by the synthesized silver nanoparticles.

Taken together, even though Pb.ext performed stronger reducing power than Ps.ext, Ps.AgNP showed markedly better antibacterial activity against *E. coli*, a common bacterium, than Pb.AgNP. This finding would be a great reference for manufacturers of antibacterial products to expand their raw materials as well as to enrich their product categories. The research also offers good recommendations for combining the two extracts to achieve antibacterial products with wide-effect on bacteria.

4. Conclusions

The appropriate aqueous extract conditions of the two *Piper* species—*P. betle* and *P. sarmentosum*, were determined for their highest total reducing capacity as 50°C in 2 h and 60°C in 1 h, respectively. Pb.ext showed better total reducing capacity with higher total polyphenol content (~125 mg GAE/mL extract) and stronger DPPH activity (IC50 was 1.45%). The ratio of 1 mM silver nitrate solution and the extracts for better nanosilver synthesis was determined as 1 : 8 (*v*/*v*). At the same dilution, both Pb.AgNP and Ps.AgNP performed significantly stronger antibacterial activity against *E. coli* compared to their initial extracts. The growth inhibition diameter caused by 10% Ps.AgNP (15.64 ± 0.14 mm) was nearly 2 times higher than that caused by 10% Pb.AgNP (8.93 ± 0.28 mm). This study would contribute useful and important information to the development of antibacterial products based on green synthesized silver nanoparticles fabricated by the extracts of the two popular plants in Southeast Asia, *P.betel* and *P. sarmentosum*. It also offered good recommendations to combine the extracts of *P. betle* and *P. sarmentosum* for wide-effect antibacterial products.

Data Availability

The experimental data used to support the findings of this study are included within the article.

Conflicts of Interest

The authors declare that there is no conflict of interest regarding the publication of this paper.

Acknowledgments

This research is funded by the Vietnam Academy of Science and Technology (VAST) under grant number NVCC19.04/21-21.

References

[1] B. Salehi, Z. A. Zakaria, R. Gyawali et al., "Piper species: a comprehensive review on their phytochemistry, biological activities and applications," *Molecules*, vol. 24, no. 7, p. 1364, 2019.

[2] S. Das, R. Parida, I. Sriram Sandeep, S. Nayak, and S. Mohanty, "Biotechnological intervention in betelvine (*Piper betle* L.): A review on recent advances and future prospects," *Asian Pacific Journal of Tropical Medicine*, vol. 9, no. 10, pp. 938–946, 2016.

[3] F. Fazal, P. P. Mane, M. P. Rai et al., "The phytochemistry, traditional uses and pharmacology of Piper betel. Linn (betel leaf): a pan-asiatic medicinal plant," *Chinese Journal of Integrative Medicine*, pp. 1–11, 2014.

[4] M. Mohd Zainudin, Z. Zakaria, and N. A. Megat Mohd Nordin, "The use of Piper sarmentosum leaves aqueous extract (Kadukmy™) as antihypertensive agent in spontaneous hypertensive rats," *BMC Complementary and Alternative Medicine*, vol. 15, no. 1, p. 54, 2015.

[5] S. Rahman, K. Sijam, and D. Omar, "Piper sarmentosum Roxb.: a mini review of ethnobotany, phytochemistry and pharmacology," *Journal of Analytical & Pharmaceutical Research*, vol. 2, no. 5, p. 00031, 2016.

[6] F. Hashim Fauzy, M. Mohd Zainudin, H. R. Ismawi, and T. F. T. Elshami, "Piper sarmentosum leaves aqueous extract attenuates vascular endothelial dysfunction in spontaneously hypertensive rats," *Evidence-based Complementary and Alternative Medicine*, vol. 2019, Article ID 7198592, 8 pages, 2019.

[7] K. Hussain, F. K. Hashmi, A. Latif, Z. Ismail, and A. Sadikun, "A review of the literature and latest advances in research of *Piper sarmentosum*," *Pharmaceutical Biology*, vol. 50, no. 8, pp. 1045–1052, 2012.

[8] S. Medici, M. Peana, V. M. Nurchi, and M. A. Zoroddu, "Medical uses of silver: history, myths, and scientific evidence," *Journal of Medicinal Chemistry*, vol. 62, no. 13, pp. 5923–5943, 2019.

[9] T. D. Nguyen, T. T. Nguyen, K. L. Ly et al., "In vivo study of the antibacterial chitosan/polyvinyl alcohol loaded with silver nanoparticle hydrogel for wound healing applications," *International Journal of Polymer Science*, vol. 2019, Article ID 7382717, 10 pages, 2019.

[10] N. T. Hiep, H. C. Khon, V. V. T. Niem et al., "Microwave-assisted synthesis of chitosan/polyvinyl alcohol silver

nanoparticles gel for wound dressing applications," *International Journal of Polymer Science*, vol. 2016, Article ID 1584046, 11 pages, 2016.

[11] N. Tra Thanh, M. Ho Hieu, N. Tran Minh Phuong et al., "Optimization and characterization of electrospun polycaprolactone coated with gelatin-silver nanoparticles for wound healing application," *Materials Science and Engineering: C*, vol. 91, pp. 318–329, 2018.

[12] I. X. Yin, J. Zhang, I. S. Zhao, M. L. Mei, Q. Li, and C. H. Chu, "The antibacterial mechanism of silver nanoparticles and its application in dentistry," *International Journal of Nanomedicine*, vol. Volume 15, pp. 2555–2562, 2020.

[13] G. Pal, P. Rai, and A. Pandey, "Green synthesis of nanoparticles: A greener approach for a cleaner future," in *Green synthesis, characterization and applications of nanoparticles*, pp. 1–26, Elsevier, 2019.

[14] W. Zhang and W. Jiang, "Antioxidant and antibacterial chitosan film with tea polyphenols-mediated green synthesis silver nanoparticle via a novel one-pot method," *International Journal of Biological Macromolecules*, vol. 155, pp. 1252–1261, 2020.

[15] S. Ahmed, Saifullah, M. Ahmad, B. L. Swami, and S. Ikram, "Green synthesis of silver nanoparticles usingAzadirachta indicaaqueous leaf extract," *Journal of Radiation Research and Applied Sciences*, vol. 9, no. 1, pp. 1–7, 2016.

[16] M. Iftikhar, M. Zahoor, S. Naz et al., "Green synthesis of silver nanoparticles using Grewia optiva leaf aqueous extract and isolated compounds as reducing agent and their biological activities," *Journal of Nanomaterials*, vol. 2020, Article ID 8949674, 10 pages, 2020.

[17] F. A. Khan, M. Zahoor, A. Jalal, and A. U. Rahman, "Green synthesis of silver nanoparticles by using Ziziphus nummularia leaves aqueous extract and their biological activities," *Journal of Nanomaterials*, vol. 2016, Article ID 8026843, 8 pages, 2016.

[18] A. Roy, O. Bulut, S. Some, A. K. Mandal, and M. D. Yilmaz, "Green synthesis of silver nanoparticles: biomolecule-nanoparticle organizations targeting antimicrobial activity," *RSC Advances*, vol. 9, no. 5, pp. 2673–2702, 2019.

[19] P. S. Praba, J. Jeyasundari, and Y. B. A. Jacob, "Synthesis of silver nano particles using Piper betle and its antibacterial activity," *European Chemical Bulletin*, vol. 3, no. 10, pp. 1014–1016, 2014.

[20] T. R. Maity, A. Samanta, B. Saha, and S. Datta, "Evaluation of Piper betle mediated silver nanoparticle in post-harvest physiology in relation to vase life of cut spike of gladiolus," *Bulletin of the National Research Centre*, vol. 43, no. 1, pp. 1–11, 2019.

[21] S. Khan, S. Singh, S. Gaikwad, N. Nawani, M. Junnarkar, and S. V. Pawar, "Optimization of process parameters for the synthesis of silver nanoparticles from Piper betle leaf aqueous extract, and evaluation of their antiphytofungal activity," *Environmental Science and Pollution Research*, vol. 27, no. 22, pp. 27221–27233, 2020.

[22] V. Raman, A. M. Galal, and I. A. Khan, "An investigation of the vegetative anatomy of *Piper sarmentosum*, and a comparison with the anatomy of *Piper betle* (Piperaceae)," *American Journal of Plant Sciences*, vol. 3, no. 8, article 22192, pp. 1135–1144, 2012.

[23] M. Tagrida and S. Benjakul, "Ethanolic extract of Betel (*Piper betle* L.) and Chaphlu (*Piper sarmentosum* Roxb.) dechlorophyllized using sedimentation process: Production, characteristics, and antioxidant activities," *Journal of Food Biochemistry*, vol. 44, no. 12, article e13508, 2020.

[24] V. Goodarzi, H. Zamani, L. Bajuli, and A. Moradshahi, "Evaluation of antioxidant potential and reduction capacity of some plant extracts in silver nanoparticles' synthesis," *Molecular Biology Research Communications*, vol. 3, no. 3, pp. 165–174, 2014.

[25] D. C. Christodouleas, C. Fotakis, K. Papadopoulos, and A. C. Calokerinos, "Evaluation of total reducing power of edible oils," *Talanta*, vol. 130, pp. 233–240, 2014.

[26] L. M. Magalhães, M. A. Segundo, S. Reis, J. L. F. C. Lima, and A. O. S. S. Rangel, "Automatic method for the determination of Folin– Ciocalteu reducing capacity in food products," *Journal of Agricultural and Food Chemistry*, vol. 54, no. 15, pp. 5241–5246, 2006.

[27] N. T. N. Hoi, "Evaluation of antioxidant and anti-aging efficacies of coffea robusta extract on human fibroblast," *Vietnam Journal of Science and Technology*, vol. 55, no. 5A, p. 34, 2017.

[28] R. Yadav and M. Agarwala, "Phytochemical analysis of some medicinal plants," *Journal of Phytology*, vol. 3, no. 12, 2011.

[29] N. T. T. le, D. T. D. Nguyen, N. H. Nguyen, C. K. Nguyen, and D. H. Nguyen, "Methoxy polyethylene glycol–cholesterol modified soy lecithin liposomes for poorlywater-solubleanticancer drug delivery," *Journal of Applied Polymer Science*, vol. 138, no. 7, p. 49858, 2021.

[30] D. H. Nguyen, J. Lee, K. Park et al., "Green silver nanoparticles formed by Phyllanthus urinaria, Pouzolzia zeylanica, and Scoparia dulcis leaf extracts and the antifungal activity," *Nanomaterials*, vol. 10, no. 3, p. 542, 2020.

[31] M. T. Vu, N. T. T. le, T. L. B. Pham, N. H. Nguyen, and D. H. Nguyen, "Development and characterization of soy lecithin liposome as potential drug carrier Systems for Codelivery of Letrozole and paclitaxel," *Journal of Nanomaterials*, vol. 2020, Article ID 8896455, 9 pages, 2020.

[32] W. Z. Sun, Y. L. Tan, M. Jia, X. M. Hu, X. C. Rao, and F. Q. Hu, "Functional characterization of the endolysin gene encoded by Pseudomonas aeruginosa bacteriophage PaP1," *African Journal of Microbiology Research*, vol. 4, no. 10, pp. 933–939, 2010.

[33] M. Balouiri, M. Sadiki, and S. K. Ibnsouda, "Methods for *in vitro* evaluating antimicrobial activity: A review," *Journal of Pharmaceutical Analysis*, vol. 6, no. 2, pp. 71–79, 2016.

[34] F. Ferreres, A. P. Oliveira, A. Gil-Izquierdo, P. Valentão, and P. B. Andrade, "*Piper betle* Leaves: Profiling Phenolic Compounds by HPLC/DAD-ESI/MS^n and Anti-cholinesterase Activity," *Phytochemical analysis*, vol. 25, no. 5, pp. 453–460, 2014.

[35] S. F. S. Ab Rahman, D. Omar, and M. Z. A. W. K. Sijam, "Identification of phenolic compounds and evaluation of antibacterial properties of *Piper sarmentosum* Roxb. against rice pathogenic bacteria," *Malaysian Journal of Microbiology*, vol. 12, no. 6, pp. 475–484, 2016.

[36] E. W. C. Chan and S. K. Wong, "Phytochemistry and pharmacology of three Piper species: an update," *International Journal of Pharmacognosy*, vol. 1, no. 9, pp. 534–544, 2014.

[37] E. E. Mgbeahuruike, T. Yrjönen, H. Vuorela, and Y. Holm, "Bioactive compounds from medicinal plants: Focus on *Piper* species," *South African Journal of Botany*, vol. 112, pp. 54–69, 2017.

[38] R. K. Ko, G. O. Kim, C. G. Hyun, D. S. Jung, and N. H. Lee, "Compounds with tyrosinase inhibition, elastase inhibition and DPPH radical scavenging activities from the branches of

Distylium racemosum Sieb. Et Zucc," *Phytotherapy Research*, vol. 25, no. 10, pp. 1451–1456, 2011.

[39] M. Asadujjaman, M. A. Hossain, and U. K. Karmakar, "Assessment of DPPH free radical scavenging activity of some medicinal plants," *Pharmacology Online*, vol. 1, pp. 161–165, 2013.

[40] M. Heidary, S. Zaker Bostanabad, S. M. Amini et al., "The antimycobacterial activity of Ag, ZnO, and Ag- ZnO nanoparticles against MDR- And XDR *Mycobacterium tuberculosis*," *Infection and Drug Resistance*, vol. Volume 12, pp. 3425–3435, 2019.

[41] E. B. Santos, N. V. Madalossi, F. A. Sigoli, and I. O. Mazali, "Silver nanoparticles: green synthesis, self-assembled nanostructures and their application as SERS substrates," *New Journal of Chemistry*, vol. 39, no. 4, pp. 2839–2846, 2015.

[42] S. Chen, S. Webster, R. Czerw, J. Xu, and D. L. Carroll, "Morphology effects on the optical properties of silver nanoparticles," *Journal of Nanoscience and Nanotechnology*, vol. 4, no. 3, pp. 254–259, 2004.

[43] J. B. Punuri, P. Sharma, S. Sibyala, R. Tamuli, and U. Bora, "Piper betle-mediated green synthesis of biocompatible gold nanoparticles," *International Nano Letters*, vol. 2, no. 1, pp. 1–9, 2012.

[44] T. P. Singh, G. Chauhan, R. K. Agrawal, and S. K. Mendiratta, "In vitro study on antimicrobial, antioxidant, FT-IR and GC–MS/MS analysis of Piper betle L. leaves extracts," *Journal of Food Measurement and Characterization*, vol. 13, no. 1, pp. 466–475, 2019.

[45] H. Duan, D. Wang, and Y. Li, "Green chemistry for nanoparticle synthesis," *Chemical Society Reviews*, vol. 44, no. 16, pp. 5778–5792, 2015.

[46] M. Ovais, A. T. Khalil, A. Raza et al., "Green synthesis of silver nanoparticles via plant extracts: beginning a new era in cancer theranostics," *Nanomedicine*, vol. 12, no. 23, pp. 3157–3177, 2016.

[47] L. Wulandari, Y. Retnaningtyas, Nuri, and H. Lukman, "Analysis of flavonoid in medicinal plant extract using infrared spectroscopy and chemometrics," *Journal of Analytical Methods in Chemistry*, vol. 2016, Article ID 4696803, 6 pages, 2016.

[48] D. Badmapriya and I. Asharani, "Dye degradation studies catalysed by green synthesized iron oxide nanoparticles," *International Journal of ChemTech Research*, vol. 9, no. 6, pp. 409–416, 2016.

[49] S. M. Amini, "Preparation of antimicrobial metallic nanoparticles with bioactive compounds," *Materials Science and Engineering: C*, vol. 103, p. 109809, 2019.

[50] B. Jayalakshmi, K. A. Raveesha, M. Murali, and K. N. Amruthesh, "Phytochemical, antibacterial and antioxidant studies on leaf extracts of Piper betle L," *International Journal of Pharmacy and Pharmaceutical Sciences*, vol. 7, no. 10, pp. 23–29, 2015.

Hindawi
Journal of Nanomaterials
Volume 2021, Article ID 6676555, 12 pages
https://doi.org/10.1155/2021/6676555

Research Article

Antibacterial Effects of Green-Synthesized Silver Nanoparticles Using *Ferula asafoetida* against *Acinetobacter baumannii* Isolated from the Hospital Environment and Assessment of Their Cytotoxicity on the Human Cell Lines

Seyedeh Narjes Abootalebi,[1,2] **Seyyed Mojtaba Mousavi**,[3] **Seyyed Alireza Hashemi**,[4] **Eslam Shorafa**,[1] **Navid Omidifar**,[1] **and Ahmad Gholami**[5]

[1]*Biotechnology Research Center, Shiraz University of Medical Sciences, Shiraz, Iran*
[2]*Division of Intensive Care Unit, Department of Pediatrics, School of Medicine, Shiraz University of Medical Sciences, Shiraz, Iran*
[3]*Department of Chemical Engineering, National Taiwan University of Science and Technology, Taipei, Taiwan*
[4]*Department of Mechanical Engineering, Center for Nanofibers and Nanotechnology, National University of Singapore, Singapore*
[5]*Pharmaceutical Sciences Research Center, Shiraz University of Medical Sciences, Shiraz, Iran*

Correspondence should be addressed to Ahmad Gholami; gholami@sums.ac.ir

Received 4 December 2020; Revised 11 April 2021; Accepted 16 April 2021; Published 3 May 2021

Academic Editor: Shahid Ali

Acinetobacter baumannii (*A. baumannii*) is a dangerous nosocomial pathogen in intensive care units, causing fatal clinical challenges and mortality. In this study, the green synthesis of silver nanoparticles (AgNPs) using the extract of *Ferula asafetida* and the chemical synthesis of AgNPs were carried out to evaluate their effects on *A. baumannii* bacterial strain and a human adenocarcinoma cell line. The NPs were characterized using several techniques, including field emission-scanning electron microscopy, X-ray diffraction, energy-dispersive X-ray spectrometry, UV-visible spectroscopy, and Fourier-transform infrared spectroscopy. After synthesis, the arrangement of AgNPs was confirmed based on the maximum absorption peak at 450 nm. The results showed that the AgNPs had a hexagonal structure. The antimicrobial activity of biogenic NPs significantly increased and reached a minimum inhibitory concentration of 2 μg/mL. The nanomaterials did not exhibit any toxic effects on the human cell line at certain concentrations and showed improvements compared to chemically synthesized AgNPs. However, at higher concentrations (100 μg/mL), the cytotoxicity increased. Finally, it was concluded that biosynthesized AgNPs had significant antimicrobial effects on *A. baumannii* isolated from intensive care units.

1. Introduction

The ESKAPE pathogens, including *Enterobacter* spp., *Pseudomonas aeruginosa*, *Enterococcus faecium*, *Acinetobacter baumannii*, *Klebsiella pneumoniae*, and *Staphylococcus aureus*, have developed multidrug resistance in clinics. These pathogens are associated with high levels of lethargy and mortality, imposing significant costs on patients and healthcare systems [1]. *Acinetobacter baumannii* is a Gram-negative, nonfastidious, nonfermenting, nonmotile coccobacillus responsible for respiratory infections, pneumonia, and urinary tract infections [2]. This pathogen attacks unhealthy hospitalized patients and severely damages their skin and the respiratory tract [3]. It can also proliferate over different temperatures and pH ranges and use different materials as a carbon source [1].

Ventilator-associated pneumonia caused by *A. baumannii* is responsible for high mortality rates and healthcare costs, particularly in intensive care units (ICUs). There is an urgent need to develop successful pharmaceuticals instead of beta-lactams (carbapenem) against this nosocomial pathogen [4]. Among metallic NPs, silver NPs (AgNPs)

are attractive biotic nanomaterials used for biomedical purposes [5]. These NPs have been applied in different scientific areas, such as environmental science, biomedicine, chemistry, and building industries, due to their unique properties. Besides, they play a remarkable role in nanotechnology and nanoscience, especially in nanomedicine [6]. They exhibit anti-inflammatory, antioxidant, antitumor, and antimicrobial properties, leading to their broad applications in biomedicine [7]. Overall, the biogenic synthesis of NPs is considered a valuable strategy by providing more profitable NPs with higher stability and biocompatibility [8].

There are around 130 *Ferula* species (Apiaceae) worldwide, thirty of which are found in Iran. There are several reports on the antibacterial, antidiabetic, hypotensive, antispasmodic, and antiviral (HIV, H1N1, HRV, and HSV) effects of *Ferula asafoetida* (*F. asafoetida*). One of the specific characteristics of this plant is its pungent odor produced by a nonubiquitous compound, as well as significant pharmacological properties due to the presence of volatile sulfide constituents [9]. Since the antibacterial mechanism of AgNPs appears to involve interactions with the bacterial cell membrane, producing free radicals and resulting in growth inhibition, we hypothesized that the extract of *F. asafoetida* might improve the antibacterial effects of AgNPs. Therefore, it is essential to select a proper reducing agent for biogenic AgNP synthesis.

Although several medicinal plant extracts containing different reducing agents, such as phenolic, polyphenol, and flavonoid compounds, have been widely applied for the green synthesis of AgNP [10–12], there are few reports on the use of *F. asafoetida* and its natural constituents for the biosynthesis of AgNPs. *Ferula asafoetida* contains many natural metabolites, including proteins, polysaccharides, alkaloids, and alcoholic compounds, which can act as reducing agents and exert beneficial biological effects. Therefore, the combination of AgNPs with *F. asafoetida* may lead to the development of a promising antimicrobial agent against serious infectious diseases with reduced cytotoxicity.

For the first time, the present study is aimed at investigating the potential application of the aqueous extract of *F. asafoetida* (FerEX) for the green synthesis of AgNPs, evaluating its effect on *A. baumannii*, isolated from patients admitted to the pediatric ICU (PICU), and examining its potential cytotoxic effects.

2. Methods

2.1. Isolation of Bacterial Strains from the PICU. Samples of *A. baumannii* were collected from the blood, respiratory emissions, urine, and skin ulcers. They were collected from patients hospitalized in the PICU of Namazi Hospital, Shiraz, Iran. They were first transferred to tubes containing normal saline (0.9%) and serially diluted tenfold. The microbiological procedures were carried out using routine laboratory tests. After transferring the microbial plates to the microbiology research facility, cultures were prepared in MacConkey agar plates (Merck, Germany). Single colonies were confined and distinguished using routine laboratory bacteriological tests based on their biochemical, culture, and microbiological features on Gram staining [13, 14].

2.2. Extraction of the Aqueous Extract of F. asafoetida. The leaves and other aerial parts of *F. asafoetida* were collected from the southern regions of Iran (Lar, Iran) in March 2019. The plant parts were then dried at room temperature. Next, the voucher specimens of *F. asafoetida* were deposited in the herbarium of the Department of Plant Protection of Shiraz University (No. #5237). After carefully washing the specimens with deionized water, different parts of *F. asafoetida* were dehydrated at 18-24°C for 14 days. Next, 41 g of powdered *F. asafoetida* was added to 500 mL of deionized water in a glass beaker and boiled for 16 hours at 50°C. Next, it was cooled, and the aqueous extract was filtered through a Whatman No. 1 filter paper. The black-brown bottle containing the extract of *F. asafoetida* (FerEX) was stored at 4°C until further analyses and biological experiments.

Fourier-transform infrared (FTIR) spectroscopy (Series Tensor II, Bruker, USA) was performed for characterization. Also, a gas chromatograph connected to a mass spectrometer (GC/MS, Agilent Technologies 5975C), which was equipped with an HP-5 MS capillary column (length of 30 m, inner diameter of 0.25 mm, and layer thickness of 0.25 μm), was used to analyze the constituents of *F. asafoetida*. The oven temperature was increased from 60°C to 250°C (5°C per minute) and kept at 250°C for ten minutes. Helium gas was used as a carrier with a flow rate of 1.1 mL/min and ionization energy of 70 eV. The interface temperature was 280°C, and the mass range was 30-600 m/z. The essential oil constituents were identified based on retention indices (by injecting C9-C20 hydrocarbons under the same conditions as essential oil) and comparison with mass spectra, according to Wiley (nl7) and Adams' mass spectral libraries [15].

2.3. Green Synthesis of AgNPs. For the green synthesis of AgNPs, 5 mL of FerEX was poured into a glass jolt by a sterile pipette. Next, 95 mL of silver nitrate (1 mM $AgNO_3$) was added and shaken at 25°C for 48 hours. Finally, the colored solution was centrifuged at 12,000 rpm for 20 minutes at 4°C and washed centrifugally three times. The obtained mass was dried using a vacuum evaporator, and biogenic *F. asafoetida* AgNP (Fer@AgNP) powder was stored in a nitrogen-filled container at 4°C.

2.4. Chemical Synthesis of AgNPs. According to a study by Abbaszadegan et al., $AgNO_3$ reduction by $NaBH_4$ was applied to synthesize chemical AgNPs. Briefly, 1 mL of $AgNO_3$ (0.1 mM) was slowly added to 20 mL of $NaBH_4$ (6.2 mM), which was previously chilled using ice and stirring [7]. This reaction was maintained in a dark room for 24 hours, and the mixture was stored at 4°C until further experiments.

2.5. Characterization. In this study, AgNPs and Fer@AgNP were characterized using FTIR spectroscopy (Tensor II, Bruker, USA), field emission-scanning electron microscopy (FE-SEM; Mira III, Tescan), energy-dispersive X-ray spectroscopy (XRD; Series S Max Finder Mira III, Tescan), and EDX mapping (Series S Max Locator Mira III, Tescan).

2.6. Antimicrobial Activity Assessment. A colony of *A. baumannii* was cultured in Luria–Bertani (LB) broth medium. A 24-hour cultured microbial strain suspension was inoculated into tubes containing 3 mL of Mueller-Hinton broth to obtain a suspension with 0.5 McFarland turbidity. The microorganism was then subjected to three types of antimicrobial tests, according to the Clinical and Laboratory Standards Institute (CLSI) 2018 guidelines, including well diffusion method, broth microdilution, and minimum bactericidal concentration (MBC) assay [16]. For preparation, the desired amounts of NPs were dispersed in a solution of double-distilled water. Next, they were exposed to ultrasonic waves for about one hour.

2.6.1. Well Diffusion Method. The well diffusion method was used to examine the antimicrobial effects in Mueller-Hinton agar plates. For this purpose, 100 μL of the microbial suspension was added to a Mueller-Hinton agar plate and cultured using a sterile swab. A well with a dimension of 6 mm × 2 cm was prepared on the surface of each agar-containing plate, containing 50 μL of each tested compound; the tested compounds included FerEX, AgNPs, and Fer@AgNPs. Carbapenem was also used as a standard antibiotic, and sterile refined water was used as control. Finally, the bacterial media were incubated at 37°C for 24 hours, and microbial colonies were examined for the developed inhibition zones; the hollow diameters (where no microorganisms grew) were measured and reported in millimeters.

2.6.2. Broth Microdilution. The broth microdilution method was used to determine the minimum inhibitory concentration (MIC) [17]. For this purpose, serial dilutions (0.5-250 μg/mL) of each compound, dissolved in Mueller-Hinton broth, were added to 96-well plates, and the microbial suspensions were immediately added to each well. Microwells containing the culture medium were considered the negative controls, and the wells containing the media and microorganisms without any effective constituents were considered the positive controls (100% viability). Carbapenem was also assessed as a standard antibiotic. Finally, the microplates were transferred to a humidified incubator and maintained overnight at 37°C. The absorption of each well was read at 600 nm using a microplate reader, and the viability percentage of microorganisms in each tested well was calculated compared to the positive control. The concentration of each compound inhibiting the growth of *A. baumannii* by 90%, as compared to the control group, was considered as the MIC.

2.6.3. MBC Assay. The microorganisms were cultured overnight in a brain-heart infusion (BHI) medium, and a stock with a concentration of 10^5-10^6 CFU/mL was prepared. Next, 50 μL of different compounds (concentrations of 0.5 to 250 μg/mL) was added to a 96-well microplate, containing 40 μL of BHI and 10 μL of *A. baumannii* suspension. The plates were incubated overnight at 37°C. A volume of 10 μL from each tested well (including the controls) was added to a BHI agar plate and transferred to an incubator for another 24 hours at 37°C to examine the bactericidal effect of each compound. The concentration of each compound causing no growth of microorganisms was regarded as the MBC.

2.7. Cytotoxicity Assay (MTT Assay). The cytotoxicity of Fer@AgNP was evaluated on the MCF-7 human cell line, using the MTT assay, according to a study by Gholami et al. [18]. In this study, the MCF-7 cell line was prepared by the Cell Bank of Pasteur Institute of Iran (NCBI code: C135). The cells were maintained in DMEM medium, containing 25 mM of glucose, 10% fetal bovine serum (FBS), penicillin (100 U/mL), and streptomycin (100 μg/mL). The cells were incubated at 37°C with 5% CO_2 at 95% humidity. Briefly, the cell lines were suspended in the RPMI-1640 medium and seeded into a cell culture plate. The cells were maintained under standard conditions (5% CO_2, 95% humidity, and temperature of 37°C) for 24 hours.

The RPMI-1640 medium was used to prepare different concentrations of each compound (1-500 μg/mL), which were later added to each well, containing cells attached to the bottom after removing the previous culture medium. The cells were incubated again for 24 hours, and 25 μL of 3-(4,5-dimethylthiazol-2-yl)-2,5-diphenyl tetrazolium bromide (MTT) solution was added to each well and incubated for four hours. To solubilize MTT-formazan crystals, 100 μL of dimethyl sulfoxide (DMSO) was added to the mixture and shaken for ten minutes [19]. An ELISA plate reader (BioTek, Winooski, VT, USA) was also utilized to calculate the absorbance of each well at a wavelength of 540 nm, compared to the equivalent well of untreated cells. Cell viability was calculated using the following equations:

$$\%\text{Cell viability} = \left(\frac{\text{OD}_{\text{cells+compounds}} - \text{OD}_{\text{compounds}}}{\text{OD}_{\text{cells+media}} - \text{OD}_{\text{media}}}\right) \times 100, \quad (1)$$

where OD represents the optical density and the cell viability percentage is the percentage of living cells after the test.

2.8. Statistical Analysis. The results of biological assays were analyzed using IBM SPSS software. One-way ANOVA, followed by Tukey's post hoc test, was used to evaluate differences between the groups. All biological experiments (both antimicrobial tests and cytotoxicity assays) were performed in triplicate, and $P \leq 0.05$ was considered statistically significant.

3. Results and Discussion

For the first time, this study is aimed at evaluating the biogenic synthesis of AgNPs using the extract of *F. asafoetida* as a reducing agent. This extract contained important biological components, such as proteins and ethylene groups, and could act as a capping/stabilizing agent. Their main components were investigated using a GC/MS apparatus.

3.1. Ferula asafoetida Constituents. A GC/MS apparatus was used to determine the major chemical components of *F. asafoetida*. The results showed that *F. asafoetida* contained 35 chemical constituents, including propenyl butyl disulfide

Table 1: The principal chemical compounds of *Ferula asafoetida* essential oil.

Number	Kovats index	Compounds	Area (%)	Analysis
1	905	3,4-Dimethylthiophene	0.05	GC
2	915	5,5-Dimethylpyrazolidin-3-one	0.03	GC
3	933	α-Pinene	1.1	GC
4	947	Camphene	0.16	GC
5	975	β-Pinene	15.69	GC
6	990	Myrcene	1.4	GC
7	999	Decane	1.02	GC
8	1012	2,3,4-Trimethylthiophene	0.62	GC
9	1016	α-Terpinene	0.04	GC
10	1029	Limonene	0.51	GC
11	1045	β-Ocimene	17.34	GC
12	1059	γ-Terpinene	0.06	GC
13	1088	α-Terpinolene	0.41	GC
14	1107	Dipropyl disulfide	0.16	GC
15	1118	Tetramethylthiophene	0.07	GC
16	1130	Alloocimene	0.66	GC
17	1163	n-Propyl sec-butyl disulfide	0.75	GC
18	1172	(E)-1-Propenyl sec-butyl disulfide	55.4	GC
19	1200	Dodecane	0.33	GC
20	1212	Bis(1-methyl propyl) disulfide	0.57	GC
21	1260	Carvacrol	0.59	GC
22	1300	Tridecane	0.05	GC
23	1392	(E)-3-Tetradecene	0.14	GC
24	1399	Tetradecane	0.22	GC
25	1452	Selin-4,7(11)-diene	0.13	GC
26	1462	α-Humulene	0	GC
27	1471	(+)-Epi-bicyclosesquiphellandrene	0.04	GC
28	1485	β-Chamigrene	0.03	GC
29	1498	Cadina-1-4-diene	0.11	GC
30	1506	β-Dihydro agarofuran	0.11	GC
31	1513	β-Bisabolene	0.07	GC
32	1520	γ-Cadinene	0.09	GC
33	1530	δ-Cadinene	0.12	GC
34	1546	Aristolene	0.02	GC
35	1600	Hexadecane	0.03	GC
36		Unknown	1.88	GC

(55.4%), α-pinene (1.1%), camphene (0.16%), β-pinene (15.69%), myrcene (1.4%), decane (1.02%), limonene (0.51%), β-ocimene (17.34%), γ-terpinene (0.06%), α-terpinolene (0.41%), carvacrol (0.59%), and n-pentacosane (2.13%). All of the main chemical constituents of *F. asafoetida* are summarized in Table 1.

Several studies have investigated the components of *F. asafoetida*. Although there are some differences in the discovered constituents and their amounts, the main components are nearly the same [20]. Among the distinguished chemical components of *F. asafoetida*, heptane belongs to the alkane group with seven carbon particles. This colorless liquid is insoluble in polar solvents, with gasoline-like smells. Besides, decane is a profoundly combustible natural compound from the alkene group. This compound is nonpolar and insoluble in water, similar to other alkanes [21].

Moreover, a cyclic monoterpene, namely, limonene, was found in *F. asafoetida*. It has a smell similar to orange and has been used to synthesize chemical materials in household cleansers and renewable energies. This hydrocarbon can be effectively oxidized in humid environments and may be a chiral particle [22].

Terpineol is a monoterpene derived from petitgrain oil, pine oil, and petroleum. It is commonly used in fragrances, makeup products, and flavors and has a pleasant odor similar to jasmine [23]. Thymol and carvacrol, as two well-known

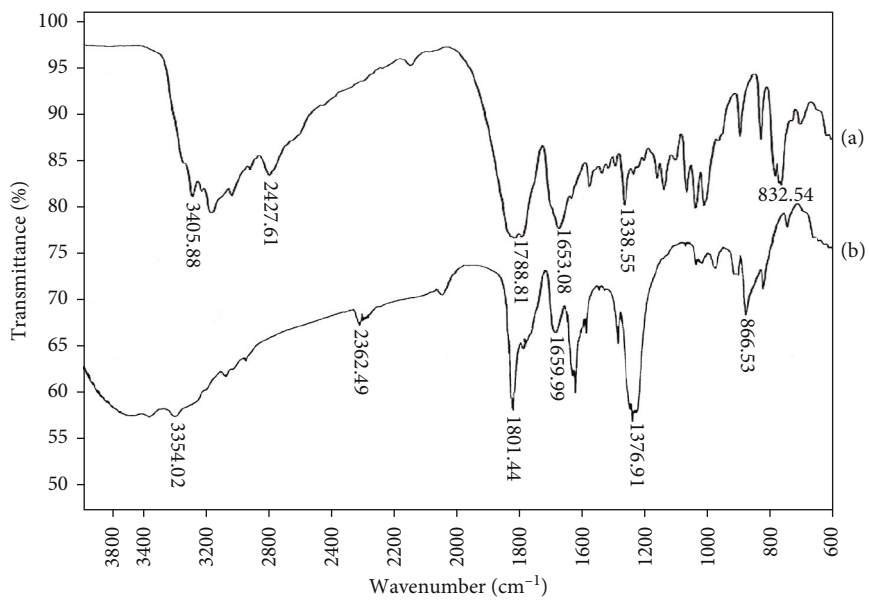

Figure 1: The FTIR spectra of (a) FerEX and (b) Fer@AgNP.

terpenes, revealed significant antioxidant, antifungal, and antibacterial activities. Besides, numerous studies showed their potential on bacterial strains at lower concentrations [24]. These compounds and some other structures found in the plant extract can functionalize AgNPs and significantly improve their biological efficacy.

3.2. Characterization of Biogenic NPs. The FTIR analysis was performed to confirm the functional groups of biomolecules involved in capping, viable stabilization, and reduction of synthesized Fer@AgNP. The FTIR spectra of FerEX and Fer@AgNP (Figure 1) showed nine peaks at 3405, 2427, 2359, 2100, 1788, 1635, 1338, 1048, and 832 cm^{-1}, respectively. The peak at 3405 cm^{-1} in the chemically synthesized AgNPs was related to the N-H bond of amide and O-H of hydroxy groups, extending to phenols/alcohols or bending/stretching hydrogen-bonded phenols/alcohols in the extract. The peak at 2427 cm^{-1} was related to the C-H bond of alkanes. Also, the peaks at 2359 cm^{-1} to 2100 cm^{-1} were related to C≡N and C≡C stretching in the aromatic/aliphatic compounds.

The peaks at 1788 to 1635 cm^{-1} were related to the C=C stretching of fragrant compounds. Another study reported that these peaks were related to the carbonyl (C=O) groups of proteins. Besides, the peak at 1338 cm^{-1} represented the CH_3 group of carbohydrates. Also, the peak at 1048 cm^{-1} was related to alkanes, ethers, esters, alcohols, and the C=O in-plane bending of carboxylic acids. Consistent with previous reports, the peak at 832 cm^{-1} was related to the =CH stretching of bicyclic monoterpenes [25]. In previous studies, the FTIR bands at 3405, 2100, 1788, 1635, 1048, and 832 cm^{-1} indicated the properties of AgNPs [26], and the presence of other bands confirmed the proximity of different biomolecules, which played a significant role in stabilizing Fer@AgNP. AbuDalo et al. also concluded that these bands represented the presence of aromatic compounds, alkanes, and amide bonds of proteins and amines in the structure of biogenic AgNPs, which contributed to the production and stability of NPs [27]. In particular, for the C=O bond, a slight shift represented adsorption on the surface and suggested that this bond is related to the hydroxyl group stretching bands in biological macromolecules, such as proteins or polysaccharides found in the *F. asafoetida*.

In Figure 2, the FE-SEM images of chemical AgNPs and green-synthesized biogenic Fer@AgNPs are presented. As shown in Figure 2, both chemical and biogenic NPs had circular structures, with an average size of 10 ± 2.77 nm for Fer@AgNP and 19.5 ± 5.1 for chemically synthesized AgNP (RSD < 3% for $n = 10$). Several studies have reported that most biogenic AgNPs have a spherical geometry, with a size range of 5 to 500 nm; however, different biological activities have been reported [27]. Our observations showed that Fer@AgNP had higher colloidal stability than chemically synthesized NPs after seven days of being maintained in the dark at 23-25°C with low particle agglomeration. It seems that the stability of Fer@AgNP is related to steric stabilization by natural surfactants [28] found in the FerEX, as described in Section 3.1.

The constituents of biogenic AgNPs were evaluated by the EDX analysis. The peaks were observed between 2 keV and 5 keV, confirming the presence of Ag. Figure 3 and Table 2 demonstrate the distinct presence of Ag peaks at 3 keV for Fer@AgNPs, which is a specific characteristic of AgNPs with weight and atomic percentages of 11.6% and 7.7%, respectively. The high atomic and weight percentages of organic elements, such as C, N, and O, revealed the possible presence of organic compounds, such as polysaccharides, phenols, and proteins; these compounds have also been reported in some studies [29].

X-ray diffractometry was used to confirm the crystalline structure of synthesized AgNPs. As shown in Figure 4, the hexagonal structure of Ag crystals was found, with Ag in a cubic form. The X-ray image indicated AgNPs, and a few diffraction peaks were observed at $2\theta = 38$, 44, 65, and 78

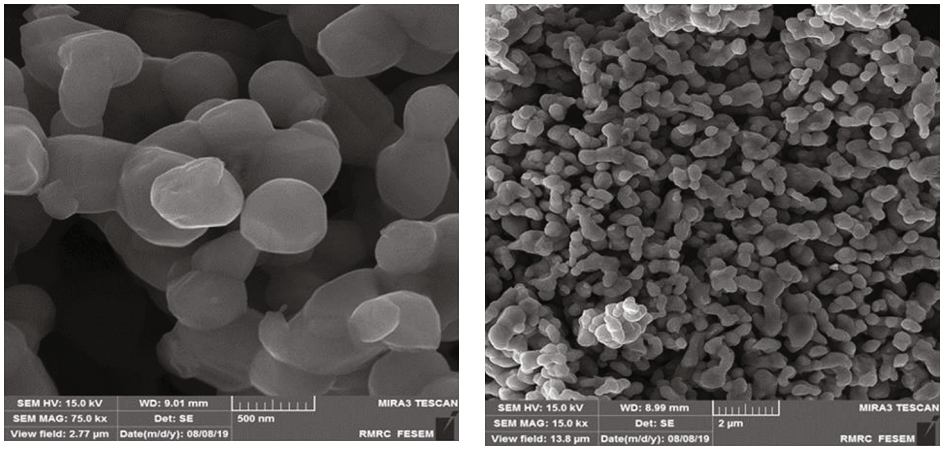

(a) (b)

Figure 2: The FE-SEM image of (a) chemically synthesized and (b) biogenic AgNPs.

corresponding to the (111), (200), (220), and (311) planes, respectively. These peaks might be attributed to the natural components of *F. asafoetida*, indicating the biogenic synthesis of Fer@AgNP [30]. In some studies, the crystalline structure of biogenic AgNPs synthesized using plant extracts is comparable with the crystalline structure of AgNPs synthesized using *F. asafoetida* [31, 32]. Equation (2) (Debye-Scherrer equation) was used to measure the average crystalline size of nanoparticles.

$$D = \frac{k\lambda}{\beta \cos\cos\theta}, \tag{2}$$

where D is the average size of the nanoparticles, k is the Scherrer equation (0.9), λ is the X-ray radiation wavelength, and β is the angular full width at half maximum (FWHM) of XRD peaks at diffraction point θ [33]. The average crystalline size of the biogenic Fer@AgNP using FerEX was ~42 nm.

As illustrated in Figure 5, a characteristic peak was observed at around λ 450 nm for AgNPs using UV-VIS spectroscopy (Figure 5(b)). The obtained range, which was consistent with previous reports, was contributed to the AgNP formation. Several studies reported the AgNP formation occurred in the wavelength of 400 to 500 nm [34]. The on-site observations and the UV-VIS spectrogram showed reducing Ag^+ ions into Ag^0, besides the green synthesis of AgNPs.

3.3. Antibacterial Effects against A. baumannii. The antimicrobial effect of Fer@AgNP against *A. baumannii* was examined using the well diffusion method, and the results were compared with those obtained for AgNPs synthesized by the chemical method. The data were also evaluated based on the MICs and MBCs. The FerEX created an inhibition hollow against the microorganisms at high concentrations (50-200 μg/mL). As shown in Figure 6, the anti-*Acinetobacter* effect of all compounds was dose-dependent. The viability of bacterial strains reduced by increasing the concentration of NPs. The Fer@AgNP showed a higher antimicrobial efficacy compared to AgNPs. The mean of three replicates for the width of the inhibition zone (in millimeter) is presented in Table 3.

Among the tested compounds, Fer@AgNP showed a more significant inhibitory effect against *A. baumannii*. At the highest concentration (200 μg/mL), the inhibition zone was measured at 14 ± 3 mm for FerEX, 19 ± 3 mm for AgNP, and 25 ± 5 mm for Fer@AgNP. There was no significant difference between Fer@AgNP and the standard antibiotic (carbapenem). Also, smaller inhibition zones were found for the FerEX. The MIC and MBC were measured to be 31.25 and 31.25 μg/mL for the chemically synthesized NPs and 2 and 2 μg/mL for the biogenic NPs, respectively. These findings revealed that the antimicrobial potential of biogenic NPs was significantly higher than chemical AgNPs (Figure 6 and Table 4). The optimal MIC and MBC were obtained by carbapenem at a concentration of 1 μg/mL. Also, the antimicrobial properties of FerEX were demonstrated at high concentrations (MIC = 125 μg/mL and MBC = 250 μg/mL).

Huang et al. synthesized biogenic AgNPs using a plant extract of *Cacumen platycladi* and evaluated their antimicrobial effects and mechanism [35]. According to their results, the MIC and MBC against *Staphylococcus aureus* and *Escherichia coli* were 5.4 and 5.4 μg/mL and 1.4 and 27 μg/mL, respectively; the present results showed better MIC and MBC values than the study by Huang and colleagues. Another study evaluated the antimicrobial effects of biogenic AgNPs using aloe vera. The MIC of aloe vera-synthesized AgNPs against *S. epidermidis* was 10 μg/mL, weaker than our finding [36]. This significant biological effect might be due to the strong antimicrobial effects of functional groups on Fer@AgNP, such as thiol groups.

The similar MBC and MIC values of nanomaterials compared to carbapenem revealed that their antimicrobial mechanisms could be bactericidal; this argument has been proposed in several previous studies [37]. On the other hand, the differences between the MIC and MBC values of FerEX might be attributed to the bacteriostatic activity of this natural product. Several studies have shown that AgNPs, green synthesized by plant extracts, have remarkable antibacterial

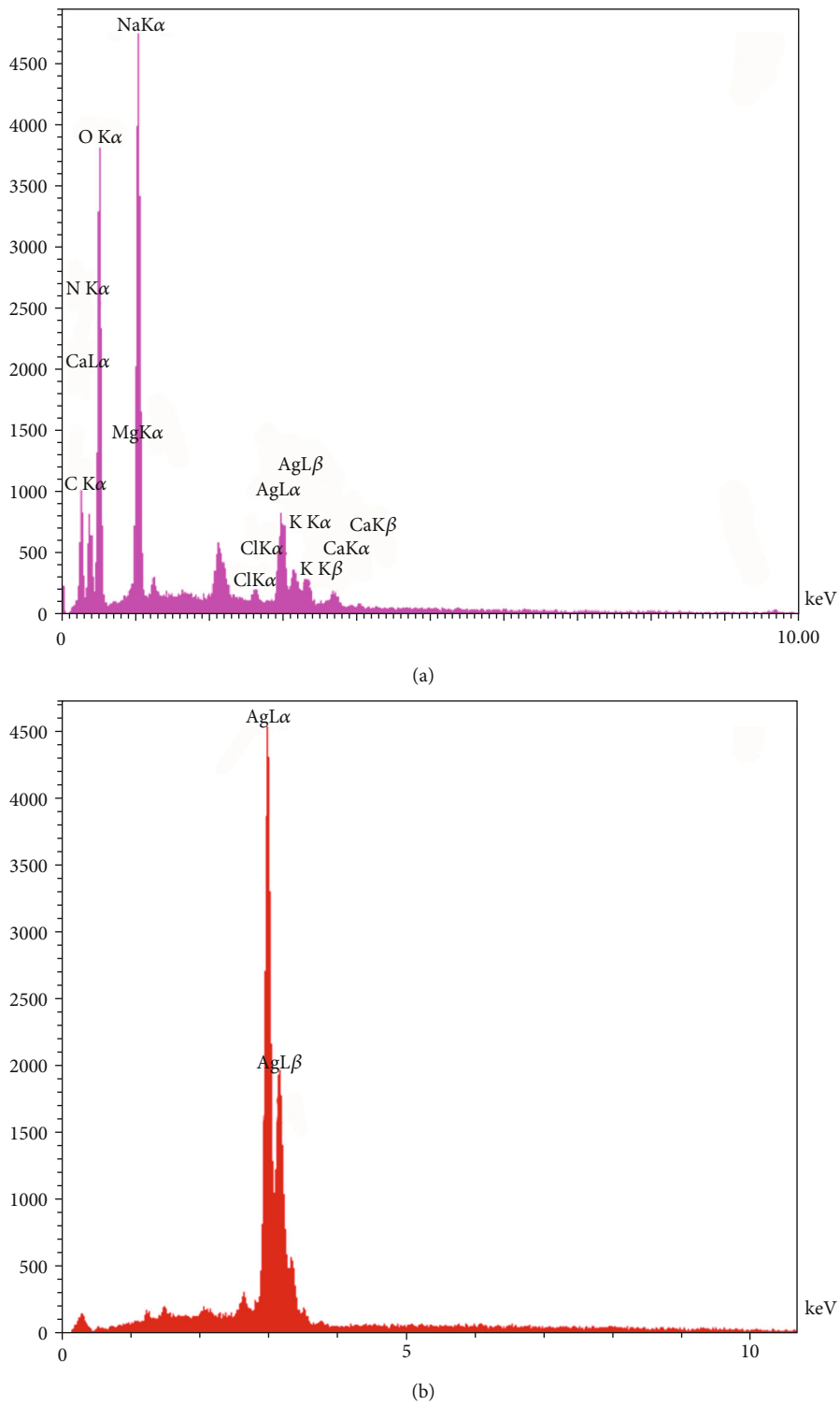

Figure 3: The EDX results of (a) chemical (AgNP) and (b) biogenic AgNPs (Fer@AgNP).

effects [38–40]. These biogenic AgNPs significantly inhibit the growth of a wide range of microbial pathogens, such as *Enterococcus faecalis*, *Escherichia coli*, *Pseudomonas aeruginosa*, *Azotobacter chroococcum*, *Bacillus licheniformis*, *Staphylococcus aureus*, and *Candida albicans*, which are involved in more common hospital-acquired infections [33, 41].

Biogenic AgNPs showed the most significant antimicrobial activity against *A. baumannii*, a dangerous pathogen in ICUs and PICUs. Our results revealed the higher viability of biogenic AgNPs against this bacterial strain than chemically synthesized AgNPs. In this regard, Singh et al. measured the MIC against *A. baumannii* to be 16 μg/mL, while the

Table 2: Quantitative EDX results of chemically synthesized (AgNP) and biogenic NPs (Fer@AgNP).

Compounds	Elements	Intensity	Weight %	Atomic %
AgNPs	Ag	1556.5	100	100
Fer@AgNP	C	79.6	13.89	18.93
	N	64.9	18.59	21.64
	O	328.0	42.20	42.42
	Na	475.2	12.30	8.60
	Ag	173.3	11.69	7.70
	Cl	7.1	0.08	0.04
	K	27.3	0.35	0.14
	Ca	19.1	0.26	0.11
	Mg	32.4	0.63	0.42

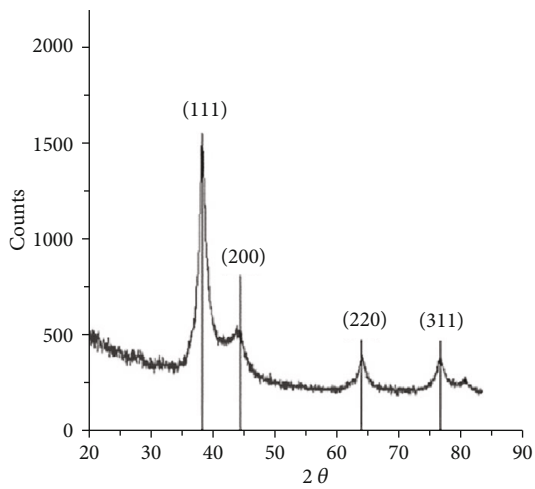

Figure 4: The XRD spectra of synthesized Fer@AgNP by FerEX for determination of Ag crystals.

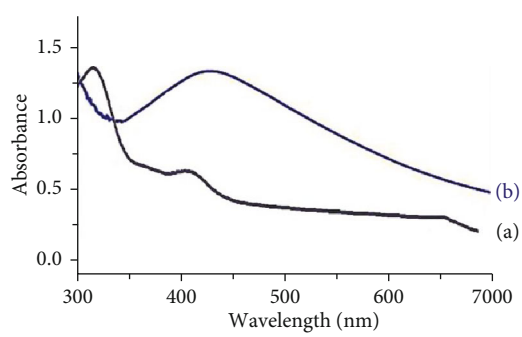

Figure 5: The UV-visible spectra of (a) the aqueous extract of FerEX and (b) biogenic AgNP.

present study found a MIC of 2 μg/mL [41]. They proposed a synergistic relationship between bacteriogenic AgNPs and some antibiotics. They clarified the potential role of these antibiotics in combination with AgNPs in facilitating the permeabilization of AgNPs through the external cell layer by displacing Mg^{2+} or Ca^{2+}, especially in the lipopolysaccharide layer. Inhibition of UDP-3-O-(R-3-hydroxymyristoyl)-N-acetylglucosamine deacetylase (LpxC) by natural compounds is another *in vivo* mechanism that disables *A. baumannii* and increases the opsonization of bacteria by macrophages [42]. This may suggest that functional groups on the surface of Fer@AgNP, particularly compounds containing thiol groups, help NPs to attach to lipopolysaccharides (LPS) of Gram-negative *A. baumannii* through biogenic synthesis and facilitate the integration of NPs.

Bhatnager et al. studied the antibacterial activity of *F. asafetida*, extracted with water (W), hexane (H), ethanol (E), and petroleum ether (P). They used biomass to calculate the zone of inhibition (*E. coli*: 8 mm (P), 8 mm (H), 12 mm (W), and 7 mm (E); *S. aureus*: 7 mm (P), 11 mm (H), 7 mm (W), and 7 mm (E); *K. pneumoniae*: 7 mm (P), 9 mm (H), 8 mm (W), and 8 mm (E); *S. flexneri*: 13 mm (P), 15 mm (H), 7 mm (W), and 11 mm (E); and *E. faecalis*: 8 mm (P), 7 mm (H), 9 mm (W), and 7 mm (E)) [43]. Although Bhatnager et al. did not investigate the concentration dependence of the antibacterial effect of FerEXs, the antimicrobial activity was observed at the highest concentrations (up to 100 μg/mL). The anti-*Acinetobacter* effect of AgNPs was increased when they were synthesized in the presence of the aqueous extract of FerEX. The increased antimicrobial effect of biogenic AgNP compared to chemical AgNP may be due to the combination of NPs with the antibacterial constituents of FerEX extract, especially thiol-containing substances.

The MIC and MBC values of Fer@AgNP against *A. baumannii* were more compelling than those obtained in other experiments using other plant extracts or living microorganisms from different plants or living organisms (*Neurada procumbens* [44], *Xanthomonas* spp. [45], *Eucalyptus citriodora* [46], and *Acinetobacter calcoaceticus*) to synthesize biogenic AgNPs. The bacterial growth was inhibited at a concentration range from 20 μg/mL to 500 μg/mL. Besides, the MIC and MBC values of Fer@AgNP revealed its higher antibacterial potential than chemically synthesized AgNPs. The superior antibacterial activity of Fer@AgNP compared to its chemically synthesized counterpart may be attributed to the smaller size of NPs, which offers a larger surface/volume ratio and results in their superior binding and transfer through the bacterial membrane or cellular proximity [47]. Besides, higher colloidal stability helps Fer@AgNP to be better distributed in biological environments as compared to AgNPs and to aggregate less [48–50]; this phenomenon increases the probability of NPs passing through biological membranes.

Although the antimicrobial mechanism of biogenic AgNPs and chemically synthesized AgNPs is still unknown, several mechanisms can play a role in their biological activities. When synthesized with various plant extracts, AgNPs can physically attach to bacteria and even eukaryotic cell surfaces and disrupt their integrity [51]. Internalization of the cytoplasm, interaction with cellular organelles and macromolecules, and finally production of reactive oxygen species (ROS) are the main biological mechanisms of biogenic AgNPs in the literature [52]. It is known that enhancement of ROS capacity causes membrane damage by increasing permeability, leading to the disruption of the electron transfer

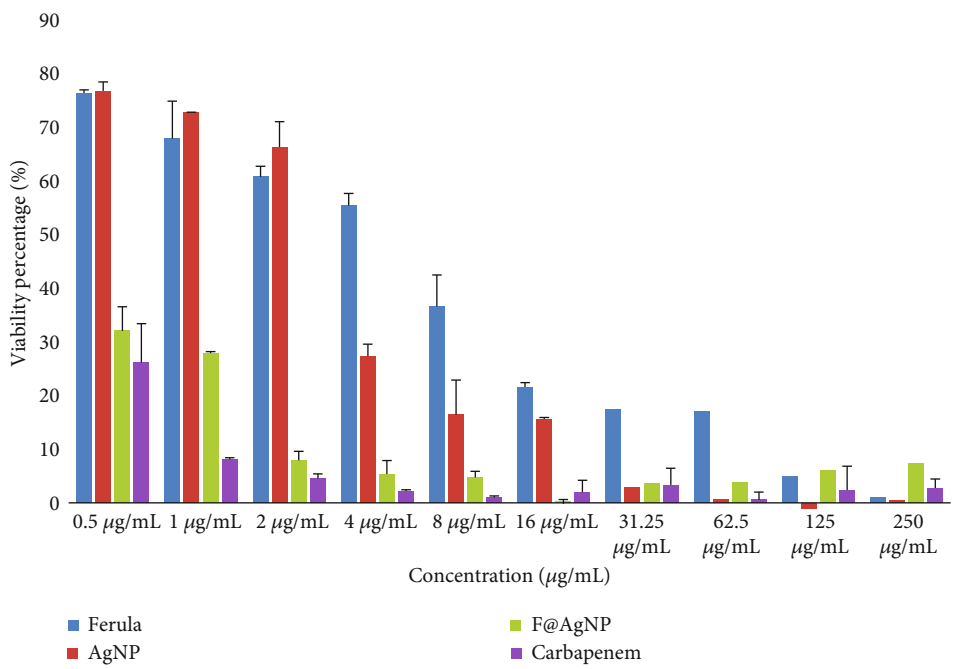

Figure 6: Antimicrobial effects of different concentrations of *Ferula asafoetida* aqueous extract (blue), chemically synthetized AgNPs (red), biogenic AgNPs (green), and carbapenem (purple) as the standard antibiotic against *A. baumannii* using the microdilution method.

Table 3: Antimicrobial susceptibility well diffusion method. Zones of inhibition of the aqueous extract of *Ferula asafoetida* (FerEX), chemically synthesized AgNPs, and green synthesized AgNPs (Fer@AgNP) against *A. baumannii*.

Compounds	Hollow diameter (mm)					
	1 μg/mL	10 μg/mL	25 μg/mL	50 μg/mL	100 μg/mL	200 μg/mL
FerEX	0 ± 0	0 ± 0	7 ± 2	9 ± 2	13 ± 2	14 ± 3
AgNP	0 ± 0	0 ± 0	9 ± 2	11 ± 3	15 ± 1	19 ± 3
Fer@AgNP	0 ± 0	8 ± 2	16 ± 3	16 ± 2	21 ± 3	25 ± 5
Carbapenem	16 ± 3	21 ± 4	23 ± 4	25 ± 2	25 ± 4	27 ± 3

Table 4: Quantitative MBC results of biosynthesized AgNPs.

Compounds	Concentrations (μg/mL)									
	0.5	1	2	4	8	16.1	31.25	62.5	125	250
FerEX	+	+	+	+	+	+	+	+	+	−
AgNP	+	+	+	+	+	+	−	−	−	−
Fer@AgNP	+	+	−	−	−	−	−	−	−	−
Carbapenem	+	−	−	−	−	−	−	−	−	−

chain and leakage of the cellular content. Besides, it can alternatively damage human cells and cause severe adverse effects. Therefore, in this study, we evaluated the effect of Fer@AgNPs on a cancerous human cell line as an indicator of cytotoxic effect and an anticancer agent.

3.4. Cytotoxic Effect of Fer@AgNPs. Several studies have assessed the anticancer effects of plant extracts. However, there is no report or article on the efficacy of synthesized Fer@AgNP in the selected cell lines. In this study, the effects of FerEX, AgNP, and Fer@AgNP were assessed on the MCF-7 human cell line by the MTT assay. Figure 7 shows that both NPs (AgNP and Fer@AgNP) showed increased cytotoxic effects against the MCF-7 cell lines at concentrations from 200 to 500 μg/mL in comparison with FerEX. By decreasing the concentration, the impact of compounds is essentially reduced. Based on the findings, at concentrations below 200 μg/mL, the effect of FerEX on the human cell lines reduced.

On the other hand, for AgNP and Fer@AgNP, the cell survivability and antioxidant levels (IC50) were 10 and 100 μg/mL, respectively, on the MCF-7. Therefore, Fer@AgNP had no antagonistic effects on the assessed cell lines as compared to AgNP, which exerted a significant cytotoxic effect on the MCF-7 cells. So far, many attempts have been designed to distinguish the effect of silver nanoparticles against various tumors. One of the broadly acknowledged hypotheses has ascribed the potential generation of reactive oxygen species created by nanoparticles and their ions, preventing cell growth and eventually cell apoptosis [8, 53].

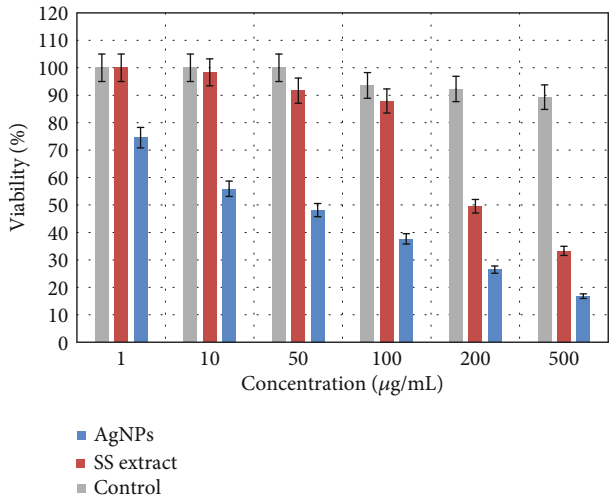

Figure 7: The MTT assay for confirming the cytotoxic effect of the extract (SS extract, red), chemically synthetized AgNPs (control, grey), and green synthesized AgNPs (AgNPs, blue) on the MCF-7 cell lines during 48 hours.

Finally, this study showed the plausibility of the biological synthesis of AgNPs using an aqueous extract of FerEX. The presence of thiol-containing groups, alkyl halides, and other reducing agents in the extract of FerEX allows for reducing Ag particles into NPs. The green-synthesized Fer@AgNP showed high antibacterial activity against *A. baumannii*. Interestingly, these green-synthesized NPs did not initiate a significant reduction in the cell viability of human adenocarcinoma cells (MCF-7), except at elevated concentrations.

The emergence of multidrug-resistant bacteria, especially in the hospital ICUs, has limited the use of standard antibiotics and has led researchers to incorporate AgNPs and natural products. In our study, *A. baumannii* isolated from the PICUs was eliminated using biogenic AgNPs. This nanomaterial is more advantageous than chemically synthesized AgNPs and even conventional antimicrobial agents. Therefore, developing this type of NPs can be considered an alternative strategy to overcome multidrug resistance in bacteria, especially *Acinetobacter* strains in ICUs.

Future studies need to examine the long-term aspects of antimicrobial activity, such as inhibition of biofilm formation, and investigate the other potential advantages of this biogenic AgNP, especially in terms of biocompatibility and biodegradability. Overall, finding newer antimicrobial agents using biocompatible nanomaterials is essential to eradicate nosocomial infections, especially those caused by *A. baumannii*. According to the present study, Fer@AgNPs could be an excellent option to overcome these infections, possibly at lower and less toxic concentrations than what is used clinically today. Also, the combination of this biogenic nanomaterial with effective antibiotics, such as carbapenem, can be investigated in future studies.

4. Conclusion

This study is the first extensive report to demonstrate the antibacterial activity of biogenic AgNPs against a nosocomial pathogen (*A. baumannii*) and evaluate its human cell cytotoxicity. The biogenic NPs exhibited significant antibacterial activities against this ESKAPE pathogen. The AgNPs produced by *F. asafoetida* inhibited bacterial growth and showed a higher potency compared to chemically synthesized AgNPs, which might be due to disruptions in the cell wall and formation of ROS. The cytotoxic assessments showed the acceptable biocompatibility of Fer@AgNPs at lower concentrations. However, it should be noted that killing bacteria is highly specific to bacterial strains in terms of cell wall composition, growth rate, biofilm formation capacity, and type of NPs. Overall, different synthesizing procedures, sizes, and shapes can render AgNPs with variable antimicrobial properties. Moreover, the binding of NPs to any microorganism depends on interactions in the available surface area. Therefore, small-sized AgNPs with a larger surface area would exhibit a more significant microbicidal activity as compared to larger AgNPs.

Data Availability

The experimental data used to support the findings of this study are included within the article.

Conflicts of Interest

The authors declare that they have no conflicts of interest.

Acknowledgments

This study was carried out after obtaining a grant (No. 98-01-36-21987). It was funded by the Vice-Chancellor for Research Affairs of Shiraz University of Medical Sciences, Shiraz, Iran. We wish to thank H. Argasi at the Research Consultation Center (RCC) of Shiraz University of Medical Sciences for his invaluable assistance in editing this manuscript.

References

[1] V. Tiwari, R. Roy, and M. Tiwari, "Antimicrobial active herbal compounds against *Acinetobacter baumannii* and other pathogens," *Frontiers in Microbiology*, vol. 6, p. 618, 2015.

[2] H. Richet and P. E. Fournier, "Nosocomial infections caused by *Acinetobacter baumannii* a major threat worldwide," *Infection Control & Hospital Epidemiology*, vol. 27, no. 7, pp. 645-646, 2006.

[3] A. Y. Peleg, H. Seifert, and D. L. Paterson, "*Acinetobacter baumannii*: emergence of a successful pathogen," *Clinical microbiology reviews.*, vol. 21, no. 3, pp. 538–582, 2008.

[4] A. Čiginskienė, A. Dambrauskienė, J. Rello, and D. Adukauskienė, "Ventilator-associated pneumonia due to drug-resistant *Acinetobacter baumannii*: risk factors and mortality relation with resistance profiles, and independent predictors of in-hospital mortality," *Medicina (Kaunas, Lithuania)*, vol. 55, no. 2, p. 49, 2019.

[5] M. Nabavizadeh, A. Abbaszadegan, A. Gholami et al., "Antibiofilm efficacy of positively charged imidazolium-based silver nanoparticles in *Enterococcus faecalis* using quantitative real-time PCR," *Jundishapur J Microbiol.*, vol. 10, no. 10, 2017.

[6] A. Abbaszadegan, A. Gholami, S. Abbaszadegan et al., "The effects of different ionic liquid coatings and the length of alkyl chain on antimicrobial and cytotoxic properties of silver nanoparticles," *Iranian endodontic journal.*, vol. 12, no. 4, pp. 481–487, 2017.

[7] A. Abbaszadegan, M. Nabavizadeh, A. Gholami et al., "Positively charged imidazolium-based ionic liquid-protected silver nanoparticles: a promising disinfectant in root canal treatment," *International Endodontic Journal*, vol. 48, no. 8, pp. 790–800, 2015.

[8] S. Zargarnezhad, A. Gholami, M. Khoshneviszadeh, S. N. Abootalebi, and Y. Ghasemi, "Antimicrobial activity of isoniazid in conjugation with surface-modified magnetic nanoparticles against *Mycobacterium tuberculosis* and nonmycobacterial microorganisms," *Journal of Nanomaterials*, vol. 2020, Article ID 7372531, 9 pages, 2020.

[9] A. Amalraj and S. Gopi, "Biological activities and medicinal properties of Asafoetida: a review," *Journal of Traditional and Complementary Medicine*, vol. 7, no. 3, pp. 347–359, 2017.

[10] S. Sarkar and V. Kotteeswaran, "Green synthesis of silver nanoparticles from aqueous leaf extract of pomegranate (*Punica granatum*) and their anticancer activity on human cervical cancer cells," *Advances in Natural Sciences: Nanoscience and Nanotechnology*, vol. 9, no. 2, article 025014, 2018.

[11] G. Arya, R. M. Kumari, N. Sharma et al., "Catalytic, antibacterial and antibiofilm efficacy of biosynthesised silver nanoparticles using *Prosopis juliflora* leaf extract along with their wound healing potential," *Journal of Photochemistry and Photobiology B: Biology*, vol. 190, pp. 50–58, 2019.

[12] G. Arya, R. Mankamna Kumari, N. Sharma et al., "Evaluation of antibiofilm and catalytic activity of biogenic silver nanoparticles synthesized fromAcacia niloticaleaf extract," *Advances in Natural Sciences: Nanoscience and Nanotechnology*, vol. 9, no. 4, article 045003, 2018.

[13] A. Gholami, S. Shahin, M. Mohkam, N. Nezafat, and Y. Ghasemi, "Cloning, characterization and bioinformatics analysis of novel cytosine deaminase from *Escherichia coli* AGH09," *International Journal of Peptide Research and Therapeutics.*, vol. 21, no. 3, pp. 365–374, 2015.

[14] S. N. Abootalebi, A. Saeed, A. Gholami et al., "Screening, characterization and production of thermostable alpha-amylase produced by a novel thermophilic *Bacillus megaterium* isolated from pediatric intensive care unit," *Journal of Environmental Treatment Techniques*, vol. 8, no. 3, pp. 952–960, 2020.

[15] A. Abbaszadegan, S. Sahebi, A. Gholami et al., "Time-dependent antibacterial effects of Aloe vera and *Zataria multiflora* plant essential oils compared to calcium hydroxide in teeth infected with *Enterococcus faecalis*," *Journal of Investigative and Clinical Dentistry*, vol. 7, no. 1, pp. 93–101, 2016.

[16] M. S. Asgari, S. Sepehri, S. Bahadorikhalili et al., "Magnetic silica nanoparticle-supported copper complex as an efficient catalyst for the synthesis of novel triazolopyrazinylacetamides with improved antibacterial activity," *Chemistry of Heterocyclic Compounds*, vol. 56, no. 4, pp. 488–494, 2020.

[17] F. Moazami, A. Gholami, V. Mehrabi, and Y. Ghahramani, "Evaluation of the antibacterial and antifungal effects of Pro-Root MTA and nano-fast cement: an *In Vitro* study," *Journal of Contemporary Dental Practice*, vol. 21, no. 7, pp. 760–764, 2020.

[18] A. Gholami, S. Rasoul-amini, A. Ebrahiminezhad, S. H. Seradj, and Y. Ghasemi, "Lipoamino acid coated superparamagnetic iron oxide nanoparticles concentration and time dependently enhanced growth of human hepatocarcinoma cell line (HepG2)," *Journal of Nanomaterials*, vol. 2015, Article ID 451405, 9 pages, 2015.

[19] R. Heiran, S. Sepehri, A. Jarrahpour et al., "Synthesis, docking and evaluation of *in vitro* anti-inflammatory activity of novel morpholine capped β-lactam derivatives," *Bioorganic Chemistry*, vol. 102, article 104091, 2020.

[20] F. Farhadi, M. Iranshahi, S. F. Taghizadeh, and J. Asili, "Volatile sulfur compounds: the possible metabolite pattern to identify the sources and types of asafoetida by headspace GC/MS analysis," *Industrial Crops and Products*, vol. 155, article 112827, 2020.

[21] Y. Ichikawa, T. Watanabe, Y. Horimoto, K. Ishii, and S. Naito, "Measurements of 50 non-polar organic compounds including polycyclic aromatic hydrocarbons, n-alkanes and phthalate esters in fine particulate matter (PM 2.5) in an industrial area of Chiba prefecture, Japan," *Asian Journal of Atmospheric Environment.*, vol. 12, no. 3, pp. 274–288, 2018.

[22] A. Rehman, A. M. López Fernández, M. F. M. Gunam Resul, and A. Harvey, "Highly selective, sustainable synthesis of limonene cyclic carbonate from bio- based limonene oxide and CO_2: a kinetic study," *Journal of CO2 Utilization*, vol. 29, pp. 126–133, 2019.

[23] C. Khaleel, N. Tabanca, and G. Buchbauer, "α-Terpineol, a natural monoterpene: a review of its biological properties," *Open Chemistry*, vol. 16, no. 1, pp. 349–361, 2018.

[24] H. Zengin and A. H. Baysal, "Antibacterial and antioxidant activity of essential oil terpenes against pathogenic and spoilage-forming bacteria and cell structure-activity relationships evaluated by SEM microscopy," *Molecules*, vol. 19, no. 11, pp. 17773–17798, 2014.

[25] P. Rajasekar, S. Priyadharshini, T. Rajarajeshwari, and C. Shivashri, "Bio-inspired synthesis of silver nanoparticles using *Andrographis paniculata* whole plant extract and their antimicrobial activity overpathogenic microbes," *International Journal of Research in Biomedicine and Biotechnology*, vol. 3, no. 3, pp. 47–52, 2013.

[26] S. Devanesan, K. Ponmurugan, M. S. AlSalhi, and N. A. al-Dhabi, "Cytotoxic and antimicrobial efficacy of silver nanoparticles synthesized using a traditional phytoproduct, asafoetida gum," *International Journal of Nanomedicine*, vol. 15, pp. 4351–4362, 2020.

[27] M. A. AbuDalo, I. R. al-Mheidat, A. W. al-Shurafat, C. Grinham, and V. Oyanedel-Craver, "Synthesis of silver nanoparticles using a modified Tollens' method in conjunction with phytochemicals and assessment of their antimicrobial activity," *PeerJ*, vol. 7, article e6413, 2019.

[28] W. Chartarrayawadee, P. Charoensin, J. Saenma et al., "Green synthesis and stabilization of silver nanoparticles using Lysimachia foenum-graecum Hance extract and their antibacterial activity," *Green Processing and Synthesis*, vol. 9, no. 1, pp. 107–118, 2020.

[29] N. E.-A. El-Naggar, M. H. Hussein, and A. A. El-Sawah, "Phycobiliprotein-mediated synthesis of biogenic silver nanoparticles, characterization, in vitro and in vivo assessment of anticancer activities," *Scientific Reports*, vol. 8, no. 1, p. 8925, 2018.

[30] S. Pirtarighat, M. Ghannadnia, and S. Baghshahi, "Green synthesis of silver nanoparticles using the plant extract of Salvia spinosa grown in vitro and their antibacterial activity

assessment," *Journal of Nanostructure in Chemistry*, vol. 9, no. 1, pp. 1–9, 2019.

[31] M. Ghaffari-Moghaddam, R. Hadi-Dabanlou, M. Khajeh, M. Rakhshanipour, and K. Shameli, "Green synthesis of silver nanoparticles using plant extracts," *Korean Journal of Chemical Engineering*, vol. 31, no. 4, pp. 548–557, 2014.

[32] A. U. Khan, Q. Yuan, Z. U. H. Khan et al., "An eco-benign synthesis of AgNPs using aqueous extract of Longan fruit peel: antiproliferative response against human breast cancer cell line MCF-7, antioxidant and photocatalytic deprivation of methylene blue," *Journal of Photochemistry and Photobiology B: Biology*, vol. 183, pp. 367–373, 2018.

[33] O. E. Rodríguez-Luis, R. Hernandez-Delgadillo, R. I. Sánchez-Nájera et al., "Green synthesis of silver nanoparticles and their bactericidal and antimycotic activities against oral microbes," *Journal of Nanomaterials*, vol. 2016, Article ID 9204573, 10 pages, 2016.

[34] M. Ndikau, N. M. Noah, D. M. Andala, and E. Masika, "Green synthesis and characterization of silver nanoparticles using *Citrullus lanatus* fruit rind extract," *International Journal of Analytical Chemistry*, vol. 2017, Article ID 8108504, 9 pages, 2017.

[35] J. Huang, G. Zhan, B. Zheng et al., "Biogenic silver nanoparticles byCacumen PlatycladiExtract: synthesis, formation mechanism, and antibacterial activity," *Industrial & Engineering Chemistry Research*, vol. 50, no. 15, pp. 9095–9106, 2011.

[36] P. Tippayawat, N. Phromviyo, P. Boueroy, and A. Chompoosor, "Green synthesis of silver nanoparticles in aloe vera plant extract prepared by a hydrothermal method and their synergistic antibacterial activity," *PeerJ*, vol. 4, article e2589, 2016.

[37] B. B. F. Mirjalili, S. Khabnadideh, A. Gholami et al., "Cu (OAc) 2 as a green promoter for one-pot synthesis of 2-amino-4, 6-diarylpyridine-3-carbonitrile as antibacterial agents," *Bulletin of the Chemical Society of Ethiopia*, vol. 34, no. 1, pp. 149–156, 2020.

[38] G. Arya, R. M. Kumari, N. Gupta, A. Kumar, R. Chandra, and S. Nimesh, "Green synthesis of silver nanoparticles using Prosopis juliflorabark extract: reaction optimization, antimicrobial and catalytic activities," *Artificial cells, Nanomedicine, and Biotechnology*, vol. 46, no. 5, pp. 985–993, 2018.

[39] S. Goyal, N. Gupta, A. Kumar, S. Chatterjee, and S. Nimesh, "Antibacterial, anticancer and antioxidant potential of silver nanoparticles engineered using Trigonella foenum-graecum seed extract," *IET nanobiotechnology.*, vol. 12, no. 4, pp. 526–533, 2018.

[40] B. Sharma, I. Singh, S. Bajar, S. Gupta, H. Gautam, and P. Kumar, "Biogenic silver nanoparticles: evaluation of their biological and catalytic potential," *Indian Journal of Microbiology.*, vol. 60, no. 4, pp. 468–474, 2020.

[41] R. Singh, J. Vora, S. B. Nadhe, S. A. Wadhwani, U. U. Shedbalkar, and B. A. Chopade, "Antibacterial activities of bacteriagenic silver nanoparticles against nosocomial *Acinetobacter baumannii*," *Journal of nanoscience and nanotechnology.*, vol. 18, no. 6, pp. 3806–3815, 2018.

[42] L. Lin, B. Tan, P. Pantapalangkoor et al., "Inhibition of LpxC protects mice from resistant *Acinetobacter baumannii* by modulating inflammation and enhancing phagocytosis," *MBio*, vol. 3, no. 5, 2012.

[43] R. Bhatnager, R. Rani, and A. S. Dang, "Antibacterial activity of *Ferula asafoetida*: a comparison of red and white type," *Journal of Applied Biology & Biotechnology*, vol. 3, pp. 18–21, 2015.

[44] F. A. Alharbi and A. A. Alarfaj, "Green synthesis of silver nanoparticles from *Neurada procumbens* and its antibacterial activity against multi-drug resistant microbial pathogens," *Journal of King Saud University - Science*, vol. 32, no. 2, pp. 1346–1352, 2020.

[45] K. Silva Santos, A. M. Barbosa, L. Pereira da Costa, M. S. Pinheiro, M. B. P. P. Oliveira, and F. Ferreira Padilha, "Silver nanocomposite biosynthesis: antibacterial activity against multidrug-resistant strains of *Pseudomonas aeruginosa* and *Acinetobacter baumannii*," *Molecules*, vol. 21, no. 9, p. 1255, 2016.

[46] P. Wintachai, S. Paosen, C. T. Yupanqui, and S. P. Voravuthikunchai, "Silver nanoparticles synthesized with *Eucalyptus critriodora* ethanol leaf extract stimulate antibacterial activity against clinically multidrug-resistant *Acinetobacter baumannii* isolated from pneumonia patients," *Microbial Pathogenesis*, vol. 126, pp. 245–257, 2019.

[47] A. S. Ethiraj, S. Jayanthi, C. Ramalingam, and C. Banerjee, "Control of size and antimicrobial activity of green synthesized silver nanoparticles," *Materials Letters*, vol. 185, pp. 526–529, 2016.

[48] A. Gholami, S. M. Mousavi, S. A. Hashemi, Y. Ghasemi, W.-H. Chiang, and N. Parvin, "Current trends in chemical modifications of magnetic nanoparticles for targeted drug delivery in cancer chemotherapy," *Drug Metabolism Reviews*, vol. 52, no. 1, pp. 205–224, 2020.

[49] F. Emadi, A. Emadi, and A. Gholami, "A comprehensive insight towards pharmaceutical aspects of graphene nanosheets," *Current Pharmaceutical Biotechnology*, vol. 21, no. 11, pp. 1016–1027, 2020.

[50] A. Abbaszadegan, Y. Ghahramani, M. Farshad, M. Sedigh-Shams, A. Gholami, and A. Jamshidzadeh, "In vitro evaluation of dynamic viscosity, surface tension and dentin wettability of silver nanoparticles as an irrigation solution," *Iranian Endodontic Journal*, vol. 14, no. 1, pp. 23–27, 2019.

[51] E. O. Mikhailova, "Silver Nanoparticles: Mechanism of action and probable bio-application," *Journal of Functional Biomaterials*, vol. 11, no. 4, p. 84, 2020.

[52] A. Roy, O. Bulut, S. Some, A. K. Mandal, and M. D. Yilmaz, "Green synthesis of silver nanoparticles: biomolecule-nanoparticle organizations targeting antimicrobial activity," *RSC Advances*, vol. 9, no. 5, pp. 2673–2702, 2019.

[53] F. Mohammadi, A. Abbaszadegan, and A. Gholami, "Recent advances in nanodentistry: a special focus on endodontics," *Micro & Nano Letters*, vol. 15, no. 12, pp. 812–816, 2020.

Hindawi
Journal of Nanomaterials
Volume 2021, Article ID 6677616, 17 pages
https://doi.org/10.1155/2021/6677616

Review Article

Uptake, Translocation, and Consequences of Nanomaterials on Plant Growth and Stress Adaptation

Shahid Ali,[1] **Asif Mehmood**,[2] **and Naeem Khan**[3]

[1]*College of Life Sciences, Northeast Forestry University, Harbin 150040, China*
[2]*Institute of Biological Sciences, Sarhad University of Science and Information Technology, Peshawar 25000, Pakistan*
[3]*Department of Agronomy, Institute of Food and Agricultural Sciences, University of Florida, Gainesville, FL 32611, USA*

Correspondence should be addressed to Shahid Ali; shahidsafi926@gmail.com and Naeem Khan; naeemkhan@ufl.edu

Received 21 December 2020; Revised 5 January 2021; Accepted 5 March 2021; Published 16 March 2021

Academic Editor: Bo Tan

Nanotechnology has shown promising potential tools and strategies at the nanometer scale to improve food production and meet the future demands of agricultural and food security. However, considering nanotechnology's potential benefits to date, their applicability has not yet reached up to field conditions. Increasing concerns regarding absorption, translocation, bioavailability, toxicity of nanoparticles, and impropriety of the regulatory framework restrict the complete acceptance and inclination of the agricultural sector to implement nanotechnologies. The biological function of nanoparticles depends on their physicochemical properties, the method of application, and concentration. The effects of the various types of nanoparticles (NPs) on plants were determined to increase seed germination and biomass or grain yield. The NPs also increased the plant's resistance to various biotic and abiotic stresses. The plant's biological functions depend on the events that occur at the molecular level. However, little progress has been made at the molecular level influenced by nanoparticles, which is an important step in evaluating potential mechanisms and plants' effects. Therefore, it is important to understand plants' underlying mechanism and response towards nanoparticles, and the gene expression changes through molecular approaches. The associations of nanomaterials with plant cells, the process of internalization, and the distribution of biomolecules using nanoparticles as a carrier are studied but not well understood. The transmission of biomolecules, such as nucleic acids, is a major obstacle due to cell walls, limiting the application of nanomaterials in crop enhancement mediated by genetic engineering. Recently, the use of different nanomaterials for nucleic acid delivery in plant cells has been published. Here, we aim to update researchers on the absorption and translocation of nanoparticles and elaborate on the importance of nanoparticles in agriculture and crop stress tolerance.

1. Introduction

Significant technical advancements and innovations have been made in recent years in agriculture to meet the growing challenges of sustainable agricultural production and food security [1, 2]. The world needs to generate 50% more food by 2050 to meet the needs of 9 billion people. This goal can only be accomplished by technical interventions to increase productivity, as land and water resources are constrained. Arable land shortage, irrigation, and reliance on conventional crops are the key concerns that have drawn the researchers' attention to using various methods. It is not surprising that attempts have been made to improve the agricultural sector using nanotechnology and nanomaterials because of nanomaterials' obvious special and incredible properties [3–5]. In particular, the use of different kinds of nanomaterials consists of metal oxides, silicates, ceramics, magnetic materials, semiconductors of quantum dots (QD), polymers, lipids, dendrimers, and emulsions [6–8]. The goals are to minimize the quantity of applied plant protection products (PPP), alleviate nutrient losses during fertilization, and maximize revenue in the agriculture sector through better nutrient management [9]. Many factors depend on the increased use of nanoparticles (NPs) in agriculture, including well-known effects, potential toxicity, monitored fate, and overdose levels. NPs can communicate with their environment, and plants are a key component of all ecosystems. Therefore, it can be concluded that NPs can communicate

with plants and that these interactions, such as their intake and their accumulation in plant biomass, will affect their environmental fate and transport [10–12]. Nanomaterials can penetrate live plant tissues, but their aggregation in the ecosystem and their effectiveness as smart delivery systems in living plants have implications. It is important to understand whether plants can consume intact NPs and transport them to other plant tissues. NPs can enter plant tissue from either the root tissues or the above-ground tissues (e.g., cuticles, stomata, hydathodes, and trichrome) as well as through root junction and wound regions.

Nanomaterials in plant science have been reported to enhance agronomic capabilities [13–15]. NPs are used as sensing materials [14, 15], herbicides, pesticides, and nanofertilizers [16, 17], improve the plant nutrients, and act as carriers for controlled release of agrochemical [18–20]. Nanomaterials also speed up plant adaptation to various climatic changes and enhance plant tolerance [21, 22]. However, certain nanoparticles (NPs) with unique physiochemical properties naturally increase plant growth and stress resistance rather than acting as nanocarriers. The biological function of nanoparticles depends on their physicochemical properties, the application method (soil, foliar, and hydroponics), and the used concentration. Nanomaterials have also demonstrated their prominent role in plant tissue in vitro cultures, such as callus induction, organogenesis, somatic embryogenesis, and secondary metabolite production [23]. Such studies suggest that plant cells can accumulate nanoparticles through their cell walls, but the mechanism is still not well understood. Although the use of nanomaterials for DNA delivery in plant cells has also been studied in the past [24], substantial developments have been made in recent years.

This study is aimed at examining in detail the role of nanotechnology in the delivery of NPs, the use of NPs in improving seed germination, and plant growth under both natural and environmental stress conditions. In addition, we elaborate the nanotechnology's current advances and associated challenges.

2. Absorption and Translocation of Nanoparticles

2.1. Mechanisms of Nanoparticle Uptake by Plants. In the soil, the NPs undergo a series of bio/geotransformations, which determine the bioavailability and toxicity of NPs. The NPs translocate to aerial portions after interacting with plant roots and accumulate in cellular or subcellular organelles. Adsorption of NPs from the soil by plant roots can be described as the first step in bioaccumulation [25]. Several researchers analyzed numerous NPs and proposed that plant accumulation occurred by root adsorption accompanied by dissemination through plant tissues by certain modifications, such as crystal phase dissolution, biotransformation, and bioaccumulation. The NP's size is directly connected to the absorption of the NPs because it is a crucial parameter that enables its entrance through cell wall pores or plant stomata. Besides, size determines their subsequent transport processes into cells (i.e., plasmodesmata) or organelles of plant cells, affecting their accumulation, toxicity, and kinetics of transport into plant cells [22]. The surface area, agglomeration, and reactivity on the cell surface or within plant structures are correlated with the NP shape [26]. To determine the specific zone of interaction between plant cell structures and NPs, the NP surface is calculated by its area and morphology, which constitute essential parameters. Due to the obvious negative charge of the cell wall, the attachment of the NPs to the surface of the plant cell relies directly on the charge of the NPs. Following the charge and particle size, the hydrophobicity present on the plant surface played a crucial role in the uptake and translocation process [27]. In addition, the basic structure of nanomaterials is complementary to the evaluation of their effect on NP absorption, translocation, and aggregation in the plant [28]. The above facts demonstrate the need to standardize laboratory experiments to assess NPs in plant tissues at various levels to determine the exact effect of NPs supported by their physical-chemical properties [29]. Therefore, to understand and elucidate the absorption, translocation, and accumulation processes, a detailed study on the nature of the NPs is needed. To determine their movement and localization to various structures and cell organelles within the plant, monitoring and tracking NPs are important.

The small NPs (diameters range from 3 to 5 nm) are reported to penetrate plant roots along with osmotic pressure, capillary forces, or passing directly through the root epidermal cells [30, 31]. The epidermal cells of the root cell wall are semipermeable containing small pores and restrict the large NPs. Some NPs induced new pores in the epidermal cell wall, which facilitated its entrance [30, 31]. After crossing the cell walls, NPs are apoplastically transported through extracellular spaces until they reach the central vascular cylinder, allowing the xylem to move unidirectionally upward. NPs, however, need to symplastically cross the Casparian strip barrier to enter the central vascular cylinder (Figure 1). This happens by binding to the endodermal cell membrane's carrier proteins through endocytosis, pore formation, and transport. NPs travel from one cell to another through the plasmodesmata as internalized in the cytoplasm [22, 32]. The NPs unable to internalize are aggregate on the Casparian strip, while the NPs that have reached to xylem are transferred to the shoots and through the phloem back to the roots [32, 33]. NPs taken up by plants may be found within the epidermal cell wall, cortical cell cytoplasm, and nuclei [33]. NPs that are not taken up on the soil aggregate's root surface can modify the absorption of nutrients [34]. Direct absorption of NPs in seeds can occur by entering the coat via parenchymatic intercellular spaces, accompanied by diffusion in the cotyledon [22].

The NPs applied by the leaves can enter the leaves through the stomata or cuticles. The cuticle acts as a primary leaf barrier, restricting the entry of NPs to a size of <5 nm. The NPs > 10 nm enter through stomata, and their cellular transport is occurring through apoplastic and symplastic routes into the vascular system of the plant [34]. The transfer of NPs (between 10 and 50 nm) is favored through the adjacent cell's cytoplasm (symplastic route). Thus, larger NPs (between 50 and 200 nm) are translocated between the cells

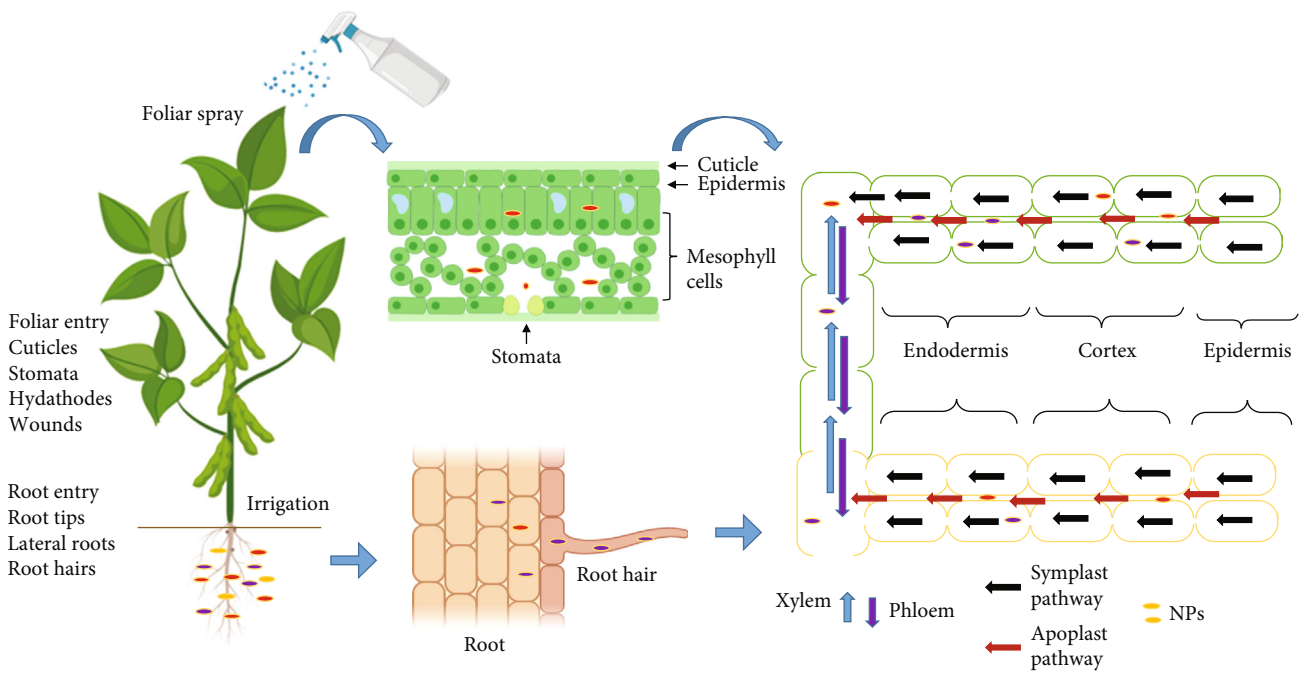

Figure 1: Schematic presentation of nanoparticle uptake through different routes and their translocation pathways in different plants' parts.

(apoplastic route). Internalized NPs are transported along with the sugar flow through the phloem sieve tubes. As a result of vascular transport by phloem, NPs can travel bidirectionally and accumulate in roots, stems, fruits, grains, and young leaves to varying degrees because these organs serve as potent sinks for the sap [22, 26, 28, 34]. The apoplastic passage is known as a nonselective direction of least resistance. It is widely agreed that many water nutrients and nonessential metal complexes favor the apoplastic route for translocation [35]. The application methods, size, concentration, and climate are the essential factors that determined the effective adsorption of NPs after foliar application [26]. Leaf morphology and its chemical composition, the presence of trichrome, and existence of leaf exudates and waxes are essential factors that affect the trapping of NPs on the surface of the leaf [36].

It is important to introduce NPs of high purity and stability to the physiological environment. The accumulation rate of NPs by the root of plants may be impacted by environmental conditions and the properties of NPs. Previous studies reported that the application of silver sulfide (Ag2S) NPs in combination with potassium chloride and ammonium thiosulfate significantly enhanced the concentration of Ag NPs in the shoot and roots of *Lactuca sativa*. (Table 1) [37]. Soil organic matter decreased cerium dioxide (CeO_2) NPs through roots in *Zea mays* (*Z. mays*) [38].

2.2. Mechanism of Nanoparticle Translocation in Plants. Studies attempted to establish the mechanisms involved in plant structures or cell organelles in the absorption, translocation, and accumulation of various NPs [27]. The translocation and accumulation of NPs in the plant depend on the plant cells' physiology and structure, the nanomaterial interaction with the soil, and the nature and stability of the NPs [39]. The cell wall of plants serves as a specific barrier that regulates the entrance of NPs into the cell and determines the ability to solubilize and allow the passage of NPs according to their nature [40, 41]. The majority of studies report that the size of the cell wall's pore is the key constraint on the entrance of NPs into the plant cell. The size of NPs is 40-50 nm to penetrate the cell from the plant surface [42]. The nature of the NPs is a second restriction factor impacting their penetration through the cell wall and cell membrane or promoting attachment to the radical surface or radical exudates [43]. The positive charging of NPs can improve their adhesion to the cell wall. Besides, morphology and NP coating can play a significant role in their behavior on the rhizosphere and their action on plants.

The nanoparticles accumulated by plant roots translocate to different tissues in the plant's aerial part, including newly developed seeds [22]. Plant characteristics and NPs all play a crucial role in the translocation of NPs. For example, previous studies have shown that gold (Au) NPs can accumulate in the shoot of *Oryza sativa* (*O. sativa*). In contrast, it cannot accumulate in the shoot of *Cucurbita pepo* and *Raphanus raphanistrum* [44]. Furthermore, plant roots take up the positively charged Au NPs most quickly.

In contrast, negatively charged Au NPs are translocated from the roots more resourcefully into plant shoots. Previous studies reported that titanium dioxide (TiO_2) and silicon dioxide (SiO_2) are the most stable NPs and can be found in their immaculate speciation in plant tissues [57, 58]. NPs like copper (II) oxide (CuO), CeO_2, lanthanum oxide (La_2O_3), and nickel oxide (NiO) are capable of transformation through disparity, resulting in accumulated plant speciation changes. The transformations of zinc oxide (ZnO) NPs were determined using synchrotron X-ray absorption (XAS) spectroscopy during exposure to different plants [59]. In *Z. mays*,

Table 1: Accumulation of NPs in various crop tissues.

NPs	Crops	Concentration (mg/L ∗ mg/kg)	Accumulation (mg/kg) Roots	Shoots	References
Ag-based	*O. sativa*	1000	20	5	[45]
	Glycine max	4000	2102	1135	[46]
	Solanum lycopersicum	250	—	50	[47]
Cu-based	*O. sativa*	1000	1544.1	17.27	[48]
	B. juncea	1500	190.4	—	[49]
	Cajanus cajan	20	5.82	19.06	[50]
	Vigna radiata	125	—	18.46	[51]
	L. sativa	250	3773	—	[52]
	Phaseolus vulgaris	100	800	—	[53]
ZnO	*S. lycopersicum*	1000	—	250	[54]
	Z. mays	100	10	30	[55]
$Mg(OH)_2$	*Z. mays*	1000	103	131	[56]
TiO_2	*S. lycopersicum*	1000	—	250	[54]

the maximum accumulation of Zn occurs in the roots and shoots under the hydroponic exposure of ZnO NPs in various forms such as Zn-phosphate. It may be due to increased dissolution in the rhizosphere, plant absorption, and translocation of Zn in the ionic form [55]. Comparable Zn accumulated speciation was also observed in soil-grown wheat crops [60, 61].

Translocation from the soil of ZnO and CeO_2 NPs into *Glycine max* (*G. max*) had been observed. The CeO_2 NPs were revealed to be translocated in the form of NPs, and Zn biotransformed into Zn-citrus inside plant tissue [46]. The transport of CuO NPs from roots to shoots via xylem took place in *Z. mays* and could be further translocated from shoots back to roots via the phloem back to roots [33]. Previous studies concluded that NP TiO_2 plays a role in the translocation in the *Triticum aestivum* (*T. aestivum* spp.). They proposed that a threshold diameter of 140 nm, above, cannot accumulate in the root. In addition, a threshold diameter of 36 nm can accumulate in the root parenchyma, could not reach the stele, and cannot be translocated into the shoot of *T. aestivum* [62].

3. Mechanisms of Nanoparticle and Plant Interaction

3.1. Effects of Nanoparticles on Plants. The NPs enter the plant system by several routes, mainly through roots and leaves. NPs interact with plants at cellular and subcellular levels after entry, promoting changes in morphological and physiological states [63]. These interactions may be positive or negative, depending on the nature of the NPs and the plant species. The chemical nature, reactivity, size, and specifically concentration of NPs in or on the plant could determine NPs' effects on plant systems [64]. The researchers used various NP application methods, such as soil application, foliar spray, or seed treatment, to examine the impact of nanoparticles on seed germination or in plant growth. Available evidence has shown that different NPs can promote seed germination [65] and plant growth and development [66–68] at concentrations below certain limits. These studies were mostly performed under artificial treatment conditions such as plate growth medium and hydrophobic or pot conditions. To understand the impact of nanoparticles on plant growth, we discuss nanoparticle's positive impact on plant seed germination and plant growth and the positive effects of NPs to improve plant stress tolerance.

3.2. Seed Germination. Germination of seeds provides a basis for the productivity, growth, and development of plants. A natural method of germination takes time, and the yield obtained is not very high indeed. But high germination has been accomplished in the case of treated seeds, making nanotechnology a potent technique for improving both germination and yield. To monitor the ability of nanoparticles to enhance germination, numerous researches have been done. The mechanism underlying the process by which NP treatments increase seed germination rates is still unclear. The NP treatments improve seed absorption and water retention; it may be attributed to increasing seed germination [69]. The tomato seeds were inoculated to media with carbon nanotubes (CNTs); after 2-day incubations, the seeds' moisture content was treated with CNTs containing 19% more than untreated seeds. These findings suggested that the CNTs promote the uptake and retention of water. The mechanism is not fully understood; maybe the CNTs create microspores [70], and water permeation channels into the seed coats [69]. It is assumed that CNTs regulate the aquaporins (AQPs) in the seed coats. The AQPs are membrane proteins and act as a water channel in the cell membrane.

Compared to the control condition, the TiO_2 (10 ppm concentration) on wheat displayed the lowest germination duration. In contrast, the shoot and seedling length was sufficiently higher at 2-10 ppm nanosized TiO_2 than that of the control [71]. However, higher TiO_2-based NP concentrations

had an inhibitory or no effect on wheat. Another research stated that the germination of aged spinach (*Spinacia oleracea*) seeds was accelerated by the nano-TiO_2 treatments at proper concentrations [72]. The *Cicer arietinum* showed that the application of nanorod hydroxylapatite (HAP) resulted in improved germination and increased growth of the plant. The better performance relative to control and other doses was found in the presence of 1 mg/mL Hap-nanorod [73]. Soybean seeds treated with super dispersive nanocrystalline powders of cobalt, iron, and copper in a zero-valent state under laboratory conditions showed increased germination frequencies relative to control conditions [74]. Data of the germination and growth impact of Ag NPs on 11 wetland plant plants, including *Eupatorium fistulosum*, *Panicum virgatum*, *Carex lurida*, *C. scoparia*, *Lolium multiflorum*, *C. vulpinoidea*, *C. crinita*, *Scirpus cyperinus*, *Phytolacca americana*, *Juncus effusus*, and *Lobelia cardinalis*, belonging to six distinct families has been shown to have differential responses to different species [75]. Accelerated seed germination was shown by the treatments of single-walled carbon nanohorns (SWCNHs) in six crop species: rice, barley, switchgrass, wheat, soybean, maize, tobacco, and tomato cell cultures [76].

3.3. Positive Impact of Nanoparticles on Plant Growth and Yield. In crop plant, the beneficial role of nanoparticles has been demonstrated: increased seed germination [77], increased shoot and root length [78], increased fruit production, improved metabolite content [79], and a substantial increase in seedling and plant vegetative biomass in many crops (Table 2). Similarly, the effect of nanoparticles has also been documented on several biochemical parameters related to plant growth and development, by increasing the nitrogen usage efficiency and enhancing the photosynthetic rate in several important crops plant, including peanuts [80], spinach [81–83], and soybeans [74]. Nanoparticles are also known for their role in improving the nutrient consumption and resistance of plants to various diseases and abiotic stresses [84]. NPs are capable of influencing plant growth and development by altering some of the physiological processes in plants. Most studies indicate that NPs can cause toxic effects above a certain concentration, and experiments based on plant toxicity evaluated their effect on the germination rate and biomass accumulation [85]. Some research has shown that NPs might also have significant effects on plants [86, 87].

The CNTs showed 100% germination in *Brassica juncea* and *Phaseolus mungo* at all concentrations and displayed a large increase in root length and amount of root hairs at 20 ppm, although a slight decrease in the number of root hairs was found at a higher concentration of 40 ppm [88]. In the seeds of *Cicer arietinum*, ZnO NPs improved the germination and growth rate [89]. In chickpea and mung at an optimal concentration of ZnO NPs, root and shoot growth improved while negative effects were observed after a certain concentration [90]. Low concentration (2 and 10 ppm) of TiO_2 NP has been shown to benefit wheat seedlings in terms of shoot lengths, higher TiO_2 NP concentrations have neutral effects, and TiO_2 bulk has inhibitory effects [91]. At a dose of 15 kg/ha of silica NPs, growth parameters such as several shoots and roots, stem height, stem diameter, leaf area, and root length of maize seedlings showed significant positive effects. In comparison, 20 kg/ha did not affect growth parameters [92]. Iron oxide (FeO) NPs are documented to promote the growth of wheat seedlings at a concentration of 100 ppm, while a high concentration of the same NPs decreased the rate of germination, root biomass, and mean time of germination [93].

Carbon dots (1.0 mg/mL) can play an important role in facilitating the growth of mung beans as they boost the beans' ability to consume and use nutrients more effectively [94]. The specific optical properties of carbon dots allow them to be transported by the vascular system through apoplastic pathways from the roots to the stems and leaves [94]. The calcium carbonate NPS accelerates growth parameters such as seed germination, root and shoot length, seedling vigor index, fresh and dry mass, and relative water content of mung (*Vigna mungo*) [95].

The positive effects of engineered nanomaterials (ENMs) on plants have also been identified as helping plants to consume more usable nutrients from fertilizers or soil water. For example, nano-ZnO in the mung bean rhizosphere has been confirmed to significantly increase the available form of P, soil microbial population, and root volume. This may be confirmed by the increased dehydrogenase activity, which is a measure of microbial activity and soil absorption of P by plants. The soil-developing microbes help maintain soil quality and structure for regular nutrient biogeochemical cycling [28]. In the plant cell, nano-ZnO is transformed into Zn_2+ ions and regulates carbonic anhydrase activity for CO_2 fixation to carbohydrates. Zinc can be used as a cofactor for several enzymes, such as catalase and superoxide dismutase, to prevent oxidative damage to plant cells [28]. SiO_2 also increases the activity of nitrate reductase in combination with TiO_2 NPs. It acts as a key point in the reduction of nitrate (NO_3-) to nitrite (NO_2-) and improved plant absorption ability to improve fertilizer and water uptake [96]. The foliar application of ZnO NPs had a beneficial impact on tomato plant growth. It, therefore, opened up the question of the possible use of ZnO NPs as a future nanofertilizer. Likewise, foliar spray of ZnO NPs in pot-grown plants at 20 mg mL^1 increases biomass production [97]. TiO_2 NPs have a beneficial effect on spinach growth by increasing the activity of Rubisco activase enzymes and enhancing the absorption of light or reducing the chloroplast oxidative stress caused by ultraviolet radiation during photosynthesis [98]. The anatase crystalline form of TiO_2 NPs exhibits the highest catalytic activity, facilitating chlorophyll and carotene synthesis in *Cucumis sativus* (*C. sativus)* [99]. Titanium dioxide enhanced the light absorption in chlorophyll-a molecules, oxygen evolution, and electron transfer rate in spinach leaves; TiO_2 NPs encourage chloroplast activity and Hill reaction [100].

The cerium (IV) oxide CeO_2 NPs increased stem elongation at 1-10 mg mL^{-1}, and a significant improvement in fruit weight was observed at 10 mg L^{-1} [101]. Higher CeO_2 NP concentrations (500 mg kg per 1) culminated in rapid shoot development with increased biomass of 31% in barley. On

Table 2: The positive responses of nanomaterials on plant growth.

Nanomaterials	Concentration	Size (nm)	Effects on plants	Crops	References
CuO	500 mg kg^{-1} sand culture		Increased biomass	*Triticum aestivum*	[60]
SiO_2	5 mM	4-10	Increased shoot biomass and grain weight	*Oryza sativa*	[104]
SWCNT	325, 1750 mg L^{-1}	8	Increased the root length	Onion and cucumber	[105]
MWCNT	49 μg mL^{-1}		Uptake nutrients (Zn, Mn, K, Ca, and Fe)	*Lycopersicon esculentum*	[106]
TiO_2	0.01-0.05%	4-6	Enhanced growth, increased glutamate dehydrogenase, and glutamic pyruvic transaminase activity	Spinach	[107]
TiO_2	300-1000 mg L^{-1}	30	Inhibition of hydraulic conductivity	*Zea mays*	[108]
TiO_2	1000 mg L^{-1}		Chlorophyll content	*T. aestivum*	[109]
Activated carbon-based TiO_2	0-500 mg L^{-1}	30-50	Improved germination	Tomato	[110]
ZnO	20 ppm foliar spray	1.2-6.8	Increased biomass	Mung bean	[111]

the contrary, soil supplemented with low CeO_2 NP concentrations (125 and 250 mg kg^1) stimulates grain production, whereas significant amounts of Ce are accumulated in grains and leaves. Besides, iron oxide NPs (IONPs) have been observed to increase the dry weight of soybean pods and leaves. IONPs have also been known as iron facilitators and aided in the transfer of iron photosynthate to peanut leaves, while IONPs increased root elongation in pumpkin, which is due to iron dissolution [96]. IONPs greatly encouraged tomato plant growth but caused green biomass to decrease [102]. The measurement of organic nitrogen in plant roots indicates that 51.1% of nitrogen (N) was present in roots relative to control [103], an indicator that TiO_2 NPs mediate the promotion of root growth by promoting N accumulation.

3.4. Positive Effects of Nanoparticles on Photosynthesis. Photosynthesis is the essential mechanism that converts light energy to chemical energy for plants on earth. All living things rely on photosynthesis either directly as their energy source or indirectly as their food's ultimate energy resource. In chloroplasts, the light source of energy is converted into a chemical form using chlorophyll, H_2O, and CO_2 as raw materials and stored in sugar molecule bonds. Several studies report that foliar application of metal NPs dramatically improves the content of chlorophyll in plants, enabling plants to synthesize more complexes for light harvesting to absorb more light energy and improve photosynthesis. TiO_2 is the most studied NP because it has a photocatalytic quality and can activate an oxidation-reduction reaction, contributing to the charge transfer between light-harvesting complexes II and TiO_2 NPs [112]. The effect of TiO_2 NPs on the photosynthetic efficiency of spinach has been reported, indicating that TiO_2 NPs can increase light absorption and accelerate light energy transport and transformation. Furthermore, due to the delay in the successful photosynthetic tenure of chloroplasts, TiO_2 NPs will prevent chloroplasts from aging. Nanoanatase TiO_2 enormously improved the electron transport chain, O_2-evolving and photophosphorylation activity, and PSII photoreduction function of chlorophyll in spinach under both visible and ultraviolet (UV) radiation [113]. Also, the soluble protein and chlorophyll content of the ZnO NP-treated plants increased by 25% and 34.5%, respectively, compared to those of the control [114]. Chlorophyll content increased from 62.67 to 227.42% with an aerosol-foliar spray with rising concentrations of TiO_2 NPs up to 500 mg kg1. The transfer of TiO_2 NPs in soil induces a maximum increase in chlorophyll content of 216.29% at a concentration of 750 mg kg^{-1} [54].

In *A. thaliana*, TiO_2 NP-treated plants have 3.83 times greater light-harvesting complex II (LHCII) content as compared to the control. The TiO_2 NPs improve the expression of LHCII b genes which play a key role in promoting chloroplast light absorption, regulating the distribution of light energy from photosystem I (PSI) to PSII by increasing the content of LHCII and accelerating the conversion of light energy to electronic energy, water photolysis, and oxygen evolution [115]. Zn is an essential plant micronutrient, whereas ZnO NPs have increased the content of chlorophyll in peanuts (1000 mg/kg) [80]. Specific ZnO NP concentrations have been found to boost the qualitative and quantitative characteristics of plants and to have higher PSII fluorescence kinetics (Phi-E0, Psi-E0, and PIABS) and lower energy flux parameter values (ABC/RC, TR0/RC, DI0/RC, and ET0/RC) [116]. In an in vitro model, manganese NPs are found to be involved in enhancing the photosynthetic electron transport rate and oxygen evolution [117]. Nanoiron, either alone or in combination with nanomagnesium, has been reported to have a major impact on chlorophyll's content [118]. In addition, the single-walled carbon nanotubes (SWCNTs) increased the rate of photosynthesis three times higher than the control by penetrating and accumulating in the lipid envelope of the extracted plant and increasing the rate of electron transport via a process consistent with amplified photoabsorption [119].

The rate of photosynthesis was significantly increased by SiO_2 NP treatments due to increased activity of carbonic anhydrase and photosynthetic pigment synthesis [120]. Treatment with ZnO NPs for 30 minutes (at 8 mg/L) has been reported to significantly increase the rate of photosynthesis and chlorophyll content, as well as increase the activity of carbonic anhydrase in tomato plants [121]. The increased rate of photosynthesis by nanoanatase TiO_2 in spinach was found to be due to the accelerated activity of Rubisco and Rubisco activase that enabled the carboxylation of Rubisco [122] (Figure 2). Rubisco activity has also been shown to be very sensitive to Ag NPs [123]. The treatments of iron sulfide NPs have been documented to enhance the growth and yield of the plant due to the activation of the Rubisco small subunit (*Rubisco S*) and Rubisco large subunit (*Rubisco L*) genes [124].

4. Role of Nanoparticles in Plant Stress Tolerance

Plants can adapt or cope with unfavorable conditions such as drought, salinity, chilling, and heat stress. Plant response to such abiotic stress is extensively studied at the cellular and molecular level [125]. A transitory provocation of cytoplasmic Ca^{2+}, ROS, abscisic acid, and increased mitogen-activated protein kinase (MAPK) pathways are included in the preliminary response of plants against abiotic stresses [126]. The advanced stage of stress response involves modulating proteins involved in cellular damage protection and regulating stress-specific gene expression.

Advances in nanomaterial engineering indicate that in existing adverse environments, nanofertilizers can improve the crop yield. In about 23% of the world's cultivated lands, salinity stress strongly limits crop production [127]. The SiO_2 NPs improve germination of seeds and increase plants' fresh and dry weight and chlorophyll content with proline accumulation under NaCl stress in tomatoes [128, 129]. The foliar spray of iron sulfate ($FeSO_4$) NPs exhibits a positive response in sunflower cultivars to salinity stress tolerance. The application of iron (II) sulfate ($FeSO_4$) NPs not only increased the leaf area, the net assimilation rate of carbon dioxide (CO_2), the chlorophyll content, the dry weight of the shoot, the substomatal concentration of CO_2, the maximum photochemical efficiency of photosystem II (Fv/Fm), and the iron (Fe) content but also decreased the significant content of sodium (Na) in the leaves [21]. Titanium dioxide (TiO_2) nanoparticles were stimulatory to the expression of antioxidant enzymes in onion seedlings, and the activity of antioxidant enzymes was further increased when TiO_2 NPs were applied in combination with Ag NPs. The low TiO_2 concentration increased seed germination and onion seedling growth, while the effect was reversed at the higher concentration (suppressed). In addition to superoxide dismutase, which displayed concentration-dependent increases, hydrolysis enzyme (amylase), catalase, and peroxidase activity were significantly induced, while enzyme activity was higher at lower TiO_2 concentrations (10-30 μg/mL) and decreased at higher TiO_2 concentrations (40 and 50 μg/mL) [130]. The use of titanium nanoparticle foliar application on wheat to mitigate the negative impact of drought stress has also demonstrated positive results for some agronomic characteristics such as starch and gluten. The findings indicated that the application of 0.02%t TiO_2 nanoparticles showed improvement in different agronomic characteristics, i.e., plant height, ear number, ear weight, number of seeds, final yield, biomass, gluten-included harvest index, and drought stress starch content [131]. Silicon can potentially be used to alleviate to some degree the effects of drought stress. Previous studies found that exposure to low sodium silicate concentrations (1.0 mM) could moderately alleviate the adverse effects of wheat drought stress. Although the precise mechanism is unknown, silicon partially improves shoot growth, increases the content of leaf chlorophyll, and retains the capacity of leaf water in stressed plants. In addition, in wheat, it also decreases membrane lipid peroxidation [132].

It has also recently been investigated that silicon nanoparticles (SiNPs) can efficiently alleviate UV-B-induced wheat stress [22]. By controlling Cd accumulation, the foliar application of nano-Si at 2.5 mM concentration greatly increases Cd stress resistance in rice plants. Nano-Si fertilizers may seem to have an advantage over conventional fertilizers in reducing the accumulation of heavy metals [40, 133]. Despite various experiments on the stimulation of plant growth and stress resistance caused by nanomaterials, the underlying mechanisms remain largely uncovered [19]. The use of nanomaterials such as nano-ZnO or nano-SiO_2 improves the accumulation of free proline and amino acids, the absorption of water and nutrients, and the activity of antioxidant enzymes such as catalase, glutathione reductase, nitrate reductase, superoxide dismutase, and peroxidase, which improve the plant tolerance to the extreme conditions [134] (Figure 3). Furthermore, nanomaterials affect the expression of stress-related genes. For example, the application of Ag NPs in *Arabidopsis* microarray analysis shows that a variety of genes that play an important role in stress tolerance have been upregulated or downregulated [135]. The upregulated genes are a large part of the response to metals and oxidative stress (cation exchanger, superoxide dismutase, peroxidase, and cytochrome P450-dependent oxidase). In comparison, downregulated genes, including systemic acquired tolerance, ethylene signaling, and auxin-regulated genes implicated in growth and organ size, are linked to the response to pathogens and hormonal stimuli [136]. In plants, certain nanomaterial-induced responses are directly involved in defense against various environmental stresses. The response of plants to nanofertilizers depends on the plant species, their growth and development stages, and the type of nanoparticles [137]. Further study is required that this technology reaches the farm gate to identify signaling pathways and regulation of gene expression by specific nanomaterials in different plant species.

Farmers have been highly dependent on pesticides to minimize crop losses, negatively affecting the environment's sustainability and human health. Recent studies have shown that nanomaterials can effectively reduce the risks of pests and diseases, thereby reducing the incidence of yield losses and environmental risks. For example, the biosynthesized Ag NPs obtained from the *Gossypium hirsutum* stem extract

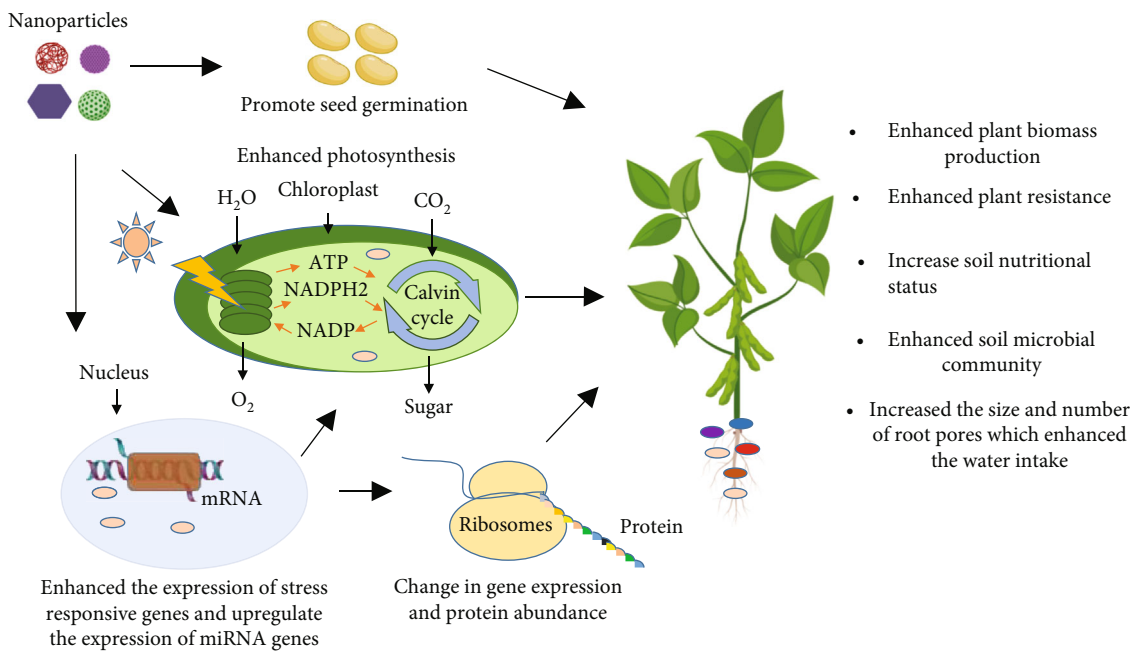

Figure 2: Positive effects of nanoparticles on plant growth and development. The optimum concentration of nanoparticles causes an alteration in different physiological processes to increase seed germination and photosynthesis of the plants. Further, the nanoparticles alter the gene expression of different genes and miRNAs that have a positive impact on stress tolerance and plant biomass.

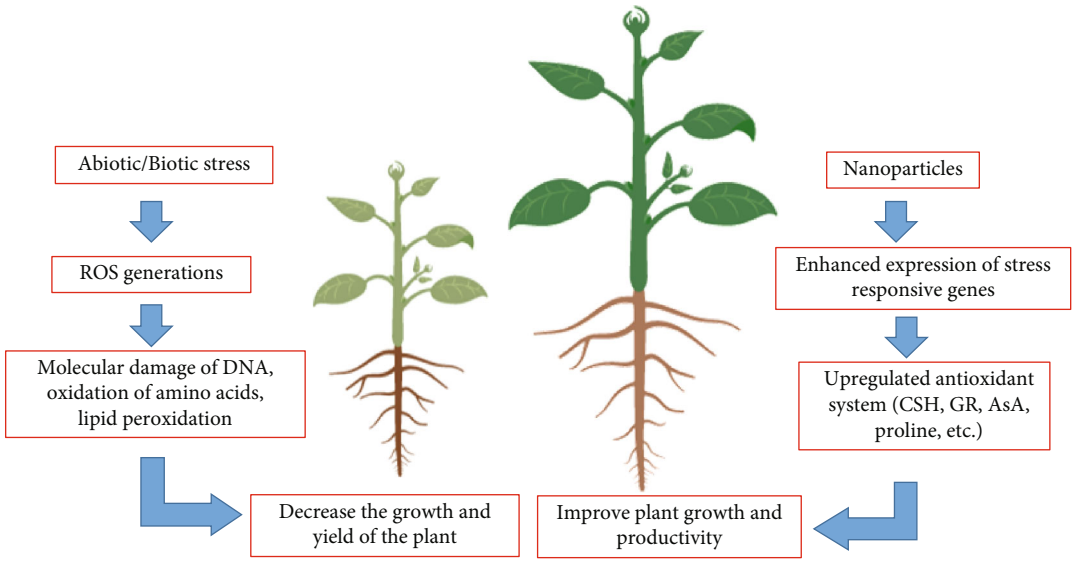

Figure 3: General mechanisms of nanoparticles increase the mitigating ability of plants under different stress environments.

have good antibacterial activity, as shown by the inhibition zone for *Xanthomonas campestris* pv. *campestris* and *Xanthomonas axonopodis* pv. *malvacearum*, two of the Malvaceae and Brassicaceae family's largest bacterial pathogens [138]. The metal oxides ZnO, CuO, and MgO could also effectively regulate many plants and soil-borne pathogen such as *Alternaria alternata*, *Botrytis cinerea*, *Colletotrichum gloeosporioides*, *Fusarium solani*, *Monilinia fructicola*, *Fusarium oxysporum* f.sp. radicis lycopersici, *Ralstonia solanacearum*, *Verticillium Dahliae*, and *Phytophthora infestans* in different plant species [139–142]. The use of the fungicide Antracol with Ag-incorporated nanocomposites (Ag@CS) has improved antifungal efficacy relative to being used alone [19].

By reducing plant membrane disruption and ion leakage, TiO_2 nanoparticles maintain the ability to decrease the negative impact of chilling tension. Photosynthesis is the plant system's integral process that is very sensitive to chilling stress [143]. The chilling stress damages the plant photosystem, reduces the chlorophyll content, absorption of CO_2, and transpiration rate, and degrades the photosystem enzyme (Rubisco) [115]. The effect of nanoparticles on the

photosystem has been achieved by increasing Rubisco enzyme production and chloroplast light immersion capacity [115] and inhibiting ROS production [119]. Exposure to TiO_2 nanoparticles increases the expression of the Rubisco and chlorophyll-binding protein gene [144], leaf pigments, and antioxidant enzyme activities [145] and improves resistance to stress chilling. Plants suffering from cold stress upregulated the genes $MeAPX_2$ and MeCu/ZnSOD and increased the activities of dehydroascorbate reductase, monodehydroascorbate reductase, and glutathione reductase that scavenge ROS, resulting in repressed oxidative stress, i.e., lipid peroxidation, degradation of chlorophyll, and production of H_2O_2, eventually ensuring stress tolerance [146]. However, increased growth and biochemical physiognomies of plants exposed to cold stress have been shown by nanoparticle exposure along with chilling stress. The low concentration of selenium (Se) nanoparticles decreased the impact of heat stress by improving the chlorophyll content, hydration ability, and plant growth [147]. The low concentration of Se nanoparticles shows plant antioxidant activities, while oxidative stress is caused by the high concentration of Se nanoparticles [148]. Plants also synthesized several heat shock proteins and molecular chaperones during heat stress. Heat shock proteins help other proteins in maintaining their constancy in stress environments and are involved in heat stress tolerance [149]. Multiwall carbon nanotubes have been documented to be involved in upregulating gene expression of heat shock proteins, such as HSP90 [150].

4.1. Molecular Mechanism of Nanoparticles to Mitigate Environmental Stresses. Plants are influenced by different environmental stresses during their life cycle and thus improve their defense against environmental stress at different stages by modulating genetic, biochemical, and physiological pathways. Plants adopt molecular routes by sufficient modification of gene expressions to cope with these stresses. Several studies have shown that the induced impact of nanoparticles on plant growth and development depends on their concentration. In plants, the signaling network stimulates the defensive system, which triggers the molecular mechanism to respond to specific stress conditions. Calcium ions involved in the transduction of signals under varying stress environments act as a second messenger [151]. Sensitivity to stress signals causes the enrichment of calcium ion level in the cytosol through calcium ion channels, which is recognized by calcium ion-binding proteins that trigger alterations in gene expression as well as plant adaptation to stress conditions [152, 153]. Nitric oxide (NO) has been shown to cause the enhancement of cytosolic calcium ions in plant cells under various biotic and abiotic stress conditions [152, 153], and thus, calcium ions persuade the synthesis of nitric oxide [154]. In *O. sativa*, the Ag nanoparticle treatment on roots showed that the nanoparticles were involved in responsive protein regulation and signaling of calcium ions, transcription, protein degradation, oxidative stress response pathways, cell wall synthesis, and cell division [155]. Ag nanoparticles are also documented to bind to calcium ion channels or Ca_1/Na_1 ion pumps through calcium ion receptors that influence cell metabolism. Besides, the association of C60 nanocrystals induced the functional regulation of Ca_1/calmodulin-dependent protein kinase II [156]. In addition, cadmium sulfide QDs induced overexpression of calcium-binding protein CML45 and calcium-dependent protein kinase 23 in *A. thaliana*. These calcium-binding proteins have been shown to regulate stress responses, and their overexpression increased plant tolerance to many abiotic stress conditions [157]. The stimulation of calcium ions by nanoparticles revealed that nanoparticles impersonate calcium ions and bind to calcium-binding proteins that activate the cascade of genes that respond to stress [158].

The exposure to zero-valent iron nanoparticles in *A. thaliana* upregulated the gene expression of *AHA2*, which is involved in stomatal opening and enhanced the tolerance of drought [159]. In *A. thaliana*, the gene expression analysis of RT-PCR and the whole-genome microarrays of cDNA expression provided new insights into the molecular mechanisms of plant responses to Ag NPs [160]. Analysis of the whole-genome cDNA microarray revealed upregulation of 286 genes, including genes mainly associated with metal and oxidative stress (e.g., cytochrome P450-dependent oxidase, vacuolar cation/proton exchanger, peroxidase superoxide, and dismutase), and downregulation of 81 genes, including plant defense and hormone stimulus genes [155]. In *A. thaliana*, the effect of zinc oxide (ZnO) [161], fullerene soot (FS), or titanium dioxide ($nTiO_2$) nanoparticles on root gene expression showed 660 up- and 826 downregulated genes, 232 up- and 189 downregulated genes, and 80 up- and 74 downregulated genes, respectively (translation gap >2-fold). The ZnO and FS mediated genes predominantly ontological groups annotated as stress responsive, including abiotic responsive genes such as drought and salinity as well as biotic genes including pathogen defense and wounding stimuli [69].

The miRNAs have been involved in the control of plant and animal biological processes and play an important role in plant responses to abiotic and biotic stresses [162]. In *A. thaliana* and *N. tabacum*, the microRNA (miRNA) gene expression was analyzed. The microRNAs are small noncoding RNAs (22-24 nucleotides), which regulate the posttranscriptional gene expression by inhibiting mRNA translation to peptides or degrading mRNA [163]. The miRNAs have been reported to mediate the stress-responsive gene expression during salt and water stress by modifying gene expression. In a tobacco cell, the nanotube stimulates the growth and gene expression [164]. It has been reported that miRNA genes are upregulated and played an important role under Al_2O_3 NP stress. With increasing concentrations of Al_2O_3 NPs, the expression of nine miRNAs (miR159, miR162, miR167, miR169, miR395, miR396, miR397, miR398, and miR399) was significantly upregulated [162, 163].

5. Nanomaterials for Genetic Engineering

Climate change and an increasing world population and genetic modification of plants have improved crop production by conferring desirable genetic traits to crops. The plant cell walls act as a barrier in the delivery of exogenous molecules into plant cells. Various strategies based on

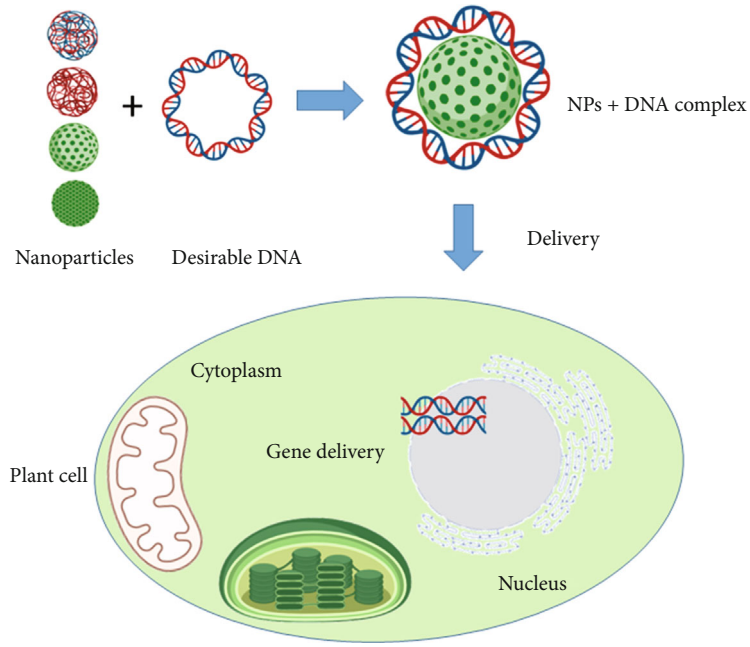

Figure 4: Graphical presentation of nanomaterials acting as a substitute of conventional gene delivery systems for plant genetic engineering.

Agrobacterium transformation or biolistic approaches are used worldwide for DNA transmission in plant cells to conquer this challenge and achieve plant genetic transformation. Limitations to these techniques are based on limited host range and extensive damage to plants, often preventing the plant development. Genetic engineering, although there is advancement in plants, has lagged and recently seen significant advancements. There are relatively fewer plants than the various and complex gene and protein distribution methods developed for animal systems. In general, modern plant genetic transformation requires two main steps: the distribution of genetic delivery and regeneration of the transformed plant, the requirement and complexity of the latter being strongly dependent on what method of delivery is used and how much the transformation is stable. There are three components of regeneration procedures: the induction of competent totipotent tissue, callus-forming tissue culture, and selection and progeny segregation.

Several of the pioneering experiments in nanomaterial-based plant genetic engineering have been carried out in plant cell cultures. Nanoparticles are attractive materials for biomolecule transmission due to their ability to penetrate plant cell walls without external force, wide host range applicability, and highly tunable physicochemical properties.

For instance, a good approach to delivering DNA in different calli (maize, soybean, tobacco, rice, and cotton) has been documented as silicon carbide-mediated transformation [165, 166]. Although lagging behind the progress made in animal systems, findings recently published in plants suggest that NMs can transcend the cell wall barrier in adult plants and reduce the limitations of current transgene delivery systems. One seminal study showed that dsRNA of various plant viruses could be loaded on nontoxic, degradable, layered double hydroxide (LDH) clay nanoparticles or BioClay. The dsRNAs and/or their RNA breakdown products offer protection in sprayed tobacco leaves against the Cauliflower Mosaic Virus (CMV), but they also confer systemic protection of the viral challenge to newly emerged, unsprayed leaves 20 days after a single tobacco spray procedure [167]. An effective, stable genetic transformation via magnetic nanoparticles (MNPs) has been achieved in cotton plants. The β-glucuronidase (GUS) reporter gene-MNP complex has been magnetically infiltrated into cotton pollen grains without affecting the pollen's viability. Cotton transgenic plants were successfully produced by pollination with magnetofected pollen, and exogenous DNA was successfully incorporated into the genome, effectively expressed, and stably inherited in the self-acquired offspring [168]. The scaffolds of carbon nanotubes applied by infusion to external plant tissue were used to transfer linear and plasmid DNA and siRNA into *E. sativa* protoplasts and *T. aestivum*, *Gossypium hirsutum*, *Eruca sativa*, and *Nicotiana benthamiana* leaves resulting in a high transient expression of Green Fluorescent Protein (GFP). The small interfering RNA (siRNA) was additionally supplied to *N. Benthamiana* plants that constitutively expressed GFP, allowing the gene to be silenced by 95% [169]. The first and most promising approach to mesoporous silica nanoparticle- (MSN-) mediated genome editing has recently been proposed. MSNs are used as carriers in *Zea mays* immature embryos to transport Cre recombinase, carrying loxP sites incorporated into chromosomal DNA. The loxP was correctly recombined after the biolistic application of engineered MSNs in plant tissues, establishing an effective genome editing [170]. As such, NP-based biomolecule delivery to plants is designed to allow DNA, single guide RNA (sgRNA), and RNP delivery for higher-throughput plant genome editing (Figure 4). Thus, it warrants a discussion on the state of the plant genome editing field.

6. Conclusion and Perspectives

In recent years, nanotechnology research has suggested the development of NPs as a powerful technique to reduce existing problems resulting from conventional fertilizers in traditional agricultural systems. The results relating to nutritional elements containing NPs (i.e., Fe, Cu, Se, and Co) have shown substantial scientific evidence of their efficacy in improving the micronutrients of the plant, which has been reflected by improved growth parameters and significant improvements at the physiological level (i.e., chlorophyll and carotenoids, photosynthetic activity, metabolic pathways, and transpiration rate). A major obstacle is the precise dosage and activity of NPs on the surface of plant targets, so minimizing the leakage of chemical products extracted from bulk materials (i.e., mineral fertilizers) has become a valuable feature that facilitates the future use of NPs. However, critical studies carried out under controlled conditions are desperately required to determine the role of NPs in and out of the plant and their effects on the environment. The basic dosage of NPs, exposure duration, translocation and accumulation, and mechanism of action on plants are important for an application strategy to be developed. In addition, the secondary effects and accumulation of soil, air, water, and biotic organisms in the ecosystem are critical in deciding the exact impacts of NPs and their effects on the ecosystem.

Data Availability

All data generated or analyzed during this study are included in this published article.

Conflicts of Interest

The authors declare no conflict of interest.

References

[1] S. Dwivedi, Q. Saquib, A. A. Al-Khedhairy, and J. Musarrat, "Understanding the role of nanomaterials in agriculture," in *Microbial Inoculants in Sustainable Agricultural Productivity*, D. P. Singh, H. B. Singh, and R. Prabha, Eds., pp. 271–288, Springer, New Delhi, India, 2016.

[2] T. J. Kou, W. W. Yu, S. K. Lam, D. L. Chen, Y. P. Hou, and Z. Y. Li, "Differential root responses in two cultivars of winter wheat (Triticum aestivum L.) to elevated ozone concentration under fully open-air field conditions," *Journal of Agronomy and Crop Science*, vol. 204, pp. 325–332, 2018.

[3] R. Grillo, A. H. Rosa, and L. F. Fraceto, "Engineered nanoparticles and organic matter: a review of the state-of-the-art," *Chemosphere*, vol. 119, pp. 608–619, 2015.

[4] C. E. Handford, M. Dean, M. Henchion, M. Spence, C. T. Elliott, and K. Campbell, "Implications of nanotechnology for the agri-food industry: opportunities, benefits and risks," *Trends in Food Science & Technology*, vol. 40, no. 2, pp. 226–241, 2014.

[5] A. Husen and K. S. Siddiqi, "Phytosynthesis of nanoparticles: concept, controversy and application," *Nanoscale Research Letters*, vol. 9, no. 1, p. 229, 2014.

[6] C. Parisi, M. Vigani, and E. Rodríguez-Cerezo, "Agricultural nanotechnologies: what are the current possibilities?," *Nano Today*, vol. 10, no. 2, pp. 124–127, 2015.

[7] Y. Bhagat, K. Gangadhara, C. Rabinal, G. Chaudhari, and P. Ugale, "Nanotechnology in agriculture: a review," *Journal of Pure and Applied Microbiology*, vol. 9, pp. 737–747, 2015.

[8] P. S. Bindraban, C. Dimkpa, L. Nagarajan, A. Roy, and R. Rabbinge, "Revisiting fertilisers and fertilisation strategies for improved nutrient uptake by plants," *Biology and Fertility of Soils*, vol. 51, no. 8, pp. 897–911, 2015.

[9] A. Servin, W. Elmer, A. Mukherjee et al., "A review of the use of engineered nanomaterials to suppress plant disease and enhance crop yield," *Journal of Nanoparticle Research*, vol. 17, pp. 1–21, 2015.

[10] K. Jeyasubramanian, U. U. G. Thoppey, G. S. Hikku, N. Selvakumar, A. Subramania, and K. Krishnamoorthy, "Enhancement in growth rate and productivity of spinach grown in hydroponics with iron oxide nanoparticles," *RSC Advances*, vol. 6, no. 19, pp. 15451–15459, 2016.

[11] N. Khan and A. Bano, "Role of plant growth promoting rhizobacteria and Ag-nano particle in the bioremediation of heavy metals and maize growth under municipal wastewater irrigation," *International Journal of Phytoremediation*, vol. 18, no. 3, pp. 211–221, 2015.

[12] F. Mirzajani, H. Askari, S. Hamzelou, M. Farzaneh, and A. Ghassempour, "Effect of silver nanoparticles on Oryza sativa L. and its rhizosphere bacteria," *Ecotoxicology and environmental safety*, vol. 88, pp. 48–54, 2013.

[13] M. L. Verma, P. Kumar, D. Sharma, A. D. Verma, and A. K. Jana, "Advances in nanobiotechnology with special reference to plant systems," in *Plant Nanobionics*, pp. 371–387, Springer, Cham, 2019.

[14] S. Chaudhary, A. Umar, K. K. Bhasin, and S. Baskoutas, "Chemical sensing applications of ZnO nanomaterials," *Materials*, vol. 11, no. 2, p. 287, 2018.

[15] J. S. Duhan, R. Kumar, N. Kumar, P. Kaur, K. Nehra, and S. Duhan, "Nanotechnology: the new perspective in precision agriculture," *Biotechnology Reports*, vol. 15, pp. 11–23, 2017.

[16] D. R. MC, C. Monreal, M. Schnitzer, R. Walsh, and Y. Sultan, "Nanotechnology in fertilizers," *Nature Nanotechnology*, vol. 5, no. 2, pp. 91–91, 2010.

[17] R. Liu and R. Lal, "Potentials of engineered nanoparticles as fertilizers for increasing agronomic productions," *Science of the Total Environment*, vol. 514, pp. 131–139, 2015.

[18] G. Medina-Pérez, F. Fernández-Luqueño, R. G. Campos-Montiel, K. B. Sánchez-López, L. N. Afanador-Barajas, and L. Prince, "Nanotechnology in crop protection: Status and future trends," in *Nano-Biopesticides Today and Future Perspectives*, pp. 17–45, Acaemic Press, 2019.

[19] Y. Shang, M. Hasan, G. J. Ahammed, M. Li, H. Yin, and J. Zhou, "Applications of nanotechnology in plant growth and crop protection: a review," *Molecules*, vol. 24, no. 14, p. 2558, 2019.

[20] J. Lv, P. Christie, and S. Zhang, "Uptake, translocation, and transformation of metal-based nanoparticles in plants: recent advances and methodological challenges," *Environmental Science: Nano*, vol. 6, pp. 41–59, 2019.

[21] S. Torabian, S. Farhangi-Abriz, and M. Zahedi, "Efficacy of FeSO 4 nano formulations on osmolytes and antioxidative

enzymes of sunflower under salt stress," *Indian Journal of Plant Physiology*, vol. 23, no. 2, pp. 305–315, 2018.

[22] D. K. Tripathi, S. Singh, V. P. Singh, S. M. Prasad, N. K. Dubey, and D. K. Chauhan, "Silicon nanoparticles more effectively alleviated UV-B stress than silicon in wheat (Triticum aestivum) seedlings," *Plant Physiology and Biochemistry*, vol. 110, pp. 70–81, 2017.

[23] D. H. Kim, J. Gopal, and I. Sivanesan, "Nanomaterials in plant tissue culture: the disclosed and undisclosed," *RSC Advances*, vol. 7, pp. 36492–36505, 2017.

[24] O. Serik, I. Ainur, K. Murat, M. Tetsuo, and I. Masaki, "Silicon carbide fiber-mediated DNA delivery into cells of wheat (Triticum acstivum L.) mature embryos," *Plant Cell Reports*, vol. 16, no. 3-4, pp. 133–136, 1996.

[25] R. Nair, S. H. Varghese, B. G. Nair, T. Maekawa, Y. Yoshida, and D. S. Kumar, "Nanoparticulate material delivery to plants," *Plant Science*, vol. 179, no. 3, pp. 154–163, 2010.

[26] W. N. Wang, J. C. Tarafdar, and P. Biswas, "Nanoparticle synthesis and delivery by an aerosol route for watermelon plant foliar uptake," *Journal of Nanoparticle Research*, vol. 15, no. 1, p. 1417, 2013.

[27] A. Kaphle, P. N. Navya, A. Umapathi, and H. K. Daima, "Nanomaterials for agriculture, food and environment: applications, toxicity and regulation," *Environmental Chemistry Letters*, vol. 16, no. 1, pp. 43–58, 2018.

[28] R. Raliya, C. Franke, S. Chavalmane, R. Nair, N. Reed, and P. Biswas, "Quantitative understanding of nanoparticle uptake in watermelon plants," *Frontiers in Plant Science*, vol. 7, p. 1228, 2016.

[29] Z. Zhang, F. Kong, B. Vardhanabhuti, A. Mustapha, and M. Lin, "Detection of engineered silver nanoparticle contamination in pears," *Journal of Agricultural and Food Chemistry*, vol. 60, pp. 10762–10767, 2012.

[30] D. Lin and B. Xing, "Root uptake and phytotoxicity of ZnO nanoparticles," *Environmental Science & Technology*, vol. 42, pp. 5580–5585, 2008.

[31] W. Du, Y. Sun, R. Ji, J. Zhu, J. Wu, and H. Guo, "TiO2 and ZnO nanoparticles negatively affect wheat growth and soil enzyme activities in agricultural soil," *Journal of Environmental Monitoring*, vol. 13, no. 4, pp. 822–828, 2011.

[32] A. Perez-de-Luque, "Interaction of nanomaterials with plants: what do we need for real applications in agriculture?," *Frontiers in Environmental Science*, vol. 5, p. 12, 2017.

[33] Z. Wang, X. Xie, J. Zhao et al., "Xylem-and phloem-based transport of CuO nanoparticles in maize (Zea mays L.)," *Environmental science & technology*, vol. 46, no. 8, pp. 4434–4441, 2012.

[34] B. Ruttkay-Nedecky, O. Krystofova, L. Nejdl, and V. Adam, "Nanoparticles based on essential metals and their phytotoxicity," *Journal of Nanbiotechnology*, vol. 15, no. 1, p. 33, 2017.

[35] S. M. Banijamali, M. Feizian, A. Alinejadian Bidabadi, and E. Mehdipour, "Evaluation uptake and translocation of iron oxide nanoparticles and its effect on photosynthetic pigmentation of chrysanthemum," *Journal of Ornamental Plants*, vol. 9, no. 4, 2019.

[36] C. Larue, H. Castillo-Michel, S. Sobanska et al., "Foliar exposure of the crop Lactuca sativa to silver nanoparticles: evidence for internalization and changes in Ag speciation," *Journal of Hazardous Materials*, vol. 264, pp. 98–106, 2014.

[37] C. L. Doolette, M. J. McLaughlin, J. K. Kirby, and D. A. Navarro, "Bioavailability of silver and silver sulfide nanoparticles to lettuce (Lactuca sativa): effect of agricultural amendments on plant uptake," *Journal of Hazardous Materials*, vol. 300, pp. 788–795, 2015.

[38] L. Zhao, J. R. Peralta-Videa, A. Varela-Ramirez et al., "Effect of surface coating and organic matter on the uptake of CeO2 NPs by corn plants grown in soil: insight into the uptake mechanism," *Journal of Hazardous Materials*, vol. 225, pp. 131–138, 2012.

[39] M. Janmohammadi, T. Amanzadeh, N. Sabaghnia, and V. Ion, "Effect of nano-silicon foliar application on safflower growth under organic and inorganic fertilizer regimes," *Botanica*, vol. 22, pp. 53–64, 2016.

[40] N. Khan and A. Bano, "Modulation of phytoremediation and plant growth by the treatment with PGPR, Ag nanoparticle and untreated municipal wastewater," *International journal of phytoremediation*, vol. 18, no. 12, pp. 1258–1269, 2016.

[41] I. S. Naruka, K. D. Gujar, and L. Gopal, "Effect of foliar application of zinc and molybdenum on growth and yield of okra (Abelmoschus esculentus L. Moench) cv. Pusa Sawani," *Haryana Journal of Horticultural Sciences*, vol. 29, no. 3/4, pp. 266-267, 2000.

[42] S. R. Mousavi, M. Galavi, and G. Ahmadvand, "Effect of zinc and manganese foliar application on yield, quality and enrichment on potato (Solanum tuberosum L.)," *Asian Journal of Plant Sciences*, vol. 6, no. 8, pp. 1256–1260, 2007.

[43] F. Ling and M. Silberbush, "Response of maize to foliar vs. soil application of nitrogen–phosphorus–potassium fertilizers," *Journal of plant nutrition*, vol. 25, no. 11, pp. 2333–2342, 2002.

[44] Z. J. Zhu, H. Wang, B. Yan et al., "Effect of surface charge on the uptake and distribution of gold nanoparticles in four plant species," *Environmental Science & Technology*, vol. 46, no. 22, pp. 12391–12398, 2012.

[45] P. Thuesombat, S. Hannongbua, S. Akasit, and S. Chadchawan, "Effect of silver nanoparticles on rice (Oryza sativa L. cv. KDML 105) seed germination and seedling growth," *Ecotoxicology and Environmental Safety*, vol. 104, pp. 302–309, 2014.

[46] J. A. Hernandez-Viezcas, H. Castillo-Michel, J. C. Andrews et al., "In situ synchrotron X-ray fluorescence mapping and speciation of CeO2 and ZnO nanoparticles in soil cultivated soybean (Glycine max)," *ACS Nano*, vol. 7, pp. 1415–1423, 2013.

[47] I. O. Adisa, S. Rawat, V. L. R. Pullagurala et al., "Nutritional status of tomato (Solanum lycopersicum) fruit grown in Fusarium-infested soil: impact of cerium oxide nanoparticles," *Journal of Agricultural and Food Chemistry*, vol. 68, no. 7, pp. 1986–1997, 2020.

[48] M. V. J. Da Costa and P. K. Sharma, "Effect of copper oxide nanoparticles on growth, morphology, photosynthesis, and antioxidant response in Oryza sativa," *Photosynthetica*, vol. 54, no. 1, pp. 110–119, 2016.

[49] S. Rao and G. S. Shekhawat, "Phytotoxicity and oxidative stress perspective of two selected nanoparticles in Brassica juncea," *3 Biotech*, vol. 3, no. 6, p. 244, 2016.

[50] S. Shende, D. Rathod, A. Gade, and M. Rai, "Biogenic copper nanoparticles promote the growth of pigeon pea (Cajanus cajan L.)," *IET Nanobiotechnology*, vol. 11, pp. 773–781, 2017.

[51] P. S. Jahagirdar, P. K. Gupta, S. P. Kulkarni, and P. V. Devarajan, "Polymeric curcumin nanoparticles by a facile in situ method for macrophage targeted delivery," *Bioengineering & Translational Medicine*, vol. 4, no. 1, pp. 141–151, 2019.

[52] T. Xiong, C. Dumat, V. Dappe et al., "Copper oxide nanoparticle foliar uptake, phytotoxicity, and consequences for sustainable urban agriculture," *Environmental Science & Technology*, vol. 51, pp. 5242–5251, 2017.

[53] S. A. Apodaca, W. Tan, O. E. Dominguez, J. A. Hernandez-Viezcas, J. R. Peralta-Videa, and J. L. Gardea-Torresdey, "Physiological and biochemical effects of nanoparticulate copper, bulk copper, copper chloride, and kinetin in kidney bean (Phaseolus vulgaris) plants," *Science of the Total Environment*, vol. 599, pp. 2085–2094, 2017.

[54] R. Raliya, R. Nair, S. Chavalmane, W. N. Wang, and P. Biswas, "Mechanistic evaluation of translocation and physiological impact of titanium dioxide and zinc oxide nanoparticles on the tomato (Solanum lycopersicum L.) plant," *Metallomics*, vol. 7, pp. 1584–1594, 2015.

[55] J. Lv, S. Zhang, L. Luo, J. Zhang, K. Yang, and P. Christied, "Accumulation, speciation and uptake pathway of ZnO nanoparticles in maize," *Environmental Science. Nano*, vol. 2, pp. 68–77, 2015.

[56] S. Shinde, P. Paralikar, A. P. Ingle, and M. Rai, "Promotion of seed germination and seedling growth of Zea mays by magnesium hydroxide nanoparticles synthesized by the filtrate from Aspergillus niger," *Arabian Journal of Chemistry*, vol. 13, no. 1, pp. 3172–3182, 2020.

[57] C. Larue, H. Khodja, N. Herlin-Boime et al., "Investigation of titanium dioxide nanoparticles toxicity and uptake by plants," *Journal of Physics: Conference Series*, vol. 304, p. 12057, 2011.

[58] A. D. Servin, H. Castillo-Michel, J. A. Hernandez-Viezcas, B. C. Diaz, J. R. Peralta-Videa, and J. L. Gardea-Torresdey, "Synchrotron micro-XRF and micro-XANES confirmation of the uptake and translocation of TiO2 nanoparticles in cucumber (Cucumis sativus) plants," *Environmental Science & Technology*, vol. 46, no. 14, pp. 7637–7643, 2012.

[59] H. A. Castillo-Michel, C. Larue, A. E. Pradas del Real, M. Cotte, and G. Sarret, "Practical review on the use of synchrotron based micro- and nano-X-ray fluorescence mapping and X-ray absorption spectroscopy to investigate the interactions between plants and engineered nanomaterials," *Plant Physiology and Biochemistry*, vol. 110, pp. 13–32, 2017.

[60] C. O. Dimkpa, J. E. McLean, D. E. Latta et al., "CuO and ZnO nanoparticles: phytotoxicity, metal speciation, and induction of oxidative stress in sand-grown wheat," *Journal of Nanoparticle Research*, vol. 14, pp. 1–15, 2012.

[61] C. O. Dimkpa, D. E. Latta, J. E. McLean, D. W. Britt, M. I. Boyanov, and A. J. Anderson, "Fate of CuO and ZnO nano- and microparticles in the plant environment," *Environmental Science & Technology*, vol. 47, no. 9, pp. 4734–4742, 2013.

[62] C. Larue, J. Laurette, N. Herlin-Boime et al., "Accumulation, translocation and impact of TiO2 nanoparticles in wheat (Triticum aestivum spp.): influence of diameter and crystal phase," *Science of the Total Environment*, vol. 431, pp. 197–208, 2012.

[63] M. R. Khan, V. Adam, T. F. Rizvi et al., "Nanoparticle–plant interactions: two-way traffic," *Small*, vol. 15, no. 37, p. 1901794, 2019.

[64] Y. Ma, L. Kuang, X. He et al., "Effects of rare earth oxide nanoparticles on root elongation of plants," *Chemosphere*, vol. 78, no. 3, pp. 273–279, 2010.

[65] M. Hatami, "Stimulatory and inhibitory effects of nanoparticulates on seed germination and seedling vigor indices," in *Nanoscience and Plant–Soil Systems*, pp. 357–385, Springer, Cham, 2017.

[66] F. Aslani, S. Bagheri, N. Muhd Julkapli, A. S. Juraimi, F. S. G. Hashemi, and A. Baghdadi, "Effects of engineered nanomaterials on plants growth: an overview," *The Scientific World Journal*, vol. 2014, 28 pages, 2014.

[67] M. C. Pallavi, R. Srivastava, S. Arora, and A. K. Sharma, "Impact assessment of silver nanoparticles on plant growth and soil bacterial diversity," *3 Biotech*, vol. 6, no. 2, p. 254, 2016.

[68] R. Nair, "Effects of nanoparticles on plant growth and development," in *Plant nanotechnology*, C. Kole, D. Kumar, and M. Khodakovskaya, Eds., pp. 95–118, Springer, Cham, 2016.

[69] M. Khodakovskaya, E. Dervishi, M. Mahmood et al., "Carbon nanotubes are able to penetrate plant seed coat and dramatically affect seed germination and plant growth," *American Chemical Society Nano*, vol. 3, pp. 3221–3227, 2009.

[70] J. R. Sanborn, X. Chen, Y. C. Yao et al., "Carbon nanotube porins in amphiphilic block copolymers as fully synthetic mimics of biological membranes," *Advanced Materials*, vol. 30, article e1803355, 2018.

[71] H. Feizi, P. R. Moghaddam, N. Shahtahmassebi, and A. Fotovat, "Impact of bulk and nanosized titanium dioxide (TiO2) on wheat seed germination and seedling growth," *Biological Trace Element Research*, vol. 146, no. 1, pp. 101–106, 2012.

[72] L. Zheng, F. Hong, S. Lu, and C. Liu, "Effect of nano-TiO_2 on strength of naturally aged seeds and growth of spinach," *Biological Trace Element Research*, vol. 104, no. 1, pp. 083–092, 2005.

[73] N. Bala, A. Dey, S. Das, R. Basu, and P. Nandy, "Effect of hydroxyapatite nanorod on chickpea (Cicer arietinum) plant growth and its possible use as nano-fertilizer," *Iranian Journal of Plant Physiology*, vol. 4, no. 3, pp. 1061–1069, 2014.

[74] Q. B. Ngo, T. H. Dao, H. C. Nguyen, T. V. TranXT Nguyen, T. D. Khuu, and T. H. Huynh, "Effects of nanocrystalline powders (Fe, Co and Cu) on the germination, growth, crop yield and product quality of soybean (Vietnamese species DT-51)," *Advances in Natural Sciences: Nanoscience and Nanotechnology*, vol. 5, pp. 1–7, 2014.

[75] L. Yin, B. P. Colman, B. M. McGill, J. P. Wright, and E. S. Bernhardt, "Effects of silver nanoparticle exposure on germination and early growth of eleven wetland plants," *PLoS One*, vol. 7, no. 10, article e47674, 2012.

[76] A. Milewska-Hendel, R. Gawecki, M. Zubko, D. Stróż, and E. Kurczynska, "Diverse influence of nanoparticles on plant growth with a particular emphasis on crop plants," *Acta Agrobotanica*, vol. 69, no. 4, 2016.

[77] K. Gopinath, S. Gowri, V. Karthika, and A. Arumugam, "Green synthesis of gold nanoparticles from fruit extract of Terminalia arjuna, for the enhanced seed germination activity of Gloriosa superba," *Journal of Nanostructure in Chemistry*, vol. 4, no. 3, p. 115, 2014.

[78] A. Hafeez, A. Razzaq, T. Mahmood, and H. M. Jhanzab, "Potential of copper nanoparticles to increase growth and yield of wheat," *Journal of Nanoscience with Advanced Technology*, vol. 1, no. 1, pp. 6–11, 2015.

[79] C. Kole, P. Kole, K. M. Randunu, P. Choudhary, R. Podila, and P. C. Ke, "Nanobiotechnology can boost crop production and quality: first evidence from increased plant biomass, fruit yield and phytomedicine content in bitter melon

(Momordica charantia)," *BMC Biotechnology*, vol. 13, no. 1, p. 37, 2013.

[80] T. N. V. K. V. Prasad, P. Sudhakar, Y. Sreenivasulu et al., "Effect of nanoscale zinc oxide particles on the germination, growth and yield of peanut," *Journal of Plant Nutrition*, vol. 35, pp. 905–927, 2012.

[81] F. Gao, F. Hong, C. Liu et al., "Mechanism of nanoanatase TiO2 on promoting photosynthetic carbon reaction of spinach," *Biological trace element research*, vol. 111, pp. 239–253, 2008.

[82] S. J. Klaine, P. J. J. Alvarez, G. E. Batley et al., "Nanomaterials in the environment: behavior, fate bioavailability, and effects," *Environmental Toxicology and Chemistry*, vol. 27, pp. 1825–1851, 2008.

[83] M. Linglan, L. Chao, Q. Chunxiang et al., "Rubisco activase mRNA expression in spinach: modulation by nanoanatase treatment," *Biological Trace Element Research*, vol. 122, no. 2, pp. 168–178, 2008.

[84] P. Wang, E. Lombi, F. J. Zhao, and P. M. Kopittke, "Nanotechnology: a new opportunity in plant sciences," *Trends in Plant Science*, vol. 21, no. 8, pp. 699–712, 2016.

[85] B. Aken Van, "Gene expression changes in plants and microorganisms exposed to nanomaterials," *Current Opinion in Biotechnology*, vol. 33, pp. 206–219, 2015.

[86] J. Yang, W. Cao, and Y. Rui, "Interactions between nanoparticles and plants, phytotoxicity and defense mechanisms," *Journal of Plant Interactions*, vol. 12, pp. 158–169, 2017.

[87] A. Rastogi, M. Zivcak, O. Sytar et al., "Impact of metal and metal oxide nanoparticles on plant, a critical review," *Frontiers in Chemistry*, vol. 5, p. 78, 2017.

[88] G. Ghodake, Y. D. Seo, D. H. Park, and D. S. Lee, "Phytotoxicity of carbon nanotubes assessed by Brassica juncea and Phaseolus mungo," *Journal of Nanoelectronics and Optoelectronics*, vol. 5, pp. 157–160, 2010.

[89] A. C. Pandey, S. S. Sharda, and R. S. Yadav, "Application of ZnO nanoparticles in influencing the growth rate of Cicer arietinum," *Journal of Experimental Nanoscience*, vol. 5, pp. 488–497, 2010.

[90] P. Mahajan, S. K. Dhoke, and A. S. Khanna, "Effect of nano-ZnO particle suspension on growth of mung (Vigna radiata) and gram (Cicer arietinum) seedlings using plant agar method," *Journal of Nanotechnology*, vol. 2011, Article ID 696535, 7 pages, 2011.

[91] A. Jaberzadeh, P. Moaveni, H. R. Tohidi Moghadam, and H. Zahedi, "Influence of bulk and nanoparticles titanium foliar application on some agronomic traits, seed gluten and starch contents of wheat subjected to water deficit stress," *Notulae Botanicae Horti Agrobotanici Cluj-Napoca*, vol. 41, no. 1, pp. 201–207, 2013.

[92] R. Suriyaprabha, G. Karunakaran, R. Yuvakkumar, V. Rajendran, and N. Kannan, "Silica nanoparticles for increased silica availability in maize (Zea mays L) seeds under hydroponic conditions," *Current Nanoscience*, vol. 8, pp. 902–908, 2012.

[93] H. Feizi, M. Kamali, L. Jafari, and M. P. Rezvani, "Phytotoxicity and stimulatory impacts of nanosized and bulk titanium dioxide on fennel (Foeniculum vulgare Mill)," *Chemosphere*, vol. 91, no. 4, pp. 506–511, 2013.

[94] J. Li, J. Hu, C. Ma et al., "Uptake, translocation and physiological effects of magnetic iron oxide (γ-Fe_2O_3) nanoparticles in corn (_Zea mays_ L.)," *Chemosphere*, vol. 159, pp. 326–334, 2016.

[95] P. Yugandhar and N. Savithramma, "Green synthesis of calcium carbonate nanoparticles and their effects on seed germination and seedling growth of Vigna mungo," *International Journal of Advanced Research*, vol. 1, no. 8, pp. 89–103, 2013.

[96] C. M. Rico, S. Majumdar, M. Duarte-Gardea, J. R. Peralta-Videa, and J. L. Gardea-Torresdey, "Interaction of nanoparticles with edible plants and their possible implications in the food chain," *Journal of Agricultural and Food Chemistry*, vol. 59, pp. 3485–3498, 2011.

[97] B. S. Sekhon, "Nanotechnology in agri-food production: an overview," *Nanotechnology, Science and Applications*, vol. 7, pp. 31–53, 2014.

[98] Z. Lei, S. Mingyu, W. Xiao et al., "Antioxidant stress is promoted by nano-anatase in spinach chloroplasts under UV-B radiation," *Biological Trace Element Research*, vol. 121, pp. 69–79, 2008.

[99] Y. Haichuan, L. Qingju, L. I. Qiang, C. Shanna, and Z. Lijuan, "Inhibitory effects of nano-TiO2 loaded Pd on cyanobacteria growth," *Acta Botanica Boreali-Occidentalia Sinica*, vol. 25, pp. 1884–1887, 2005.

[100] W. Xuming, G. Fengqing, M. Linglan et al., "Effects of nano-anatase on ribulose-1, 5-bisphosphate carboxylase/oxygenase mRNA expression in spinach," *Biological Trace Element Research*, vol. 126, pp. 280–289, 2008.

[101] Q. Wang, X. Ma, W. Zhang, H. Pei, and Y. Chen, "The impact of cerium oxide nanoparticles on tomato (Solanum lycopersicum L.) and its implications for food safety," *Metallomics*, vol. 4, no. 10, pp. 1105–1112, 2012.

[102] K. S. Siddiqi and A. Husen, "Plant response to engineered metal oxide nanoparticles," *Nanoscale research letters*, vol. 12, pp. 1–8, 2017.

[103] N. Khan and A. Bano, "Exopolysaccharide producing rhizobacteria and their impact on growth and drought tolerance of wheat grown under rainfed conditions," *PLoS One*, vol. 14, no. 9, article e0222302, 2019.

[104] C. Liu, F. Li, C. Luo et al., "Foliar application of two silica sols reduced cadmium accumulation in rice grains," *Journal of Hazardous Materials*, vol. 161, pp. 1466–1472, 2009.

[105] J. E. Cañas, M. Long, S. Nations et al., "Effects of functionalized and nonfunctionalized single-walled carbon nanotubes on root elongation of select crop species," *Environmental Toxicology and Chemistry*, vol. 27, pp. 1922–1931, 2008.

[106] D. K. Tiwari, N. Dasgupta-Schubert, L. V. Cendejas, J. Villegas, L. C. Montoya, and S. B. García, "Interfacing carbon nanotubes (CNT) with plants: enhancement of growth, water and ionic nutrient uptake in maize (Zea mays) and implications for nano-agriculture," *Applied Nanoscience*, vol. 4, no. 5, pp. 577–591, 2014.

[107] F. Rezaei, P. Moaveni, and H. Mozafari, "Effect of different concentrations and time of nano TiO2 spraying on quantitative and qualitative yield of soybean (Glycine max L.) at Shahr-e-Qods, Iran," *Biological Forum*, vol. 7, pp. 957–964, 2015.

[108] G. Ghodake, Y. D. Seo, and D. S. Lee, "Hazardous phytotoxic nature of cobalt and zinc oxide nanoparticles assessed using Allium cepa," *Journal of Hazardous Materials*, vol. 186, pp. 952–955, 2011.

[109] H. Mahmoodzadeh, M. Nabavi, and H. Kashefi, "Effect of nanoscale titanium dioxide particles on the germination and growth of canola (Brassica napus)," *Journal of Ornamental and Horticultural Plants*, vol. 3, pp. 25–32, 2013.

[110] P. Singh, R. Singh, A. Borthakur et al., "Effect of nanoscale TiO2-activated carbon composite on Solanum lycopersicum (L.) and Vigna radiata (L.) seeds germination," *Energy, Ecology and Environment*, vol. 1, no. 3, pp. 131–140, 2016.

[111] S. K. Dhoke, P. Mahajan, R. Kamble, and A. Khanna, "Effect of nanoparticles suspension on the growth of mung (Vigna radiata) seedlings by foliar spray method," *Nanotechnology Development*, vol. 3, no. 1, article e1, 2013.

[112] T. Y. Kuang, Ed., *Mechanism and Regulation of Primary Energy Conversion Process in Photosynthesis*, Science and Technology Press, Jiangsu, Nanjing, 2003.

[113] Z. Lei, S. Mingyu, L. Chao et al., "Effects of nanoanatase TiO2 on photosynthesis of spinach chloroplasts under different light illumination," *Biological Trace Element Research*, vol. 119, pp. 68–76, 2007.

[114] R. Raliya, J. C. Tarafdar, and P. Biswas, "Enhancing the mobilization of native phosphorus in the mung bean rhizosphere using ZnO nanoparticles synthesized by soil fungi," *Journal of Agricultural and Food Chemistry*, vol. 64, no. 16, pp. 3111–3118, 2016.

[115] Y. Ze, C. Liu, L. Wang, M. Hong, and F. Hong, "The regulation of TiO2 nanoparticles on the expression of light-harvesting complex II and photosynthesis of chloroplasts of Arabidopsis thaliana," *Biological Trace Element Research*, vol. 143, pp. 1131–1141, 2011.

[116] A. Singh, S. M. Prasad, and S. Singh, "Impact of nano ZnO on metabolic attributes and fluorescence kinetics of rice seedlings," *Environmental Nanotechnology, Monitoring & Management*, vol. 9, pp. 42–49, 2018.

[117] S. Pradhan, P. Patra, S. Das et al., "Photochemical modulation of biosafe manganese nanoparticles on Vigna radiata, a detailed molecular, biochemical, and biophysical study," *Environmental Science & Technology*, vol. 47, pp. 13122–13131, 2013.

[118] M. Delfani, M. B. Firouzabadi, N. Farrokhi, and H. Makarian, "Some physiological responses of black-eyed pea to iron and magnesium nanofertilizers," *Communications in soil science and plant analysis*, vol. 45, no. 4, pp. 530–540, 2014.

[119] J. P. Giraldo, M. P. Landry, S. M. Faltermeier et al., "Plant nanobionics approach to augment photosynthesis and biochemical sensing," *Nature Materials*, vol. 13, pp. 400–408, 2014.

[120] M. H. Siddiqui and M. H. Al-Whaibi, "Role of nano-SiO2 in germination of tomato (Lycopersicum esculentum seeds Mill.)," *Saudi journal of biological sciences*, vol. 21, pp. 13–17, 2014.

[121] M. Faizan, A. Faraz, M. Yusuf, S. T. Khan, and S. Hayat, "Zinc oxide nanoparticle-mediated changes in photosynthetic efficiency and antioxidant system of tomato plants," *Photosynthetica*, vol. 56, pp. 678–686, 2017.

[122] F. Q. Gao, F. S. Hong, C. Liu et al., "Mechanism of nanoanatase TiO2 on promoting photosynthetic carbon reaction of spinach, inducing complex of rubiscoe rubisco activase," *Biological Trace Element Research*, vol. 111, pp. 239–253, 2006.

[123] H. S. Jiang, L. Y. Yin, N. N. Ren et al., "Silver nanoparticles induced reactive oxygen species via photosynthetic energy transport imbalance in an aquatic plant," *Nanotoxicology*, vol. 11, pp. 157–167, 2017.

[124] S. Rawat, V. L. Pullagurala, M. Hernandez-Molina et al., "Impacts of copper oxide nanoparticles on bell pepper (Capsicum annum L.) plants: a full life cycle study," *Environmental Science: Nano*, vol. 5, pp. 83–95, 2018.

[125] F. K. Choudhury, R. M. Rivero, E. Blumwald, and R. Mittler, "Reactive oxygen species, abiotic stress and stress combination," *The Plant Journal*, vol. 90, no. 5, pp. 856–867, 2017.

[126] Z. Zhang, S. Ali, T. Zhang, W. Wang, and L. Xie, "Identification, evolutionary and expression analysis of PYL-PP2C-SnRK2s gene families in soybean," *Plants*, vol. 9, no. 10, p. 1356, 2020.

[127] G. Onaga and W. Kerstin, "Advances in plant tolerance to biotic stresses," in *Plant Genomics*, I. Y. Abdurakhmonov, Ed., pp. 167–228, InTech, Rijeka, Croatia, 2016.

[128] A. Y. Mushtaq, S. A. Rizwan, N. E. Jamil et al., "Influence of silicon sources and controlled release fertilizer on the growth of wheat cultivars of Balochistan under salt stress," *Pakistan Journal of Botany*, vol. 51, no. 5, pp. 1561–1567, 2019.

[129] M. H. Gowayed, H. S. Al-Zahrani, and E. M. Metwali, "Improving the salinity tolerance in potato (Solanum tuberosum) by exogenous application of silicon dioxide nanoparticles," *International Journal of Agriculture and Biology*, vol. 19, no. 1, 2017.

[130] S. L. Laware and S. Raskar, "Effect of titanium dioxide nanoparticles on hydrolytic and antioxidant enzymes during seed germination in onion," *International Journal of Current Microbiology and Applied Sciences*, vol. 3, no. 7, pp. 749–760, 2014.

[131] N. Khan and A. Bano, "Effects of exogenously applied salicylic acid and putrescine alone and in combination with rhizobacteria on the phytoremediation of heavy metals and chickpea growth in sandy soil," *International journal of phytoremediation*, vol. 20, no. 5, pp. 405–414, 2018.

[132] Z. F. Pei, D. F. Ming, D. Liu et al., "Silicon improves the tolerance to water-deficit stress induced by polyethylene glycol in wheat (Triticum aestivum L.) seedlings," *Plant Growth Regulation*, vol. 29, no. 1, pp. 106–115, 2010.

[133] Z. Iqbal, A. Sarkhosh, R. Balal et al., "Silicon alleviate hypoxia stress by improving enzymatic and non-enzymatic antioxidants and regulating nutrient uptake in muscadine grape (Muscadinia rotundifolia Michx.)," *Frontiers in Plant Science*, vol. 11, 2020.

[134] T. Elsakhawy, A. E. D. Omara, T. Alshaal, and H. El-Ramady, "Nanomaterials and plant abiotic stress in agroecosystems," *Environment, Biodiversity and Soil Security*, vol. 2, no. 2018, pp. 73–94, 2018.

[135] S. D. Gupta, A. Agarwal, and S. Pradhan, "Phytostimulatory effect of silver nanoparticles (AgNPs) on rice seedling growth: an insight from antioxidative enzyme activities and gene expression patterns," *Ecotoxicology and Environmental Safety*, vol. 161, pp. 624–633, 2018.

[136] C. L. Zhang, H. S. Jiang, S. P. Gu et al., "Combination analysis of the physiology and transcriptome provides insights into the mechanism of silver nanoparticles phytotoxicity," *Environmental Pollution*, vol. 252, no. Part B, pp. 1539–1549, 2019.

[137] F. Zulfiqar, M. Navarro, M. Ashraf, N. A. Akram, and S. Munné-Bosch, "Nanofertilizer use for sustainable agriculture: advantages and limitations," *Plant Science*, vol. 289, p. 110270, 2019.

[138] G. L. Vanti, V. B. Nargund, R. Vanarchi et al., "Synthesis of Gossypium hirsutum-derived silver nanoparticles and their antibacterial efficacy against plant pathogens," *Applied Organometallic Chemistry*, vol. 33, no. 1, article e4630, 2019.

[139] J. J. G. Guerrero, P. Songkumarn, T. U. Dalisay, I. B. Pangga, and N. D. Organo, "Toxicity of CuO and ZnO nanoparticles

and their bulk counterparts on selected soil-borne fungi," *Agriculture and Natural Resources*, vol. 54, no. 3, pp. 325–332, 2020.

[140] J. Chen, L. Wu, M. Lu, S. Lu, Z. Li, and W. Ding, "Comparative study on the fungicidal activity of metallic MgO nanoparticles and macroscale MgO against soilborne fungal phytopathogens," *Frontiers in Microbiology*, vol. 11, p. 365, 2020.

[141] L. Cai, J. Chen, Z. Liu, H. Wang, H. Yang, and W. Ding, "Magnesium oxide nanoparticles: effective agricultural antibacterial agent against Ralstonia solanacearum," *Frontiers in Microbiology*, vol. 9, p. 790, 2018.

[142] M. R. Khan, F. Ahamad, and T. F. Rizvi, "Effect of nanoparticles on plant pathogens," in *Advances in Phytonanotechnology*, pp. 215–240, Academic Press, 2019.

[143] R. Mohammadi, R. Maali-Amiri, and A. Abbasi, "Effect of TiO2 nanoparticles on chickpea response to cold stress," *Biological Trace Element Research*, vol. 152, pp. 403–410, 2013.

[144] H. Hasanpour, R. Maali-Amiri, and H. Zeinali, "Effect of TiO2 nanoparticles on metabolic limitations to photosynthesis under cold in chickpea," *Russian Journal of Plant Physiology*, vol. 62, pp. 779–787, 2015.

[145] R. Mohammadi, R. MaaliAmiri, and N. Mantri, "Effect of TiO2 nanoparticles on oxidative damage and antioxidant defense systems in chickpea seedlings during cold stress," *Russian Journal of Plant Physiology*, vol. 61, no. 6, pp. 768–775, 2014.

[146] J. Xu, J. Yang, X. Duan, Y. Jiang, and P. Zhang, "Increased expression of native cytosolic Cu/Zn superoxide dismutase and ascorbate peroxidase improves tolerance to oxidative and chilling stresses in cassava (Manihot esculenta Crantz)," *BMC Plant Biology*, vol. 14, no. 1, p. 208, 2014.

[147] M. Haghighi, R. Abolghasemi, and J. A. Teixeira da Silva, "Low and high temperature stress affect the growth characteristics of tomato in hydroponic culture with Se and nano-Se amendment," *Scientia Horticulturae*, vol. 178, pp. 231–240, 2014.

[148] M. Hasanuzzaman, K. Nahar, and M. Fujita, "Silicon and selenium: two vital trace elements that confer abiotic stress tolerance to plants," in *Emerging Technologies and Management of Crop Stress Tolerance*, pp. 377–422, Elsevier, The Netherlands, 2014.

[149] A. Wahid, "Physiological implications of metabolites biosynthesis in net assimilation and heat stress tolerance of sugarcane (Saccharum officinarum) sprouts," *Journal of Plant Research*, vol. 120, pp. 219–228, 2007.

[150] M. V. Khodakovskaya, K. de Silva, D. A. Nedosekin et al., "Complex genetic, photothermal, and photoacoustic analysis of nanoparticle-plant interactions," *Proceedings of the National Academy of Sciences of the United States of America*, vol. 108, no. 3, pp. 1028–1033, 2011.

[151] S. Ali, K. Hayat, A. Iqbal, and L. Xie, "Implications of abscisic acid in the drought stress tolerance of plants," *Agronomy*, vol. 10, no. 9, p. 1323, 2020.

[152] M. I. R. Khan, S. Syeed, R. Nazar, and N. A. Anjum, "An insight into the role of salicylic acid and jasmonic acid in salt stress tolerance," in *Phytohormones and Abiotic Stress Tolerance in Plants*, N. A. Khan, R. Nazar, N. Iqbal, and N. A. Anjum, Eds., pp. 277–300, Springer Verlag, 2012.

[153] M. N. Khan, M. H. Siddiqui, F. Mohammad, and M. Naeem, "Interactive role of nitric oxide and calcium chloride in enhancing tolerance to salt stress," *Nitric Oxide*, vol. 27, no. 4, pp. 210–218, 2012.

[154] S. U. Jalil and M. I. Ansari, "Nanoparticles and abiotic stress tolerance in plants: synthesis, action, and signaling mechanisms," in *Plant Signaling Molecules*, pp. 549–561, Woodhead Publishing, 2019.

[155] F. Mirzajani, H. Askari, S. Hamzelou et al., "Proteomics study of silver nanoparticles toxicity on Oryza sativa L.," *Ecotoxicology and Environmental Safety*, vol. 108, pp. 335–339, 2014.

[156] M. R. Maghsoodi, L. Ghodszad, and B. A. Lajayer, "Dilemma of hydroxyapatite nanoparticles as phosphorus fertilizer: potentials, challenges and effects on plants," *Environmental Technology & Innovation*, vol. 19, article 100869, 2020.

[157] M. Boudsocq and J. Sheen, "CDPKs in immune and stress signaling," *Trends in Plant Science*, vol. 18, no. 1, pp. 30–40, 2013.

[158] Z. M. Almutairi, "Effect of nano-silicon application on the expression of salt tolerance genes in germinating tomato (Solanum lycopersicum L.) seedlings under salt stress," *Plant Omics*, vol. 9, pp. 106–114, 2016.

[159] J. H. Kim, Y. Oh, H. Yoon, I. Hwang, and Y.-S. Chang, "Iron nanoparticle-induced activation of plasma membrane Hþ-ATPase promotes stomatal opening in Arabidopsis thaliana," *Environmental Science & Technology*, vol. 49, pp. 1113–1119, 2015.

[160] R. Kaveh, Y. S. Li, S. Ranjbar, R. Tehrani, C. L. Brueck, and B. Van Aken, "Changes in Arabidopsis thaliana gene expression in response to silver nanoparticles and silver ions," *Environmental Science & Technology*, vol. 47, no. 18, pp. 10637–10644, 2013.

[161] P. Landa, R. Vankova, J. Andrlova et al., "Nanoparticle-specific changes in Arabidopsis thaliana gene expression after exposure to ZnO, TiO2, and fullerene soot," *Journal of Hazardous Materials*, vol. 241, pp. 55–62, 2012.

[162] T. P. Frazier, C. E. Burklew, and B. Zhang, "Titanium dioxide nanoparticles affect the growth and microRNA expression of tobacco (Nicotiana tabacum)," *Functional & integrative genomics*, vol. 14, no. 1, pp. 75–83, 2014.

[163] S. Singh, K. Vishwakarma, S. Singh et al., "Understanding the plant and nanoparticle interface at transcriptomic and proteomic level: a concentric overview," *Plant Gene*, vol. 11, pp. 265–272, 2017.

[164] G. Mustafa and S. Komatsu, "Nanoparticles mediated soybean response mechanism at morphological, physiological, and proteomic level," *Current Proteomics*, vol. 14, no. 1, pp. 3–12, 2017.

[165] S. Asad and M. Arsh, "Silicon carbide whisker-mediated plant transformation," in *Properties and Applications of Silicon Carbide*, R. Gerhardt, Ed., pp. 1–16, BoD-Books on Deman, Rijeka, 2012.

[166] H. Y. Lau, H. Wu, E. J. H. Wee, M. Trau, Y. Wang, and J. R. Botella, "Specific and sensitive isothermal electrochemical biosensor for plant pathogen DNA detection with colloidal gold nanoparticles as probes," *Scientific Reports*, vol. 7, p. 38896, 2017.

[167] N. Mitter, E. A. Worrall, K. E. Robinson et al., "Clay nanosheets for topical delivery of RNAi for sustained protection against plant viruses," *Nature plants*, vol. 3, p. 16207, 2017.

[168] X. Zhao, Z. Meng, Y. Wang et al., "Pollen magnetofection for genetic modification with magnetic nanoparticles as gene carriers," *Nature Plants*, vol. 3, no. 12, pp. 956–964, 2017.

[169] G. S. Demirer, H. Zhang, J. L. Matos et al., "High aspect ratio nanomaterials enable delivery of functional genetic material without DNA integration in mature plants," *bioRxiv*, vol. 10, pp. 1–32, 2018.

[170] S. Martin-Ortigosa, D. J. Peterson, J. S. Valenstein et al., "Mesoporous silica nanoparticle-mediated intracellular Cre protein delivery for maize genome editing via loxP site excision," *Plant Physiology*, vol. 164, pp. 537–547, 2013.

Hindawi
Journal of Nanomaterials
Volume 2021, Article ID 6693302, 16 pages
https://doi.org/10.1155/2021/6693302

Research Article

Biosynthesis of Copper Oxide Nanoparticles Using *Streptomyces* MHM38 and Its Biological Applications

Sarah I. Bukhari,[1] **Moaz M. Hamed**,[2] **Mohamed H. Al-Agamy**,[1,3] **Hanaa S. S. Gazwi**,[4] **Hesham H. Radwan**,[1] **and Asmaa M. Youssif**[5]

[1]*Department of Pharmaceutics, College of Pharmacy, King Saud University, Riyadh, Saudi Arabia*
[2]*Marine Microbiology Lab., Marine Environmental Division, National Institute of Oceanography and Fisheries, Egypt*
[3]*Department of Microbiology and Immunology, Faculty of Pharmacy, Al-Azhar University, Cairo, Egypt*
[4]*Department of Agricultural Chemistry, Faculty of Agriculture, Minia University, El-Minia, Egypt*
[5]*Department of Botany and Microbiology, Faculty of Science, Alexandria University, Alexandria, Egypt*

Correspondence should be addressed to Mohamed H. Al-Agamy; malagamy@ksu.edu.sa

Received 8 November 2020; Revised 7 December 2020; Accepted 18 December 2020; Published 4 January 2021

Academic Editor: Shahid Ali

Biosynthesis methods employing microorganisms have emerged as an eco-friendly, clean, and viable alternative to chemical and physical processes. The present study reports the synthesis of copper oxide nanoparticles (CuONPs) using cell-free culture supernatant of marine *Streptomyces* sp. MHM38. For the optimized production of CuONPs, the influence of some parameters, such as the concentration of copper sulfate ($CuSO_4$), reaction time, filtrate to substrate ratio, and pH, was studied. 5 mM of $CuSO_4$ was optimal for nanoparticle (NP) production. Well-defined CuONP formation occurred after 60 min of incubation when an equal volume of filtrate (cell-free supernatant) to substrate ($CuSO_4$ solution) was added. UV-visible spectroscopy analysis of CuONPs exhibited a peak at 550 nm, which corresponds to the surface plasmon resonance of CuONPs. Most of the particles were spherical and were 1.72–13.49 nm when measured using a transmission electron microscope. The antimicrobial activity of CuONPs was determined using a well diffusion method against *Enterococcus faecalis* ATCC 29212, *Salmonella typhimurium* ATCC 14028, *Pseudomonas aeruginosa* ATCC 9027, *Escherichia coli* ATCC 8939, fungi (*Rhizoctonia solani*, *Fusarium solani*, and *Aspergillus niger*), and yeast (*Candida albicans* ATCC 10237). The highest antimicrobial activities were recorded against *Candida albicans* ATCC 10237, whereas *Salmonella typhimurium* ATCC 14028 and *Escherichia coli* ATCC 8939 showed the less activity. The biochemical findings of the CuONP groups were significant ($p < 0.05$) with diminished levels of alanine aminotransferase (ALT), aspartate aminotransferase (AST), alkaline phosphatase (ALP), lactate dehydrogenase (LDH), total and direct bilirubin, urea, and creatinine compared with the paracetamol group. Nonenzymatic and enzymatic antioxidants of the CuONP groups were significantly elevated ($p < 0.05$) in SOD and GSH levels, and exceptionally low nitric oxide (NO) and malondialdehyde (MAD) levels were found for the paracetamol group. The histopathological examination of the CuONP groups assured the impact of improving CuONPs against paracetamol-induced liver damage.

1. Introduction

Metal nanoparticles are synthesized and used because of their unique electrical, optical, catalytic, and magnetic characteristics [1–3], which differ from the characteristics of bulk materials. Recently, many chemical and physical methods have achieved the synthesis of inorganic nanoparticles. However, biological synthesis is realized globally as being dangerous, expensive, and not an environmentally friendly chemical process [4, 5]. Therefore, it is essential to develop fast, cost-effective, ecological friendly, and easy-to-scale synthetic approaches of manufacturing nanoparticles of metal using biological systems. It is well established that in harsh conditions microbes develop mechanisms to survive in toxic metals by turning toxic metal ions into their corresponding nontoxic forms of metal sulfide/oxide [6]. Many of the destructive impacts of physical and chemical methods can be resolved by the green synthesis of NPs using various

biological entities. These involve the mild pH, pressure, and temperature for biosynthesis of NPs and do not include harmful or hazardous substances and prohibit the addition of external reducing, capping, and stabilizing agents [7]. The specifics of nanotransformation mechanisms are not well known. In the case of copper, a wide range of biological tools, such as bacteria [8, 9], fungi [10], algae [11], and plants [12], can be used to synthesize nanoparticles. A substantial proportion of the world's population uses nanoparticles to treat some diseases. Recent studies have indicated that CuNPs have broad biological properties [13]. Actinomycetes are a diverse group of Gram-positive bacteria that are common in soil and widely distributed in different environments, and they are known to generate many forms of novel secondary metabolites [14]. The bioactive compounds of actinomycetes are active against bacteria, fungi, and viruses [15]. Actinomycetes are highly regarded as being important candidates for metal nanoparticle synthesis [16]. They are stable and polydisperse, making them an effective candidate for intracellular and extracellular metal nanoparticle synthesis. The electron binding of Ag^+ ions to a mycelial cell wall enzyme carboxylate group results in intracellular nanoparticular synthesis [17–19]. *Streptomyces* are a commonly used actinomycetes species in nanoparticulate biosynthesis [20], and they have been documented to produce silver, gold, manganese, copper, and zinc nanoparticles [21, 22]. Copper nanoparticles (CuNPs) have important applications in various fields [23–25]. Copper oxide nanoparticles (CuONPs) have essential antimicrobial properties by inhibiting bacterial, fungal, viral, and algal growth [26, 27]. Nanosized copper oxide has a longer shelf life than other organic antimicrobials, such as silver and gold [28]. Copper oxide nanoparticles synthesized with actinomycetes show antibacterial properties [29]. Paracetamol is a medication with antipyretic and analgesic impacts that is broadly utilized by the wider community and taken freely without supervision. However, high doses of paracetamol can cause liver damage. Paracetamol is expected to be a significant factor causing severe liver damage [30]. This study was designed to use a marine actinobacterial *Streptomyces* sp. strain that was screened for biosynthesis, optimization, and characterization of produced copper oxide nanoparticles (CuONPs), which were evaluated for their acceptability to animal tissue, antioxidant and hepatoprotective activity, and inhibitory action against some pathogenic microorganisms.

2. Material and Method

2.1. Microorganisms and Cultural Conditions. Streptomyces sp. MHM38 was isolated from a marine sediment sample in the Suez gulf and deposited in GenBank as *Streptomyces* sp. MHM38 with accession number KU764745 by Dr. Moaz M. Hamed. This marine actinobacterial isolate was maintained on slant containing starch nitrate agar medium (SNM) with a specific composition (g/l: starch, 20; K_2HPO_4,1.0; KNO_3, 2.0; $MgSO_4$, 0.5; and agar 18.0; H_2O, 1.0 l). Components were dissolved in 0.5 l of distilled water and 0.5 l of seawater [31]. Measures of 50 and 20 $\mu g\,ml^{-1}$ tetracycline and nystatin, respectively, were applied as antibacterial and antifungal agents to prevent bacterial and fungal infection following autoclaving and solidification. The strain was incubated for seven days at 30°C–32°C. The isolate was stored as spore suspension in 20% (*v*/*v*) glycerol at −20°C for subsequent investigation.

2.2. Inoculum Preparation. A 250 ml Erlenmeyer flask was used containing 50 ml of SNM. This flask was inoculated with old stock culture and incubated for five days in a rotator incubator shaker at 30°C–32°C and 200 rpm, and it was used as an inoculum for subsequent experiments.

2.3. Extracellular Synthesis of CuONPs. The isolate was freshly inoculated in an Erlenmeyer flask containing 50 ml of the abovementioned production medium to screen *Streptomyces* sp. MHM38 for the synthesis of CuONPs. The culture was centrifuged at 10,000 rpm at the end of the incubation, and supernatants were used to detect copper nanoparticles. The supernatants (biomass filtrate) were used for green synthesis of CuONPs. A volume of 15 ml of 1 mM $CuSO_4$ was added to 15 ml of the isolate supernatant in 100 ml Erlenmeyer flasks. The flasks were incubated at 30°C–32°C and observed for color change. Two controls were used: the first control (sterile media mixed with 1 mM copper sulfate) was used to establish that media components cannot reduce copper ions to copper nanoparticles. In the negative control (copper sulfate solution), no color change was observed over time. The flasks were monitored daily for any visual color change. UV-visible spectroscopy in the range of 200–800 nm was conducted for flasks with color adjustment [4].

2.4. Optimization of Different Factors on the Production of Copper Oxide Nanoparticles by Streptomyces sp. MHM38

2.4.1. Effect of Copper Concentration on Nanoparticle Production. 15 ml of cell-free supernatant was added to 15 ml of 1 to 10 mM $CuSO_4$. The blend was incubated as above, and UV-vis spectroscopy was used to study CuONPs.

2.4.2. Effect of Reaction Time on Nanoparticle Production. Nanoparticle synthesis and stability are influenced by reaction time. 15 ml of cell-free supernatant was added to 15 ml of 5 mM $CuSO_4$ solution. The mixture was incubated for various periods as above, and a UV-visible spectroscopy analysis was performed to analyze CuONPs.

2.4.3. Effect of the Substrate to Filtrate Ratio on Nanoparticle Production. Three flasks were prepared to study the effect of different substrate to filtrate ratios on CuONP formation: in the first, 15 ml of cell-free supernatant was added to 15 ml of 5 mM $CuSO_4$ solution; in the second, 15 ml of cell-free supernatant was added to 7.5 ml of 5 mM $CuSO_4$ solution; and in the third, 15 ml of cell-free supernatant was added to 30 ml of 5 mM $CuSO_4$ solution. The mixture was incubated statically for 60 min, and the formed CuONPs were analyzed using UV-visible spectroscopy.

2.4.4. Effect of pH on Nanoparticle Production. Cell-free supernatant was exposed to 5 mM $CuSO_4$ at pH of 6, 7, and 8 and incubated for 60 min to investigate the impact of pH

on CuONP production. UV-visible spectroscopy was used to analyze the formed CuONPs.

2.5. Characterization of Copper Oxide Nanoparticles

2.5.1. UV-Visible Spectral Analysis. Color changes were observed for biosynthesized copper oxide nanoparticles using the cell-free supernatant. CuONPs were characterized using UV-visible spectroscopy (Double Beam Spectrophotometer 6800, JENWAY) in the range of 200–800 nm, at regular intervals.

2.5.2. Transmission Electron Microscope Analysis. CuONP solution was diluted and sonicated. A drop was placed on a carbon-coated grid, and water was evaporated. Measurements were performed on a JEM-100-CX at a voltage acceleration of 80 KV dry. Then, samples were examined with a transmission electron microscope (TEM) at the Faculty of Science, Alexandria University.

2.5.3. Energy Dispersive X-Ray Spectroscopy Analysis. The technique described by Jyoti et al. [32] was used to determine the elementary structure of samples and confirm that the nanoparticle suspension contained only copper [33]. This analysis was conducted using the powder of lyophilized CuONPs. A sample was analyzed using the Oxford instrument attached to a scanning electron microscope at the Electron Microscope Unit, Faculty of Science, Alexandria University.

2.5.4. X-Ray Diffraction Analysis. CuONP samples were dried for X-ray diffraction (XRD) pattern analysis, which was recorded in the transmission mode on a Shimadzu XRD7000 instrument (at the Central Laboratory, the City of Scientific Research and Technological Applications, Egypt) operating at 40 KV current 30 mA with Cu Ka radiation ($\lambda = 1.5404$ A) [34]. A monochromatic X-ray beam with a lambda wavelength was used to analyze the crystalline nature of the samples [35].

2.6. Biotechnological Application of Copper Nanoparticles

2.6.1. Antimicrobial Activity of Copper Nanoparticles Using the Agar Diffusion Method. Biosynthesized CuONPs were examined for antimicrobial activity against Gram-positive bacterial pathogens (*Enterococcus faecalis* ATCC 29212), Gram-negative bacteria (*Salmonella typhimurium* ATCC 14028, *Pseudomonas aeruginosa* ATCC 9027, and *Escherichia coli* ATCC 8939), fungi (*Rhizoctonia solani*, *Fusarium solani*, and *Aspergillus niger*), and yeast (*Candida albicans* ATCC 10237) using the well diffusion method: Mueller-Hinton Agar was used for bacteria, Sabouraud Dextrose Agar was used for *C. albicans*, and potato D-glucose agar was used for fungi. A 100 μl bacterial suspension was used to prepare bacterial lawns for each bacterial test organism. These bacterial pathogens were kindly provided by the staff members of the National Institute of Oceanography and Fisheries (NIOF), Alexandria branch, and the Assiut University Mycological Center (AUMMC), Assiut, Egypt, also supplied fungal cultures. An 8 mm diameter agar well was made using a sterilized cork borer in stainless steel. The wells were loaded with 100 μl of 200 mg/ml concentrations of CuONP solution and 100 μl of culture broth from *Streptomyces* sp. MHM38 cell-free supernatant, and DMSO was used as a solvent. The plates were incubated for 24 h at 37°C for bacteria and 120 h at 28°C for fungi. Then, they were examined for inhibition zones. The diameter of inhibition areas was measured, and the mean value was recorded in millimeters for each organism [36].

2.6.2. Effect of Copper Oxide Nanoparticles against Oxidative Stress

(1) Animal and Experimental Design. Eighty healthy, eight-week-old, male albino Sprague-Dawley rats weighing 180–200 g were obtained and housed in the biology lab in the Agricultural Chemistry Department, Faculty of Agriculture, Minia University, at a controlled temperature of 25°C ± 2°C with a 12 h dark/light photoperiod for an adaptation period of two weeks. The study protocol was approved by the Agricultural Chemistry Department Ethics Committee, Minia University Faculty of Agriculture. Rats were randomly divided into eight groups with 10 rats in each group and subjected for 21 days to one of eight treatments: control (group 1), administered orally with 500 mg/kg b.wt paracetamol (PAC) daily for the last five days [37] (group 2), administered orally with 1 mg of CuONPs/kg b.wt daily for 21 days (group 3), administered orally with 2 mg of CuONPs/kg b.wt daily for 21 days (group 4), administered orally with 5 mg of CuONPs/kg b.wt daily for 21 days (group 5), administered with 1 mg of CuONPs/kg b.wt for 16 days and then received both CuONPs and paracetamol in the last five days (group 6), administered with 2 mg of CuONPs/kg b.wt for 16 days and then received both CuONPs and paracetamol in the last five days (group 7), and administered with 5 mg of CuONPs/kg b.wt for 16 days and then received both CuONPs and paracetamol in the last five days (group 8). After 24 hours, rats were sacrificed under light ether narcosis followed by decapitation to obtain biomaterials (blood and liver) for research. The blood sample was collected from the portal vein in the tubes that do not contain anticoagulants. The blood samples obtained were centrifuged at 1200 g for 15 min to separate the serum. The serum obtained was used to conduct biochemical analyses of alanine aminotransferase (ALT), aspartate aminotransferase (AST), lactate dehydrogenase (LDH), alkaline phosphatase (ALP), total and direct bilirubin, urea, and creatinine, which were measured according to El-Naggar and Abdelwahed [36], Al-Rubaei et al. [37], Davies et al. [38], Montgomery and Dymock [39], Ohkawa et al. [40], and Kakkar et al. [41], respectively. The liver was homogenized in homogenization buffer PBS (pH 7.4), and then, homogenates were centrifuged at 10,000 g for 30 min (+4°C) to obtain supernatants. The supernatants of liver tissues of rats were used to analyze glutathione (GSH) levels following Davies et al. [38], nitric oxide (NO) following Montgomery and Dymock [39], malondialdehyde (MDA) following Ohkawa et al. [40], and superoxide dismutase (SOD) following Kakkar et al. [41]. Liver tissues were also fixed in neutral buffered 10% formalin, dehydrated, cleared, and paraffin ionized for paraffin blocks, and 5-micron sections were obtained,

mounted on a glass slide, and stained with hematoxylin and eosin and Prussian blue reaction [42].

(2) Statistical Analysis. Data are presented as the mean ± standard error of the means (SEM). One-way analysis of variance followed by Tukey post hoc test using the Statistical Package for the Social Sciences (SPSS software V. 18.0) was performed to compare groups. p values < 0.05 were considered significant.

3. Results and Discussion

3.1. Evaluation of Biosynthesis of Copper Oxide Nanoparticles Using Streptomyces sp. MHM38. Streptomyces sp. MHM38 reduced the copper ions to copper nanoparticles. The biosynthesis of CuONPs was indicated by changing the soft blue reaction blend to green after 1% (v/v) of 1 mM aqueous $CuSO_4$ was added to the cell-free *Streptomyces* sp. MHM38 supernatant. By comparison, no color change was observed in aqueous $CuSO_4$ incubated under the same conditions without cell-free supernatant (Figure 1). The formation of colors depends on the surface vibration of plasmon [4, 43]. Our results agree with Shantkriti and Rani [4], who mentioned that when cell-free supernatant of *Pseudomonas fluorescens* was added to $CuSO_4$ solution and incubated for 48 h the color of the reaction mixtures changed from blue to dark green. Therefore, isolate CA-1 was considered the most potent isolate by endophytic actinomycetes due to color changes and maximum absorption peaks [44].

3.2. UV-Visible Spectral Analysis. The presence of nanoparticles was confirmed by UV-visible spectrophotometry within the 200–800 nm range the CuONPs formed by the *Streptomyces* sp. MHM38 which showed an absorption peak of 550 nm (Figure 2) of the different surface plasmon resonance (SPR) spectra, indicating the existence of CuONPs. Depending on individual particle properties, such as size, shape, and capping agents, the exact location of the SPR band can vary [45]. Brause and his team [46] reported that SPR is dominant in the optical absorption of metal nanoparticles, and particle size is linked to the absorption pick. The SPR of CuONPs in aqueous solution increases to longer wavelengths, with particle size increasing. The position and form of copper nanocluster absorption of plasmon are strongly dependent on particle size, stabilizing molecules or surface adsorbed particles, and the media's bioelectricity [47]. Our results agree with Ghorbani et al. [48], who mentioned that the copper SPR band of *Salmonella typhimurium* occurred at 565 nm [4]. The copper SPR band of *Pseudomonas fluorescens* exhibits a distinct absorption peak in the region of 550-650 nm.

3.3. Optimization of Copper Oxide Nanoparticles Using Box-Behnken Design

3.3.1. Effect of Copper Concentration on Nanoparticle Production. From Figure 3, it is clear that the rate of formation of CuONPs increased with increasing substrate concentration, reaching its maximum at 5 mM of $CuSO_4$. The addition of various concentrations of $CuSO_4$ solution to the pellet did not reveal any color change. Our results agree with

Figure 1: Visible observation of copper oxide nanoparticle biosynthesis by *Streptomyces* sp. MHM38 (left) 1 mM $CuSO_4$ solution (right).

Shantkriti and Rani, who mentioned that the color of the reaction mixtures changed from blue to dark green after 5 mM $CuSO_4$ was added to the supernatant of *Pseudomonas fluorescens* [4], and they were similar to a finding of a dark green solution when 5 mM of $CuSO_4$ was added to a flask containing *Morganella* sp. [49].

3.3.2. Effect of Reaction Time on Copper Oxide Nanoparticle Production. Reaction time is essential to the synthesis and stability of nanoparticles. Absorption at 550 nm was shown to increase progressively to 60 min, so there was no change (Figure 4). This suggests that CuONP development increased and size decreased over time. At the same time, Kimber et al. mentioned a complete reduction of $CuSO_4$ solution to CuNPs by *Shewanella oneidensis* after 96 h [50], and Hamid said that the CuNPs of *Salmonella typhimurium* formed after 20 min [48]. However, Shantkriti and his team [4] found that CuONPs formed using *Pseudomonas fluorescens* 90 min after adding 5 mM of $CuSO_4$ solution.

3.3.3. Effect of a Substrate to Filtrate Ratio on Copper Oxide Nanoparticle Production. Different volumes of $CuSO_4$ solutions have been used to understand the $CuSO_4$ volume required for the efficient production of NPs. When samples were taken at 60 min, the ratio of filtrate (cell-free supernatant) to substrate ($CuSO_4$ solution) was 1 : 1; the absorbance of CuONPs at 550 nm gave a high value compared with the ratio of filtrate (cell-free supernatant) to substrate ($CuSO_4$ solution), which was 1 : 1/2, or ratio of filtrate (cell-free supernatant) to substrate ($CuSO_4$ solution), which was 1 : 2, as shown in Figure 5.

3.3.4. Effect of pH on Copper Nanoparticle Production. Altering pH is thought to help control the shape and size of nanoparticles [51]. The peaks of an acidic pH of 6 were not typical of CuONPs (Figure 6). The alkaline pH provided a high absorption peak at 550 nm, and a characteristic peak of CuONPs was formed by *Pseudomonas fluorescens* at a neutral pH. After optimization, we estimated that the optimum conditions for CuONPs were a substrate concentration of 5 mM. An equal volume of filtrate and substrate was added,

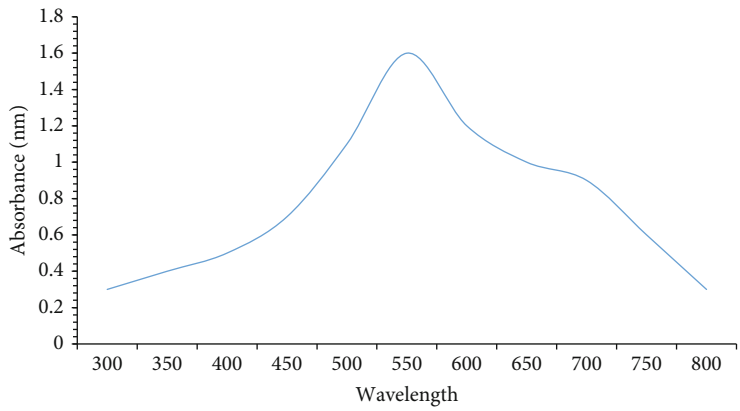

Figure 2: UV-visible absorption spectrum of copper nanoparticles synthesized using 15 ml of cell-free *Streptomyces* sp. MHM38 supernatant of 72 h old culture added to 15 ml of 1 mM $CuSO_4$ solution and incubated statically.

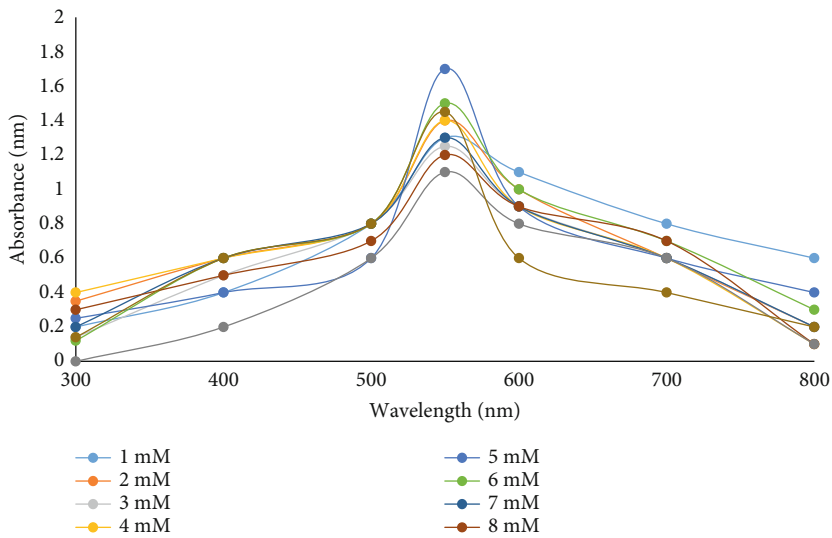

Figure 3: Effect of different copper sulfate ($CuSO_4$) concentrations on the production of copper oxide nanoparticles by *Streptomyces* sp. MHM38.

the pH was adjusted to eight, and the mixture was incubated statically for 60 min [4]. As showed in Figure 7, the color of the solution changed to green when we applied the preview conditions, indicating high levels of production of CuONPs.

3.4. Characterization of Copper Oxide Nanoparticles

3.4.1. TEM. Many studies have classified the shape and size of copper nanoparticles using TEM structures [52]. The present work revealed the spherical form of nanoparticles in the TEM images of copper nanoparticles (Figure 8). TEM analysis of CuONPs produced using *Streptomyces* sp. MHM38 showed that they were relatively uniform in shape. In general, spherical particles appeared with an average dimensional size of 1.72–13.49 nm, which is smaller than the CuNPs formed by *Pseudomonas fluorescens*, showing an extent of 20–80 nm [4]. Kimber et al. [50] mentioned that *Shewanella oneidensis* produced spherical CuNPs in the range of 20–50 nm.

3.4.2. XRD Analysis. The XRD pattern of nanoparticles showed intensive peaks throughout the two-party scope of the value 20–80, similar to the Bragg's copper oxide nanoparticle reflection. Thus, the reaction mixture indicated the formation of copper oxide nanoparticles. CuONPs produced using *Streptomyces* sp. MHM38 distinguished XRD peaks with 2θ values of prominent XRD peaks with 2θ values of 35°, 38°, 48°, 53°, 58°, 65°, 67°, and 72° which were observed (Figure 9). These peaks are assigned to the (111), (202), (020), (202), and (113) reflection planes of face-centered-cubic (fcc) copper, respectively. Our results agree with Chen et al. [53], who mentioned that the XRD pattern of the copper nanoparticles synthesized using N,N′-di-carboxy methyl perylene diimide (PDI) functionalized CuO nanocomposites showed at 2θ values of 35°, 38°, 48°, 53°, 58°, 65°, 67°, and 72°, corresponding to XRD planes (111), (202), (020), (202), and (113) Bragg's reflection based on the fcc structure of CuONPs.

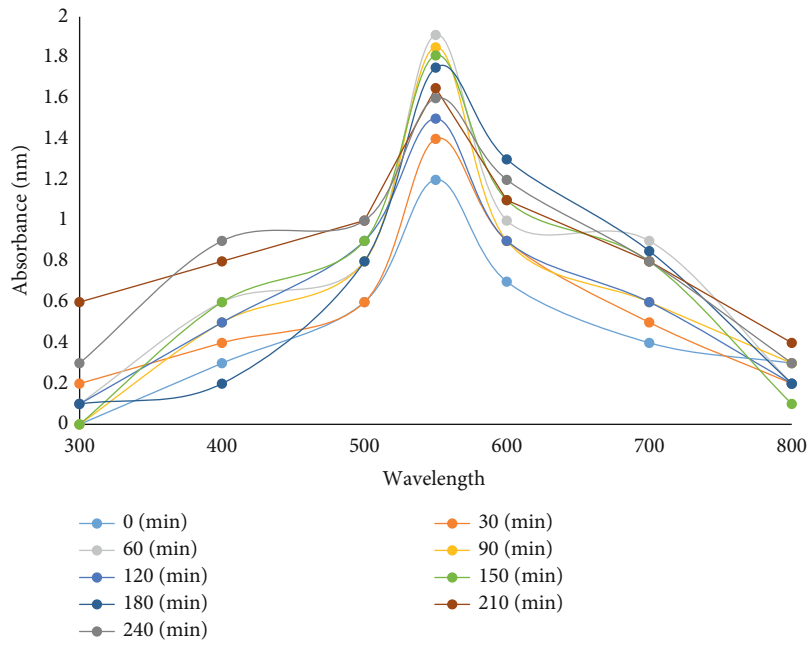

Figure 4: Effect of reaction time on the production of copper oxide nanoparticles using *Streptomyces* sp. MHM38.

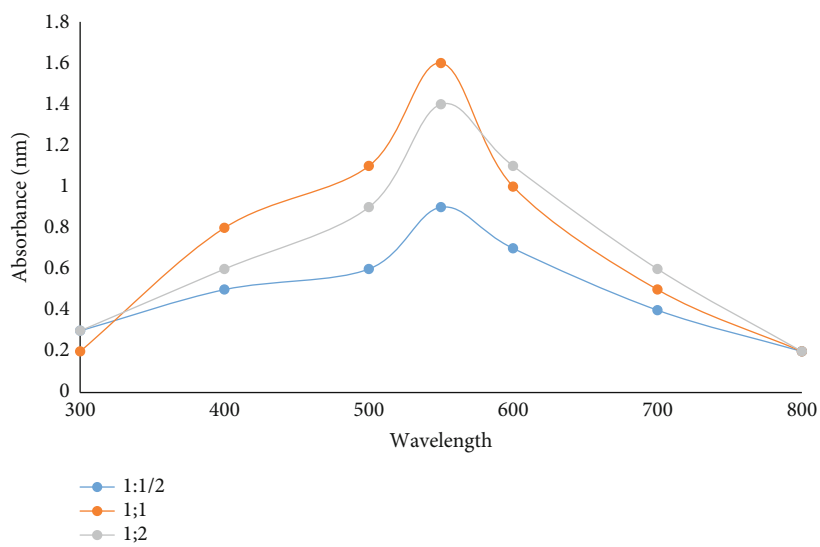

Figure 5: Effect of the ratio between filtrate (cell-free supernatant) to substrate ($CuSO_4$ solution) concentration on the production of copper oxide nanoparticles using *Streptomyces* sp. MHM38.

3.4.3. Energy Dispersive X-Ray (EDX) Spectroscopy Analysis. EDX and elementary mapping determined the purity and elemental composition of the nanoparticles. In the current research, EDX spectroscopy analysis was performed for CuONPs produced using *Streptomyces* sp. MHM38 (Figure 10), which confirmed the presence of elemental copper based on the signals. In the EDX spectrum, the nanoparticles displayed a peak at eight keV, which is due to the absorption of copper oxide nanocrystallites corresponding to SPR [54]. The optical absorption band peak for nanoparticles produced by *Streptomyces* sp. MHM38 was in the range of 1 to 9 keV, which is typical for the absorption of copper oxide nanocrystallites. The primary component observed was copper oxide (90%), and other elements were regarded, such as calcium, phosphate, and carbon. The use of a TEM network triggered the carbon distribution. However, there were other EDX peaks for calcium, phosphorus, and copper (5%, 10%, and 2%, respectively), which represent an essential ingredient in bacterial structural proteins that have functional groups, suggesting that they were mixed precipitates from the centrifuged supernatant/metal solution.

3.5. Antimicrobial Activity. Nanoparticles have an elevated surface-volume ratio, tiny size, and elevated dispersion

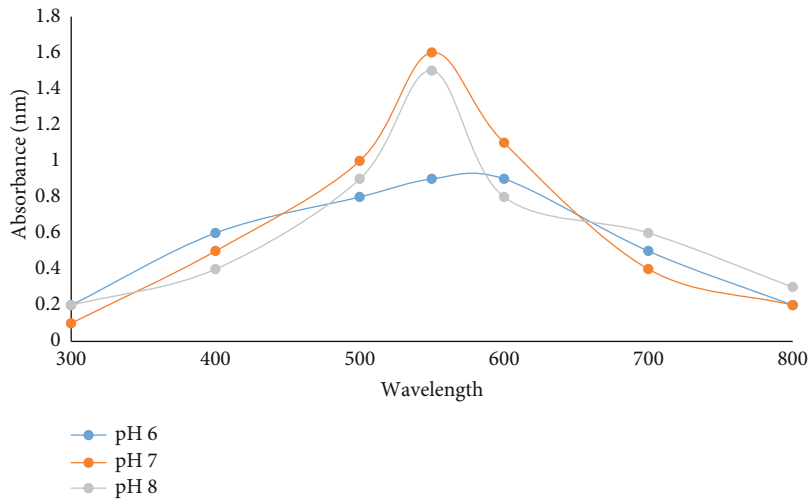

Figure 6: Effect of pH on the production of copper oxide nanoparticles using *Streptomyces* sp. MHM38.

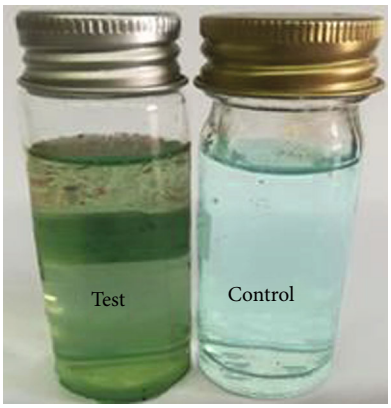

Figure 7: Visible observation of optimized copper oxide nanoparticle biosynthesis by *Streptomyces* sp. (Left: 15 ml of supernatant was added to 15 ml of 5 mM $CuSO_4$ at pH 8. Right: 15 ml of media was added to 15 ml of 5 mM $CuSO_4$ at pH 8.)

characteristics that enable them to interact with microbial surfaces. The large surface area of CuONPs enhances their interaction with microbes to perform wide antimicrobial operations [55]. However, the few reports on CuONP antimicrobial research have shown that CuONPs are effective against multiple pathogenic microorganisms [56]. The antimicrobial activity of CuONPs was determined on pathogenic bacterial strains Gram-positive bacteria (*Enterococcus faecalis* ATCC 29212), Gram-negative bacteria (*Salmonella typhimurium* ATCC 14028, *Pseudomonas aeruginosa* ATCC 9027, and *Escherichia coli* ATCC 8939), fungi (*Rhizoctonia solani*, *Fusarium solani*, and *Aspergillus niger*), and yeast (*Candida albicans* ATCC 10237) using the method of well diffusion, and the inhibition area values are shown in Table 1 and Figure 11. In each plate, DMSO as control, cell-free supernatant broth with no $CuSO_4$ addition is maintained. The highest antimicrobial activity was observed against *Candida albicans* ATCC 10237 and *Pseudomonas aeruginosa* ATCC 9027, whereas a lower activity was found against *Salmonella typhimurium* ATCC 14028 and *Escherichia coli* ATCC 8939. These findings are consistent with previous studies that examined *Candida albicans* and *Pseudomonas aeruginosa* antimicrobial activity of CuNPs [56]. The appearance of the inhibition area showed that in these locations there was no growth of bacteria. This shows how biosynthesized CuONPs interact with a smaller part/high surface area, of which CuONPs have been adsorbed onto the surface of the microorganism cell wall. As a result of this, cell walls that destroy human pathogens were demolished and disrupted by the resistance property of biosynthesized CuONPs. The antibacterial activity of copper metal is licensed by the United States Environmental Protection Agency as an antimicrobial agent [57]. The inhibitory action of CuONPs can be due to their small size and high volume-to-volume surface area, allowing it to interact with the microbial cell membrane [58]. Also, their inhibitory action is related to the production of hydroxyl radicals that ruin the helical structure of DNA by binding it and harm vital proteins by binding amino sulfhydryl and carboxyl amino acid groups and then inactivate necessary enzymes [59]. Santo et al. [60] showed the inhibitory action of CuONPs associated with an inactivated surface protein responsible for transporting material across cytoplasmic membranes and destroying selective permeability. Marine actinomycetes have recently revealed biosynthesis of CuONPs and their applications against pathogenic microbes [61]. Green-synthesized AgNPs by *Penicillium chrysogenum* strain F9 can be used to overcome the resistance pattern of *Candida* spp. and recommended as an anti-*Candida* agent [62].

3.6. The Effect of Copper Oxide Nanoparticles Produced Using Streptomyces sp. MHM38 against Paracetamol-Induced Liver and Kidney Damage. Tests for ALT, AST, ALP, and bilirubin are essential in diagnosing the condition of the liver. When liver cells (hepatitis) deteriorate, they are released into the bloodstream and level above the normal range. Urea and creatinine are both metabolic wastes excreted by the kidneys through urine, and only a small amount remains in the blood. If there is a disorder of kidney function, then there is an expansion in these two parameters. LDH is a conspicuous

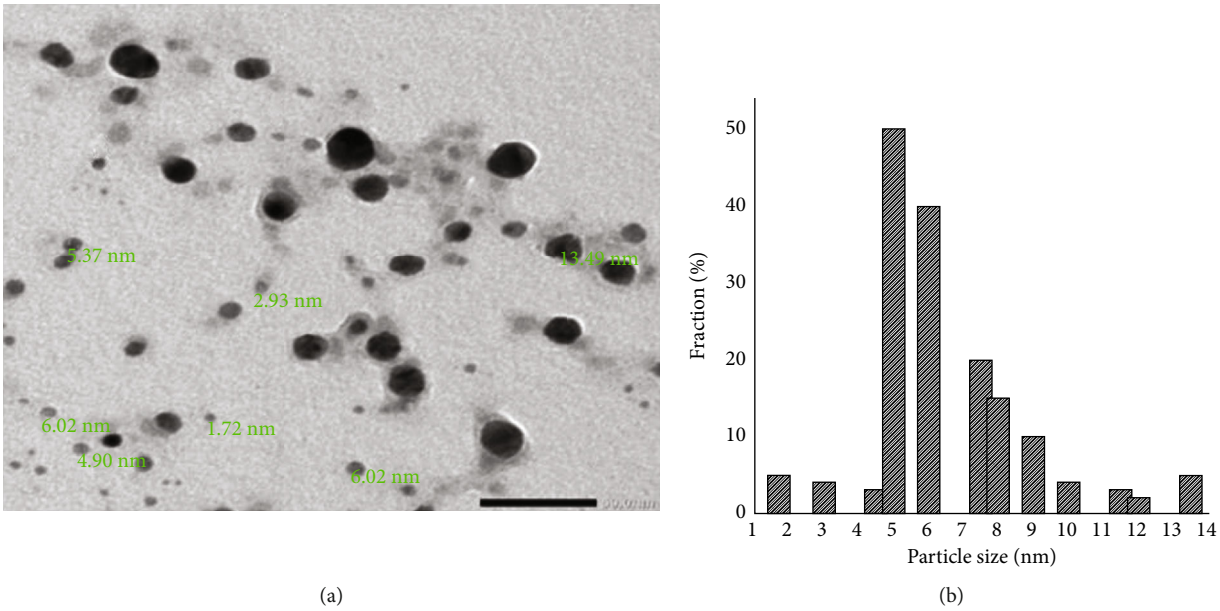

Figure 8: Transmission electron microscope image of produced spherical copper oxide nanoparticles using cell-free supernatant of *Streptomyces* sp. MHM38 (a). Histogram of CuONP size distribution (b).

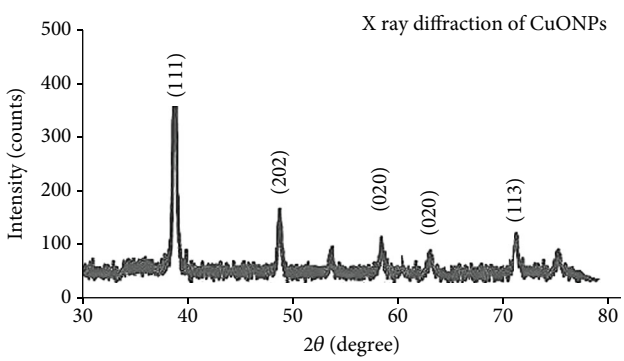

Figure 9: X-ray diffraction pattern with regard to the copper oxide nanoparticles biosynthesized using *Streptomyces* sp. MHM38.

marker and a diagnostic tool for tissue injury. As shown in Table 2, there were no significant differences in ALT, AST, ALP, LDH, total and direct bilirubin, urea, and creatinine between the groups treated with CuONPs compared with the control group. However, these parameters increased with an increasing dose of CuONPs. Conversely, significant increases were demonstrated in the ALT, AST, ALP, LDH, total and direct bilirubin, urea, and creatinine levels in paracetamol-treated rats compared with the controlled value. Meanwhile, pretreatment with CuONPs recorded suppression with these values, as shown in Table 2. These results were in agreement with Ravindran et al. [63], who explained that paracetamol increased levels of ALT, AST, ALP, bilirubin, urea, and creatinine. Paracetamol turned into water-soluble products through drug metabolism enzymes and was excreted in the urine in a therapeutic dose [64]. Excess paracetamol is oxidized by the hepatic cytochrome p450 system (CYP450) to N-acetyl-p-benzoquinone imine (NAPQI), which is toxic [65]. Detoxification is usually expelled from NAPQI by GSH. GSH depletion occurs when using high doses of paracetamol, and consequently, the toxic NAPQI accumulation binds to cellular proteins via cysteinyl sulfhydryl groups and forms NAPQI-protein adducts [66]. This case results in the formation of reactive oxygen species (ROS), such as superoxide anion (O_2^-), hydrogen peroxide (H_2O_2), and a hydroxyl root (OH^-) that impacts the cell membrane and stimulates lipid peroxide and also leads to liver necrosis [67]. Liver cell injuries lead to cellular enzymes leaking into the bloodstream and can be measured in serum. The increase in the production of ROS causes damage to the kidney tissue, resulting in a higher level of urea and creatinine [68]. Farghaly and Hussein [69] reported that paracetamol caused an increase in the level of LDH. Paracetamol works to accumulate Ca^{2+} intracellularly, which activates anaerobic glycolysis and phosphofructokinase, forming lactate and increasing LDH [70]. Returning these enzymes to normal levels demonstrates the protective effect of CuONPs against liver and kidney damage and their ability to regenerate liver and kidney cells, which is in agreement with Zhang et al. [71]. Green-synthesized nanoparticles exhibit a beneficial effect against liver and kidney degradation because the bacteria used in nanoparticle synthesis have medicinal properties. These results are consistent with Ghaffar et al. [72]. The protective activity of CuONPs may be attributed to their role in preventing cellular leakage and losing the functional integrity of the cellular membrane in hepatocytes and kidney.

3.7. The Effect of Copper Oxide Nanoparticles Produced Using Streptomyces sp. MHM38 against Paracetamol-Induced Oxidative Stress. The oral administration of biosynthesized CuONPs alone did not induce any evident changes in most biochemical parameters compared with the control group. Paracetamol administration produced a significant increase

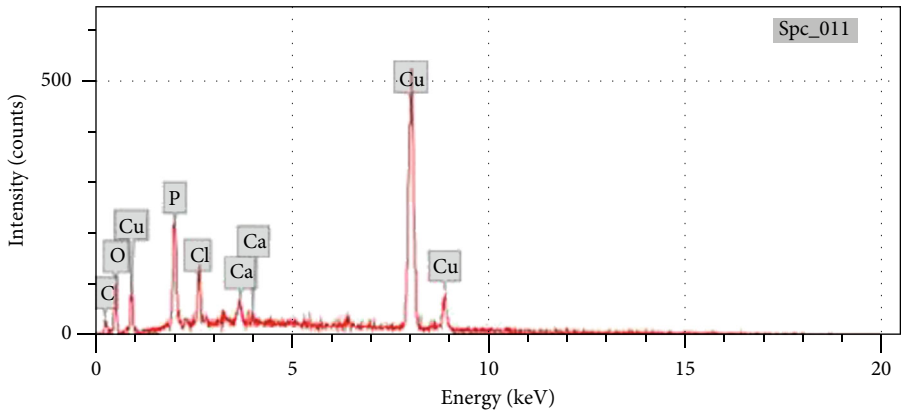

Figure 10: Energy dispersive X-ray spectrum of copper oxide nanoparticles formed using *Streptomyces* sp. MHM38, showing a peak between 1, 8, and 9 keV.

Table 1: Antimicrobial activity of copper nanoparticles produced using *Streptomyces* sp. MHM38.

Microorganism	Inhibition zone diameter (mm)		
	Free supernatant	CuONPs	DEMSO
Enterococcus faecalis ATCC 29212	0.0	20.0 ± 0.3	0.0
Salmonella typhimurium ATCC 14028	0.0	18.0 ± 0.4	0.0
Pseudomonas aeruginosa ATCC 9027	16.0 ± 0.6	20.0 ± 0.5	0.0
Escherichia coli ATCC 8939	0.0	18.0 ± 0.5	0.0
Rhizoctonia solani	0.0	0.0	0.0
Fusarium solani	0.0	0.0	0.0
Aspergillus niger	0.0	0.0	0.0
Candida albicans ATCC 10237	18.0 ± 0.5	22.0 ± 0.5	0.0

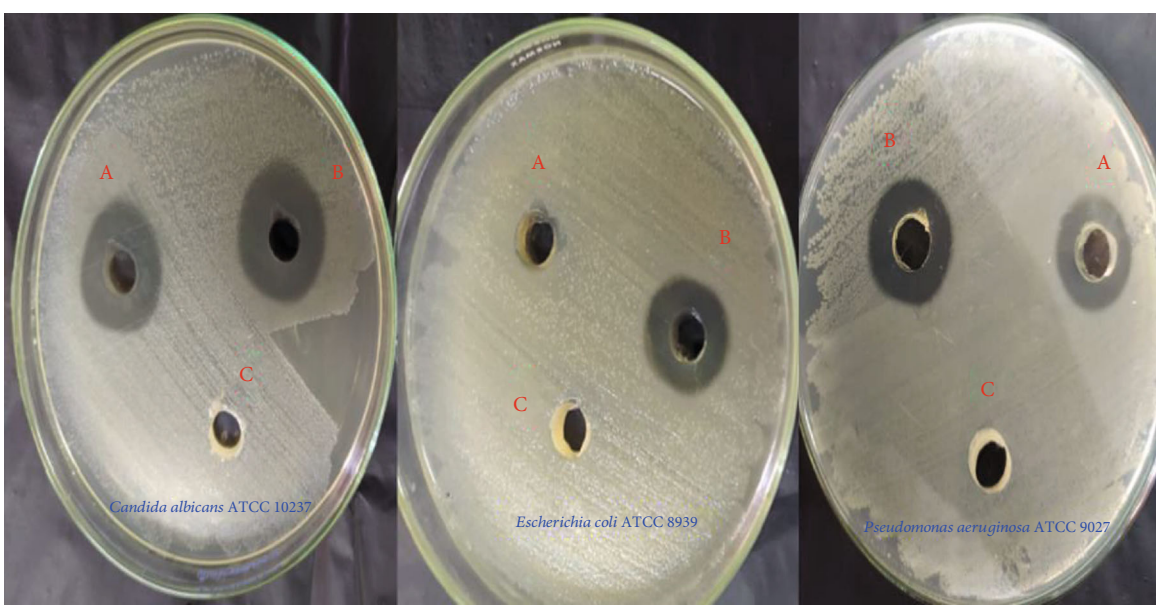

Figure 11: Antibacterial activity of copper nanoparticles against *Candida albicans* ATCC 10237, *Escherichia coli* ATCC 8939, and *Pseudomonas aeruginosa* ATCC 9027 ((a) cell-free supernatant, (b) copper nanoparticles produced using *Streptomyces* sp. MHM38, and (c) DMSO).

Table 2: Effect of copper oxide nanoparticles produced using *Streptomyces* sp. MHM38 on biochemical parameters.

Groups Parameters	Control	PAC	CuONPs (1 mg/kg b.wt)	CuONPs (2 mg/kg b.wt)	CuONPs (5 mg/kg b.wt)	CuONPs (1 mg/kg b.wt)+PAC	CuONPs (2 mg/kg b.wt)+PAC	CuONPs (5 mg/kg b.wt)+PAC
ALT (U/l)	22.53 ± 0.59	82.90 ± 3.06	25.60^{b}±0.78	24.40^{b}±1.21	26.35^{b}±0.64	42.23^{ab}±1.88	39.50^{ab}±0.89	52.37^{ab}±2.42
AST (U/l)	80.80 ± 1.73	223.65^{a}±7.59	82.48^{b}±6.15	73.65^{b}±1.99	85.17^{b}±1.85	136.25^{ab}±2.28	109.65^{ab}±0.43	153.95^{ab}±0.84
ALP (U/l)	223.2 ± 3.67	611.1^{a}±5.77	229.4^{b}±1.09	226.95^{b}±3.95	231.80^{b}±7.63	338.67^{ab}±5.27	360.03^{ab}±25.12	411.87^{ab}±9.61
Total bilirubin (mg/dl)	0.65 ± 0.03	2.27^{a}±0.09	0.75^{b}±0.03	0.7^{b}±0.06	0.8^{b}±0.06	1.23^{ab}±0.13	0.95^{ab}±0.03	1.7^{ab}±0.06
Direct bilirubin (mg/dl)	0.4 ± 0.06	0.99^{a}±0.06	0.4^{b}±0.12	0.38^{b}±0.18	0.45^{b}±0.02	0.58^{ab}±0.02	0.51^{ab}±0.2	0.7^{ab}±0.05
Urea (mg/dl)	23.45 ± 1.59	50.97^{a}±1.42	24.5^{b}±1.10	23.83^{b}±0.80	27.13^{b}±0.57	33.2^{ab}±0.35	31.70^{ab}±0.23	40.15^{ab}±0.02
Creatinine (mg/dl)	1.25 ± 0.03	2.82^{a}±0.03	1.31^{b}±0.03	1.30^{b}±0.06	1.35^{b}±0.03	1.70^{ab}±0.06	1.58^{ab}±0.03	1.9^{ab}±0.11
LDH (U/l)	145.7 ± 0.14	374.4^{a}±7.04	155.7^{b}±2.59	146.0^{b}±1.73	158.25^{b}±0.14	262.85^{ab}±10.59	235.7^{ab}±2.59	283.5^{ab}±2.02

Results are expressed as the mean ± standard error ($n = 10$) where the mean is significant at $p < 0.05$. [a]Compared with the control group; [b]compared with the paracetamol group.

Table 3: Effect of copper oxide nanoparticles produced using *Streptomyces* sp. MHM38 on nitric oxide, malondialdehyde, superoxide dismutase, and glutathione.

Groups Parameters	Control	PAC	CuONPs (1 mg/kg b.wt)	CuONPs (2 mg/kg b.wt)	CuONPs (5 mg/kg b.wt)	CuONPs (1 mg/kg b.wt)+PAC	CuONPs (2 mg/kg b.wt)+PAC	CuONPs (5 mg/kg b.wt)+PAC
NO (μmol/g tissue)	46.92 ± 0.15	66.65^{a}±1.69	51.67^{b}±0.07	51.27^{b}±0.14	51.17^{b}±1.48	60.35^{ab}±1.68	54.58^{ab}±1.57	61.49^{ab}±1.49
MDA (nmol/g tissue)	8.15 ± 0.53	24.40^{a}±0.23	9.40^{b}±0.46	8.60^{b}±0.40	9.50^{b}±0.25	12.27^{ab}±0.28	15.10^{ab}±0.06	17.19^{ab}±1.88
SOD (U/g protein)	23.58 ± 2.00	9.84^{a}±1.54	21.34^{b}±0.64	23.61^{b}±0.59	23.05^{b}±1.69	12.65^{ab}±0.37	19.41^{ab}±1.49	17.13^{ab}±1.38
GSH (nmol/g tissue)	4.45 ± 0.17	1.54^{a}±0.02	4.46^{b}±0.03	4.02^{b}±0.01	4.18^{b}±0.33	3.50^{ab}±0.23	3.00^{ab}±0.1	2.92^{ab}±0.01

Results are expressed as mean ± SE ($n = 10$) where mean is significant at $p < 0.05$. [a]Compared with the control group; [b]compared with the paracetamol group.

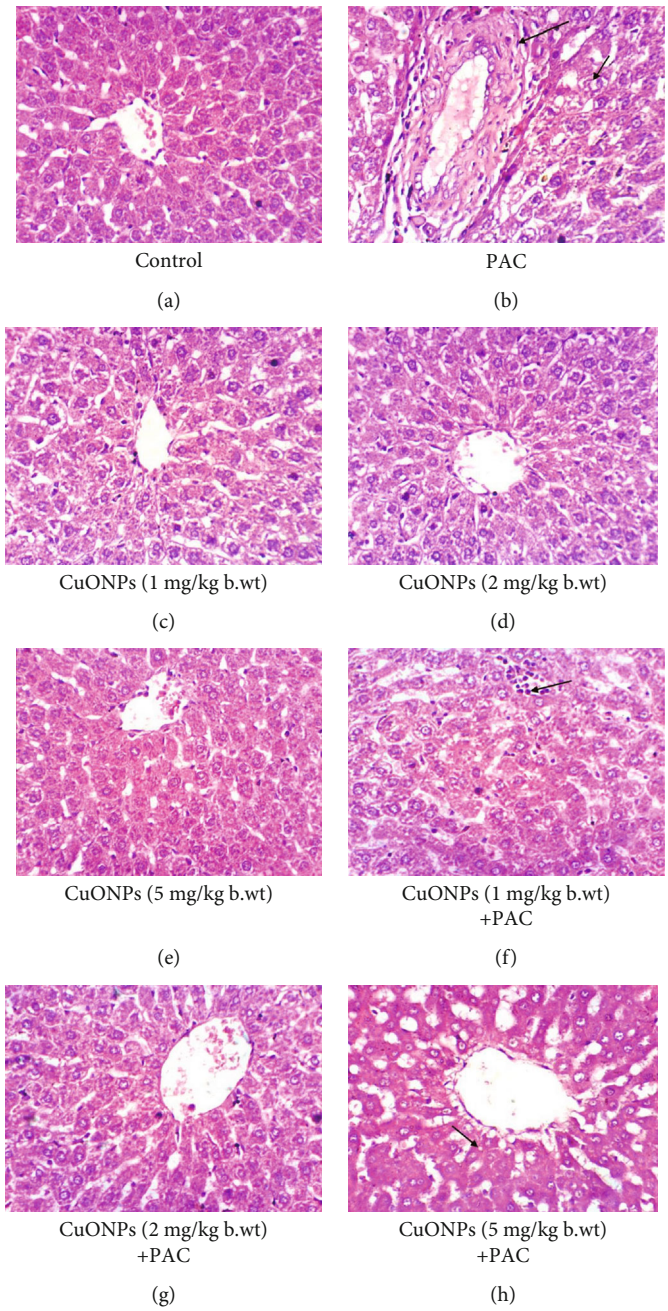

Figure 12: Section of rat's livers.

in NO and MAD content accompanied by a marked inhibition of GSH and SOD activities compared with the control group. The administration of biosynthesized CuONPs led to a significant decrease in NO and MAD content and increased GSH and SOD levels compared with the paracetamol group (Table 3). Nonenzymatic antioxidants (GSH) and enzymatic antioxidants (SOD) in natural conditions regulate free radical removal and production and thus maintain the ROS level. Therefore, this antioxidant protects the body from oxidative stress. Ravindran et al. [63] explain that consuming high doses of paracetamol reduces the activity of these enzymatic antioxidants and makes cells more vulnerable to injury caused by free radicals. Madkour and Abdel-Daim [73] showed that high doses of paracetamol cause oxidative stress and damage the liver, causing increased levels of MDA and NO and a decrease in the activities of SOD compared with the control group. Cytotoxicity occurs due to oxidative stress when the level of free radicals is increased to the point that cells cannot remove them and prevent their formation. An increased level of MDA and NO and decreased SOD and GSH levels indicate tissue damage and failure of an antioxidant system. It is assumed that the high antioxidant state by CuONPs (1, 2, and 5 mg/kg b.wt) protects against lipid peroxide by scavenging free radicals. From these results, we conclude that the CuONPs positively modify the state of antioxidants and restore them to an almost regular rate

(Table 3). Our findings are consistent with Zhang et al. [71], who have shown that AgNPs have a positive impact on the liver in terms of lipid peroxides. Administration with AgNPs was effective in relieving CCl_4 injuries [74]. Mohanta et al. [75] showed that biosynthesized AgNPs have potent antioxidant activities, as they have a protective impact on free radical generation or inhibit their production.

3.8. The Effect of Copper Oxide Nanoparticles Produced Using Streptomyces sp. MHM38 against Paracetamol-Induced Liver Tissue Damage. The results of the histopathological examination conducted in this study showed that the average group exhibited a standard lobular structure and normal hepatic cells (Figure 12(a)). Simultaneously, significant vacuolar degeneration of hepatocytes and fibroplasia occurred in the portal triad in the paracetamol-treated group (Figure 12(b)). These results are consistent with Madkour and Abdel-Daim [73], who explained that paracetamol caused inflammatory necrosis in liver tissue. Treatment with CuONPs reduced the pathological changes of paracetamol, which enhanced its ability to protect the liver from paracetamol toxicity (Figures 12(f)–12(h)). These results are consistent with Keshari et al. [76]. Bhuvaneswari et al. [77] showed that nanoparticle ameliorates liver tissue for CCl_4-treated rats. The drug's ability to reduce injuries or maintain physiological liver function after induction of poisoning indicates its hepatoprotective impact [78].

4. Conclusions

Biosynthesis of CuONPs using actinomycetes is an emerging trend in bio-nanotechnology and thus has a broad range of implementation in the biomedical field due to its eco-friendly nature and biocompatibility. The extensive function of *Streptomyces* sp. MHM38 is very useful for generating CuONPs in a nontoxic manner. The biosynthesized CuONPs were characterized by UV-vis spectroscopy, XRD, EDX, and TEM analysis. The formed CuONPs showed a prominent antimicrobial activity at different concentrations against the pathogens, viz., *Candida albicans* ATCC 10237, *Salmonella typhimurium* ATCC 14028, *Escherichia coli* ATCC 8939, *Pseudomonas aeruginosa* ATCC 9027, and *Enterococcus faecalis* ATCC 29212. In addition, CuONPs biosynthesized from marine *Streptomyces* sp. MHM38 had no toxic effect on the liver of the studied rats. It also mitigated the adverse impact of paracetamol, indicating that it can be used for several beneficial purposes, including as a prophylactic, without implications for the liver. Finally, this research opens up new ways to explore the role of biologically synthesized nanostructured substances for multiaction use in medical purposes.

Data Availability

Data are available on request. Please contact Mohamed Alagamy.

Conflicts of Interest

The authors declare that they have no conflicts of interest.

Authors' Contributions

Moaz M.H., Hanaa S.S.G., Asmaa M.Y., Sarah I.B., and Mohamed H.A. performed the methodology. Moaz M.H. was responsible for the software. Moaz M.H., Hanaa S.S.G., and Asmaa M.Y. contributed in writing. Mohamed H.A. contributed in data curation, writing, review, and editing. Hesham H.R. was responsible for the supervision. All authors read and approved the final manuscript.

Acknowledgments

The authors extend their appreciation to the Deputyship for Research & Innovation, "Ministry of Education" in Saudi Arabia, for funding this research work through the project no. IFKSURG-038.

References

[1] X.-F. Zhang, Z.-G. Liu, W. Shen, and S. Gurunathan, "Silver nanoparticles: synthesis, characterization, properties, applications, and therapeutic approaches," *International journal of molecular sciences*, vol. 17, no. 9, p. 1534, 2016.

[2] J. Jeevanandam, A. Barhoum, Y. S. Chan, A. Dufresne, and M. K. Danquah, "Review on nanoparticles and nanostructured materials: history, sources, toxicity and regulations," *Beilstein Journal of Nanotechnology*, vol. 9, no. 1, pp. 1050–1074, 2018.

[3] I. Khan, K. Saeed, and I. Khan, "Nanoparticles: properties, applications and toxicities," *Arabian Journal of Chemistry*, vol. 12, no. 7, pp. 908–931, 2019.

[4] S. Shantkriti and P. Rani, "Biological synthesis of copper nanoparticles using *Pseudomonas fluorescens*," *International Journal of Current Microbiology and Applied Sciences*, vol. 3, no. 9, pp. 374–383, 2014.

[5] A. Fouda, G. Abdel-Maksoud, M. A. Abdel-Rahman, S. S. Salem, S. E.-D. Hassan, and M. A.-H. El-Sadany, "Eco-friendly approach utilizing green synthesized nanoparticles for paper conservation against microbes involved in biodeterioration of archaeological manuscript," *International Biodeterioration & Biodegradation*, vol. 142, pp. 160–169, 2019.

[6] G.-T. Tenkouano, *Paleolimnological reconstruction of the environmental impact of the Deloro industrial site on Moira Lake (Ontario)*, Doctoral dissertation, 2017.

[7] S. S. Salem and A. Fouda, "Green synthesis of metallic nanoparticles and their prosective biotechnological applications: an overview," *Biological Trace Element Research*, vol. 199, pp. 344–370, 2021.

[8] A. V. Singh, R. Patil, A. Anand, P. Milani, and W. Gade, "Biological synthesis of copper oxide nano particles using *Escherichia coli*," *Current Nanoscience*, vol. 6, no. 4, pp. 365–369, 2010.

[9] R. Usha, E. Prabu, M. Palaniswamy, C. K. Venil, and R. Rajendran, "Synthesis of metal oxide nano particles by *Streptomyces* sp. for development of antimicrobial textiles," *Global Journal of Biotechnology and Biochemistry*, vol. 5, no. 3, pp. 153–160, 2010.

[10] M. R. Salvadori, L. F. Lepre, R. A. Ando, C. A. O. do Nascimento, and B. Corrêa, "Biosynthesis and uptake of copper nanoparticles by dead biomass of *Hypocrea lixii* isolated from the metal mine in the Brazilian Amazon region," *PLoS One*, vol. 8, no. 11, p. e80519, 2013.

[11] P. R. Ghosh, D. Fawcett, S. B. Sharma, and G. E. Poinern, "Production of high-value nanoparticles via biogenic processes using aquacultural and horticultural food waste," *Materials*, vol. 10, no. 8, p. 852, 2017.

[12] S. Harne, A. Sharma, M. Dhaygude, S. Joglekar, K. Kodam, and M. Hudlikar, "Novel route for rapid biosynthesis of copper nanoparticles using aqueous extract of *Calotropis procera* L. latex and their cytotoxicity on tumor cells," *Colloids and Surfaces B: Biointerfaces*, vol. 95, pp. 284–288, 2012.

[13] S. K. Murthy, "Nanoparticles in modern medicine: state of the art and future challenges," *International journal of nanomedicine*, vol. 2, no. 2, pp. 129–141, 2007.

[14] L. Han, G. Zhang, G. Miao, X. Zhang, and J. Feng, "*Streptomyces kanasensis* sp. nov., an antiviral glycoprotein producing actinomycete isolated from forest soil around kanas lake of China," *Current Microbiology*, vol. 71, no. 6, pp. 627–631, 2015.

[15] V. R. Sultanpuram, T. Mothe, and F. Mohammed, "*Nocardioides solisilvae* sp. nov., isolated from a forest soil," *Antonie Van Leeuwenhoek*, vol. 107, no. 6, pp. 1599–1606, 2015.

[16] P. Golinska, M. Wypij, A. P. Ingle, I. Gupta, H. Dahm, and M. Rai, "Biogenic synthesis of metal nanoparticles from actinomycetes: biomedical applications and cytotoxicity," *Applied Microbiology and Biotechnology*, vol. 98, no. 19, pp. 8083–8097, 2014.

[17] M. Składanowski, M. Wypij, D. Laskowski, P. Golińska, H. Dahm, and M. Rai, "Silver and gold nanoparticles synthesized from *Streptomyces* sp. isolated from acid forest soil with special reference to its antibacterial activity against pathogens," *Journal of Cluster Science*, vol. 28, no. 1, pp. 59–79, 2017.

[18] P. Singh, Y.-J. Kim, D. Zhang, and D.-C. Yang, "Biological synthesis of nanoparticles from plants and microorganisms," *Trends in Biotechnology*, vol. 34, no. 7, pp. 588–599, 2016.

[19] S. Abdeen, R. R. Isaac, S. Geo, S. Sornalekshmi, A. Rose, and P. Praseetha, "Evaluation of antimicrobial activity of biosynthesized iron and silver nanoparticles using the fungi *Fusarium oxysporum* and *Actinomycetes* sp. on human pathogens," *Nano Biomedicine & Engineering*, vol. 5, no. 1, 2013.

[20] N. F. Zonooz, M. Salouti, R. Shapouri, and J. Nasseryan, "Biosynthesis of gold nanoparticles by *Streptomyces* sp. ERI-3 supernatant and process optimization for enhanced production," *Journal of Cluster Science*, vol. 23, no. 2, pp. 375–382, 2012.

[21] S. S. Waghmare, A. M. Deshmukh, and Z. Sadowski, "Biosynthesis, optimization, purification and characterization of gold nanoparticles," *African Journal of Microbiology Research*, vol. 8, no. 2, pp. 138–146, 2014.

[22] B. A. Omran, "Prokaryotic microbial synthesis of nanomaterials (the world of unseen)," in *Nanobiotechnology: A Multidisciplinary Field of Science*, pp. 37–79, Springer, 2020.

[23] A. Fouda and T. I. Shaheen, "Silver nanoparticles: biosynthesis, characterization and application on cotton fabrics," *Microbiology Research Journal International*, vol. 20, no. 1, pp. 1–14, 2017.

[24] Z. Issaabadi, M. Nasrollahzadeh, and S. M. Sajadi, "Green synthesis of the copper nanoparticles supported on bentonite and investigation of its catalytic activity," *Journal of Cleaner Production*, vol. 142, pp. 3584–3591, 2017.

[25] M. Ismail, S. Gul, M. Khan, M. A. Khan, A. M. Asiri, and S. B. Khan, "Green synthesis of zerovalent copper nanoparticles for efficient reduction of toxic azo dyes congo red and methyl orange," *Green Processing and Synthesis*, vol. 8, no. 1, pp. 135–143, 2019.

[26] H. Almasi, P. Jafarzadeh, and L. Mehryar, "Fabrication of novel nanohybrids by impregnation of CuO nanoparticles into bacterial cellulose and chitosan nanofibers: characterization, antimicrobial and release properties," *Carbohydrate Polymers*, vol. 186, pp. 273–281, 2018.

[27] K. Rajesh, B. Ajitha, Y. A. K. Reddy, Y. Suneetha, and P. S. Reddy, "Assisted green synthesis of copper nanoparticles using *Syzygium aromaticum* bud extract: Physical, optical and antimicrobial properties," *Optik*, vol. 154, pp. 593–600, 2018.

[28] F. Ijaz, S. Shahid, S. A. Khan, W. Ahmad, and S. Zaman, "Green synthesis of copper oxide nanoparticles using *Abutilon indicum* leaf extract: antimicrobial, antioxidant and photocatalytic dye degradation activitie," *Tropical Journal of Pharmaceutical Research*, vol. 16, no. 4, pp. 743–753, 2017.

[29] M. I. Nabila and K. Kannabiran, "Biosynthesis, characterization and antibacterial activity of copper oxide nanoparticles (CuO NPs) from actinomycetes," *Biocatalysis and Agricultural Biotechnology*, vol. 15, pp. 56–62, 2018.

[30] N. Nerdy and K. Ritarwan, "Hepatoprotective activity and nephroprotective activity of peel extract from three varieties of the passion fruit (*Passiflora* sp.) in the albino rat," *Open Access Macedonian Journal of Medical Sciences*, vol. 7, no. 4, p. 536, 2019.

[31] N. A. El-Sersy, H. Abd-Elnaby, G. M. Abou-Elela, H. A. Ibrahim, and N. M. El-Toukhy, "Optimization, economization and characterization of cellulase produced by marine *Streptomyces ruber*," *African Journal of Biotechnology*, vol. 9, no. 38, pp. 6355–6364, 2010.

[32] K. Jyoti, M. Baunthiyal, and A. Singh, "Characterization of silver nanoparticles synthesized using *Urtica dioica* Linn. leaves and their synergistic effects with antibiotics," *Journal of Radiation Research and Applied Sciences*, vol. 9, no. 3, pp. 217–227, 2019.

[33] K. Roy, S. Biswas, and P. Banerjee, "'Green' synthesis of silver nanoparticles by using grape (*Vitis vinifera*) fruit extract: characterization of the particles and study of antibacterial activity," *Research Journal of Pharmaceutical, Biological and Chemical Sciences*, vol. 4, no. 1, pp. 1271–1278, 2013.

[34] A. M. Fayaz, M. Girilal, M. Rahman, R. Venkatesan, and P. Kalaichelvan, "Biosynthesis of silver and gold nanoparticles using thermophilic bacterium *Geobacillus stearothermophilus*," *Process Biochemistry*, vol. 46, no. 10, pp. 1958–1962, 2011.

[35] L. Karthik, G. Kumar, A. V. Kirthi, A. Rahuman, and K. B. Rao, "*Streptomyces* sp. LK3 mediated synthesis of silver nanoparticles and its biomedical application," *Bioprocess and Biosystems Engineering*, vol. 37, no. 2, pp. 261–267, 2014.

[36] N. E.-A. El-Naggar and N. A. Abdelwahed, "Application of statistical experimental design for optimization of silver nanoparticles biosynthesis by a nanofactory *Streptomyces viridochromogenes*," *Journal of Microbiology*, vol. 52, no. 1, pp. 53–63, 2014.

[37] Z. Al-Rubaei, T. U. Mohammad, and L. K. Ali, "Effects of local curcumin on oxidative stress and total antioxidant capacity in vivo study," *Pakistan Journal of Biological Sciences*, vol. 17, no. 12, pp. 1237–1241, 2014.

[38] M. Davies, D. Birt, and R. Schnell, "Direct enzymatic assay for reduced and oxidized glutathione," *Journal of Pharmacological Methods*, vol. 12, no. 3, pp. 191–194, 1984.

[39] H. Montgomery and J. F. Dymock, *Determination of nitrite in water*, ROYAL SOC CHEMISTRY THOMAS GRAHAM HOUSE, SCIENCE PARK, MILTON RD, CAMBRIDGE, 1961.

[40] H. Ohkawa, N. Ohishi, and K. Yagi, "Assay for lipid peroxides in animal tissues by thiobarbituric acid reaction," *Analytical Biochemistry*, vol. 95, no. 2, pp. 351–358, 1979.

[41] P. Kakkar, B. Das, and P. Viswanathan, *A modified spectrophotometric assay of superoxide dismutase*, 1984.

[42] J. D. Bancroft and M. Gamble, *Theory and Practice of Histological Techniques*, Elsevier health sciences, 2008.

[43] A. A. Mohamed, A. Fouda, M. A. Abdel-Rahman et al., "Fungal strain impacts the shape, bioactivity and multifunctional properties of green synthesized zinc oxide nanoparticles," *Biocatalysis and Agricultural Biotechnology*, vol. 19, p. 101103, 2019.

[44] S. E.-D. Hassan, S. S. Salem, A. Fouda, M. A. Awad, M. S. El-Gamal, and A. M. Abdo, "New approach for antimicrobial activity and bio-control of various pathogens by biosynthesized copper nanoparticles using endophytic actinomycetes," *Journal of Radiation Research and Applied Sciences*, vol. 11, no. 3, pp. 262–270, 2019.

[45] D. Mott, J. Galkowski, L. Wang, J. Luo, and C.-J. Zhong, "Synthesis of size-controlled and shaped copper nanoparticles," *Langmuir*, vol. 23, no. 10, pp. 5740–5745, 2007.

[46] R. Brause, H. Moeltgen, and K. Kleinermanns, "Characterization of laser-ablated and chemically reduced silver colloids in aqueous solution by UV/VIS spectroscopy and STM/SEM microscopy," *Applied Physics B*, vol. 75, no. 6-7, pp. 711–716, 2002.

[47] C. Krishnaraj, E. Jagan, S. Rajasekar, P. Selvakumar, P. Kalaichelvan, and N. Mohan, "Synthesis of silver nanoparticles using *Acalypha indica* leaf extracts and its antibacterial activity against water borne pathogens," *Colloids and Surfaces B: Biointerfaces*, vol. 76, no. 1, pp. 50–56, 2010.

[48] H. R. Ghorbani, F. P. Mehr, and A. K. Poor, "Extracellular synthesis of copper nanoparticles using culture supernatants of *Salmonella typhimurium*," *ORIENTAL JOURNAL OF CHEMISTRY*, vol. 31, no. 1, p. 3, 2015.

[49] R. Ramanathan, S. K. Bhargava, and V. Bansal, "Biological synthesis of copper/copper oxide nanoparticles," in *Chemeca 2011: Engineering a Better World*, pp. 18–21, Sydney Hilton Hotel, NSW, Australia, 2011.

[50] R. L. Kimber, E. A. Lewis, F. Parmeggiani et al., "Biosynthesis and characterization of copper nanoparticles *UsingShewanella oneidensis*: application for click chemistry," *Small*, vol. 14, no. 10, 2018.

[51] S. Gurunathan, K. Kalishwaralal, R. Vaidyanathan et al., "Biosynthesis, purification and characterization of silver nanoparticles using *Escherichia coli*," *Colloids and Surfaces B: Biointerfaces*, vol. 74, no. 1, pp. 328–335, 2009.

[52] R. Singh, U. U. Shedbalkar, S. A. Wadhwani, and B. A. Chopade, "Bacteriagenic silver nanoparticles: synthesis, mechanism, and applications," *Applied Microbiology and Biotechnology*, vol. 99, no. 11, pp. 4579–4593, 2015.

[53] M. Chen, Y. Ding, Y. Gao et al., "N,N′-di-caboxy methyl perylene diimide (PDI) functionalized CuO nanocomposites with enhanced peroxidase-like activity and their application in visual biosensing of H_2O_2 and glucose," *RSC Advances*, vol. 7, no. 41, pp. 25220–25228, 2017.

[54] Q. Maqbool, M. Nazar, A. Maqbool et al., "CuO and CeO_2 nanostructures green synthesized using olive leaf extract inhibits the growth of highly virulent multidrug resistant bacteria," *Frontiers in Pharmacology*, vol. 9, p. 987, 2018.

[55] S. Shende, A. P. Ingle, A. Gade, and M. Rai, "Green synthesis of copper nanoparticles by *Citrus medica* Linn.(Idilimbu) juice and its antimicrobial activity," *World Journal of Microbiology and Biotechnology*, vol. 31, no. 6, pp. 865–873, 2015.

[56] R. Hassanien, D. Z. Husein, and M. F. Al-Hakkani, "Biosynthesis of copper nanoparticles using aqueous *Tilia* extract: antimicrobial and anticancer activities," *Heliyon*, vol. 4, no. 12, p. e01077, 2018.

[57] S. E.-D. Hassan, A. Fouda, A. A. Radwan et al., "Endophytic actinomycetes *Streptomyces* spp mediated biosynthesis of copper oxide nanoparticles as a promising tool for biotechnological applications," *JBIC Journal of Biological Inorganic Chemistry*, vol. 24, no. 3, pp. 377–393, 2019.

[58] M. S. Usman, M. E. El Zowalaty, K. Shameli, N. Zainuddin, M. Salama, and N. A. Ibrahim, "Synthesis, characterization, and antimicrobial properties of copper nanoparticles," *International Journal of Nanomedicine*, vol. 8, p. 4467, 2013.

[59] K.-Y. Yoon, J. H. Byeon, J.-H. Park, and J. Hwang, "Susceptibility constants of *Escherichia coli* and *Bacillus subtilis* to silver and copper nanoparticles," *Science of the Total Environment*, vol. 373, no. 2-3, pp. 572–575, 2007.

[60] C. E. Santo, N. Taudte, D. H. Nies, and G. Grass, "Contribution of copper ion resistance to survival of *Escherichia coli* on metallic copper surfaces," *Applied and Environmental Microbiology*, vol. 74, no. 4, pp. 977–986, 2008.

[61] U. Rasool and S. Hemalatha, "Marine endophytic actinomycetes assisted synthesis of copper nanoparticles (CuNPs): characterization and antibacterial efficacy against human pathogens," *Materials Letters*, vol. 194, pp. 176–180, 2017.

[62] A. M. Soliman, W. Abdel-Latif, I. H. Shehata, A. Fouda, A. M. Abdo, and Y. M. Ahmed, "Green approach to overcome the resistance pattern of *Candida* spp. using biosynthesized silver nanoparticles fabricated by *Penicillium chrysogenum* F9," *Biological Trace Element Research*, vol. 199, no. 2, pp. 800–811, 2020.

[63] C. A. Ravindran, V. Murugaiyah, P. Khiang, and R. Xavior, "Hepatoprotective activity of leaf of methanol extract of *Laurus nobilis* L. against paracetamol induced hepatotoxicity in rats," *Asian Journal of Pharmaceutical and Clinical Research*, vol. 6, no. 4, pp. 153–157, 2013.

[64] J. A. Hinson, D. W. Roberts, and L. P. James, "Mechanisms of acetaminophen-induced liver necrosis," in *Adverse drug reactions*, pp. 369–405, Springer, 2010.

[65] F.-L. Yen, T.-H. Wu, L.-T. Lin, and C.-C. Lin, "Hepatoprotective and antioxidant effects of *Cuscuta chinensis* against acetaminophen-induced hepatotoxicity in rats," *Journal of Ethnopharmacology*, vol. 111, no. 1, pp. 123–128, 2007.

[66] M. Subramanian, S. Balakrishnan, S. K. Chinnaiyan, V. K. Sekar, and A. N. Chandu, "Hepatoprotective effect of leaves of *Morinda tinctoria* Roxb. against paracetamol induced liver damage in rats," *Drug Invention Today*, vol. 5, no. 3, pp. 223–228, 2013.

[67] Y.-H. Chen, F.-Y. Lin, P.-L. Liu et al., "Antioxidative and hepatoprotective effects of magnolol on acetaminophen-induced liver damage in rats," *Archives of pharmacal research*, vol. 32, no. 2, pp. 221–228, 2009.

[68] P. Moshaie-Nezhad, S. M. Hosseini, M. Yahyapour, M. Iman, and A. Khamesipoure, "Protective effect of ivy leaf extract on

paracetamol-induced oxidative stress and nephrotoxicity in mice," *Journal of Herbmed Pharmacology*, vol. 8, no. 1, 2019.

[69] H. S. Farghaly and M. A. Hussein, "Protective effect of curcumin against paracetamol-induced liver damage," *Australian Journal of Basic and Applied Sciences*, vol. 4, no. 9, pp. 4266–4274, 2010.

[70] D. Landowne and J. Ritchie, "On the control of glycogenolysis in mammalian nervous tissue by calcium," *The Journal of Physiology*, vol. 212, no. 2, pp. 503–517, 1971.

[71] H. Zhang, J. A. Jacob, Z. Jiang et al., "Hepatoprotective effect of silver nanoparticles synthesized using aqueous leaf extract of *Rhizophora apiculata*," *International Journal of Nanomedicine*, vol. Volume 14, pp. 3517–3524, 2019.

[72] T. Ghaffar, M. Irshad, Z. Anwar et al., "Recent trends in lactic acid biotechnology: a brief review on production to purification," *Journal of radiation research and applied Sciences*, vol. 7, no. 2, pp. 222–229, 2019.

[73] F. F. Madkour and M. Abdel-Daim, "Hepatoprotective and antioxidant activity of *Dunaliella salina* in paracetamol-induced acute toxicity in rats," *Indian journal of pharmaceutical sciences*, vol. 75, no. 6, pp. 642–648, 2013.

[74] A. V. D'Antoni, "All-in-One Anatomy Exam Review: Volumes 1–5 by Carlos Suárez-Quian and Joel A. Vilensky, 2015, iBooks downloaded from the Apple store. Total cost for all five volumes $15.95 (volumes can be purchased separately)," *Clinical Anatomy*, vol. 29, no. 6, pp. 814–814, 2016.

[75] Y. K. Mohanta, S. K. Panda, R. Jayabalan, N. Sharma, A. K. Bastia, and T. K. Mohanta, "Antimicrobial, antioxidant and cytotoxic activity of silver nanoparticles synthesized by leaf extract of *Erythrina suberosa* (Roxb.)," *Frontiers in Molecular Biosciences*, vol. 4, p. 14, 2017.

[76] A. K. Keshari, R. Srivastava, P. Singh, V. B. Yadav, and G. Nath, "Antioxidant and antibacterial activity of silver nanoparticles synthesized by _Cestrum nocturnum_," *Journal of Ayurveda and Integrative Medicine*, vol. 11, no. 1, pp. 37–44, 2020.

[77] R. Bhuvaneswari, N. Chidambaranathan, and K. Jegatheesan, "Hepatoprotective effect of *Embilica officinalis* and its silver nanoparticles against CCl_4 induced hepatotoxicity in Wistar albino rats," *Digest Journal of Nanomaterials & Biostructures*, vol. 9, no. 1, 2014.

[78] N. Yadav and V. Dixit, "Hepatoprotective activity of leaves of *Kalanchoe pinnata* Pers.," *Journal of Ethnopharmacology*, vol. 86, no. 2-3, pp. 197–202, 2003.